Aging processes of sealing materials

Von der Naturwissenschaftlichen Fakultät der
Gottfried Wilhelm Leibniz Universität Hannover
zur Erlangung des Grades
Doktor der Naturwissenschaften
Dr.rer.nat.

genehmigte Dissertation

von

Yuichi Aoyagi, M. Engineering (Japan)

geboren am 24.Mai.1981 in Aichi, Japan

Zusammenfassung

Dichtungsmaterialien werden in der Praxis immer unter Deformation eingesetzt und unterliegen verschiedenen Alterungsprozessen in Abhängigkeit der Umgebungsparameter wie z. B. der Temperatur und Sauerstoff, was sich häufig in einer für die Langzeitfunktion der Dichtung kritisch beeinflussten Spannungsrelaxation darstellt. Daher hat diese Arbeit das Ziel, zu einem detaillierten Verständnis des speziellen Alterungsmechanismus der Spannungsrelaxation von EPDM Elastomeren beizutragen.. Zu diesem Zweck wurde der Einfluss von Material- und Umweltparametern auf irreversible Änderungen der Vernetzung und der chemischen Strukturen der Polymermatrix unter mechanischer Beanspruchung umfangreich betrachtet. Im Einzelnen wurden die Einflüsse der Materialparameter wie Vernetzungsmittel, Vernetzungsdichte, Ruß, Antioxidantien, Sauerstoff und Polymermikrostruktur von EPDM untersucht. Um das o. a. Ziel zu erreichen, wurden neuartige Charakterisierungstechniken wie Niedrigfeld-NMR-Relaxationszeit-Spektroskopie mit Inverser Laplace Transformation (ILT) und Chemilumineszenz unter Dehnung weiterentwickelt und optimiert. Die NMR-Methode und die hier weiterentwickelte Auswertemethode der ILT wurden verwendet, um die Strukturänderung im Netzwerk und der Kettenbeweglichkeit möglichst exakt zu beschreiben.

Mit Hilfe dieser Methode konnte eine Quantifizierung von Strukturveränderungen wie Quervernetzungen, Anteile freier Kettenenden und freier Kettenfragmente, die während des Alterungsprozesses gebildet werden, vorgenommen werden. Es wurde festgestellt, dass all die o. a. Materialparameter einen signifikanten Einfluss auf die alterungsbedingte Änderung der Spannungsrelaxation bei konstanter Deformation haben. Es wurde auch gezeigt, dass die Geschwindigkeit der thermischen Oxidation unter Verformung höher ist als im nicht verformten Zustand. Die neuen Charakterisierungsmethoden ermöglichen eine wesentlich genauere Beschreibung und somit ein deutlich besseres Verständnis des Spannungsrelaxationsmechanismus von Elastomeren.

Schlagwörter:

Abstract

In practice, sealing materials are always used under deformation and are subject to various aging processes as a function of ambient parameters such as, for example, temperature and oxygen, frequently manifested in stress relaxation impacted critically with respect to the long-term functioning of the seal. This study thus aims to contribute to a detailed understanding of the specific aging mechanism of stress relaxation in the case of EPDM elastomers. To this end, the influence of material and ambient parameters on irreversible changes in the crosslinking and chemical structures of the polymer matrix under mechanical load was extensively examined. In point of detail, the effects of material parameters like crosslinking agent, crosslinking density, carbon black, antioxidants, oxygen, and the polymer microstructure of EPDM were closely studied. Attainment of the targeted objective of this study involved further development and optimization of innovative characterization methods like low-field time-domain NMR spectroscopy with inverse Laplace transformation (ILT) and chemiluminescence under strain. The NMR methods and the ILT analysis methods further developed here were used to describe as precisely as possible the structural changes occurring in the network and with respect to chain mobility.

With the help of this method, it was possible to quantify structural changes like crosslinking, the share of free chain ends and free chain fragments formed during the aging process. All the aforementioned material parameters were found to have a significant impact on the aging-related change in stress relaxation at constant deformation. The rate of thermal oxidation under deformation was also shown to be greater than in a non-deformed state. The new characterization methods allow for a much more precise description, and thus a markedly better understanding, of the stress relaxation mechanism among elastomers.

Table of Contents

Chapter 1

Introduction

1.1   Motivation and introduction

Seals can be seen as one of the most indispensable machine element. The main function of seals is to fill the gap between two components in order to prevent any leakage of gas or liquid to the inside or the outside. In addition, seals are used to prevent the entry of dust or other contaminations.

Therefore, Seals Market is expected to expand due to growth of Automobile industry. From the report of "Gaskets and Seals Global Market Outlook (2017-2023) [1], the Global Gasket & Seals Market is valued at $59.73 billion in 2016 and is expected to reach $97.16 billion by 2023 growing at a CAGR of 7.2% from 2016 to 2023 since vehicle production market has grown up. Asia Pacific is expected to grasp major revenue shares in gasket & seals market. This growth is attributed to rising demand from the automotive industry in emerging economies like India and China.

Seals are made of a various materials such as thermoplastic polymers or duromers, rubber including silicone, fiberglass and metal. Nevertheless, the most typical material for seals is rubber because of its characteristic rubber elasticity.

Its characteristic rubber elasticity leads the suitability of rubber materials for sealing applications. This allows the shape of the material to recover flexibly because seals are used typically under compression. The elastic properties of rubber provide enough reaction force enable to prevent leakage.

However, up to the point at which leakages actually occur, reaction force gradually decreases as a function of time. This is called "stress relaxation". As a result of stress relaxation, the reaction force reaches finally to zero. Then this is the end of a seals life and leakage is observed [2, 3, 4]. This stress relaxation mechanism lies on "aging" of materials. Aging is a gradual process of the change of material properties over time due to thermal, chemical, physical or biological factors etc.

During the aging process, rubber structure is largely degraded and therefore rubber loses its original length, the flexibility to adapt the shape to the gap between components. Therefore ,it can be concluded, that the service life of seals is largely determined by the intensity of the degradation processes, which is dependent on the one hand the environmental conditions as temperature, oxygen ,UV exposure, humidity and etc moreover on the other hand the material sensitivity to

degradation processes. Besides, aging in the actual process in machine is accelerated by several complex factors such as deformation, mechanical fatigue, chemical media or diffusion processes [5, 6, 7, 8, 9].

Especially, in static applications, where mechanical fatigue can play a neglectable role the life of sealing materials are largely determined by the pure thermal or thermal oxidative aging process [10, 11, 12, 13, 14].

1.2   Aims

Because of these back ground, giving a deeper insight of the rubber structural change due to aging and influential factors on aging has been greatly interesting for the rubber industry. Besides, the investigation can contribute the development of high resistance materials and prediction of its life time.

Hence, the aims of this research are:
- To provide a better understanding of the aging mechanism, especially, focus on thermal oxidation during the stress relaxation process.
- To clarify the effect of key factors of environment and materials on the aging process above. (e.g. strain, oxygen and temperature as environmental factors and polymer composition, crosslink density, co-agent amount, antioxidant and carbon black filler as material parameters)

In order to achieve these aims, the principal objectives of this research are:
- Evaluating the influence of different material parameters as polymer type, crosslinking density, carbon black filler type, antioxidant and co-agent on the material aging sensitivity by performing stress relaxation measurements
- Introducing a common index called characteristic aging time constant and the aging activation energy in order to quantify the material aging sensitivity
- Identifying and developing characterization methods to characterize the material structure changes during aging
- Establishing a correlation between the results derived by the different methods and the stress relaxation behavior
- Deriving a model description of the aging process

1.3 Scientific approach

In order to achieve a comprehensive understanding of the complex mechanism on the stress relaxation of rubber, this research is conducted following the scheme as shown in Fig.1.1.

This thesis starts from the review of the fundamentals of the rubber elasticity, the detailed description of EPDM as the used polymer and the description of crosslinking mechanism in Chapter 2.

The stress relaxation theory and the processes taking place during stress relaxation are discussed in depth in Chapter 3.

The influential factors of aging mechanism regarding environment ,main material and ingredients in this work are discussed in Chapter 4. (e.g temperature, oxygen, deformation, EPDM polymer, peroxide crosslink agent, carbon black, antioxidant and co-agent.)

Novel characterization methods, which have been developed during this thesis in order to evaluate the material structural changes, are introduced in Chapter 5. The basic theories of these characterization methods are reviewed here.

Chapter 6 contains the experimental part, the description of the applied equipment as well as the materials and method parameters used in this research. The results are summarized and discussed in Chapter 7.Chapter 8 and 9 contain the summary and final conclusion as well as the proposal of further research to be conducted.

Theoretical aspects   Aging mechanism of rubber

Chain mobility analysis   Physical test   Chemical analysis
NMR   Correlation   Stress relaxation   Correlation   Chemiluminescense

characterization   characterization

Crosslink structurer ,chemical structural change

Material and experimental method

Experiment

Method development
Crosslink structural analysis using NMR with ILT   Correlation

Mechanism   Material parameters investigation   Characteristic
Crosslink ,Filler ,Antioxidant, micro structure of polymer   aging time constant

Method development   Physical test
NMR and Chemiluminescence under stress condition   Stress relaxation

Mechanism   Environmental factor investigation   Activation energy
Stress(Static deformation)
Correlation

Fig.1.1: Strategy of this study

Chapter 2

Theory of rubber elasticity and crosslinking

<u>2.1 Rubber elasticity</u>

"Elastomer" is a coined word of elastic-polymer [15]. "Rubber" can be defined as a polymer which has "rubber elasticity". Rubber elasticity is originated from the polymer chain in a crosslinked network acting as an entropic spring. This elasticity possesses several characteristic features [16].

1) Rubbers deform under the application of relatively small force, in other words, they have a comparable small Young´s modulus (1-3 MPa) in comparison with other materials (e.g. Steel: 10^6 MPa).

2) Rubbers can deform to a large extend (in case of usual unfilled rubber, 500-1000 % of their original length) and recover to the initial dimension after releasing the applied deformation reversibly. Vice versa, materials such as metals can deform with high stress but the elastic limit is under 1%. Besides that, high deformation of metals leads to plastic deformation (permanent deformation) which is irreversible, they will not return to their original shape.

3) Rubbers are designed as polymers having a glass transition temperature (Tg) under 0°C [17]. Tg is the temperature at which a polymer turns from soft to hard or brittle materials. Each polymer with an amorphous structure has its own unique glass transition temperature.

In sum, rubbers are possible to deform largely with small force but recover to original shape reversibly over 0°C. Therefore, rubber is suitable for seals and its rubber elasticity is the most important parameter making rubber so valuable for the sealing industry.

For a further understanding of rubber elasticity, Fig.2.1 shows a microscopic view of the non-stretched and stretched thermodynamics condition of the crosslinked rubber network. In Fig.2.1, lines show the polymer entanglements and blue dot show crosslink points.
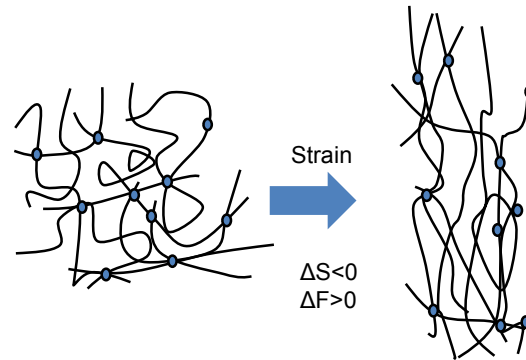
Fig.2.1: The model of unstretched and stretched rubber network

An un-crosslinked network can be described as an ensemble of long-chain molecules which are entangled. Polymer chain entanglements which are developed by the polymeric random-coil chains cause visco-elasticity [18, 19, 20]. Considering practical applications for industry, un-crosslinked rubber cannot maintain its original shape following a large deformation or high forces. Therefore, "crosslinking" is essential. Crosslinking is incorporating a number of intermolecular chemical bonds between polymer molecules to obtain a loose three-dimensional molecular network from an un-crosslinked rubber structure. As a result of crosslinking, crosslinked material obtains rubber elasticity.

The rubber elasticity can be understood with molecular chains through the thermodynamics theory. It is possible to describe the relationship between the temperature T, the internal energy U and the thermodynamic parameter entropy S with the Helmholtz free energy F by the following relation.

$$F = U - TS \quad (2.1)$$

The unstretched condition can be written as:

$$F_u = U - TS_u \quad (2.2)$$

Besides, the stretched condition can be described as:

$$F_s = U - TS_s \quad (2.3)$$

The difference of the Helmholtz Free Energy *F* between unstretched and stretched state can be described as:

$$\Delta F = -T(S_s - S_u) = -T\Delta S, \ \Delta S < 0, \Delta F > 0 \ (2.4)$$

Due to stretching of the molecular chain the number of possible conformations the chain can arrange itself are reduced .This results in a reduction of the entropy $\Delta S < 0$, and an increase in the Helmholtz Free Energy $\Delta F > 0$. The magnitude of the kinetic tensile force can be calculated from the following thermodynamic equation.

$$f = -\left(\frac{\partial F}{\partial l}\right)_T = -T\left(\frac{\partial S}{\partial l}\right)_T, \left(\frac{\partial S}{\partial l}\right)_T < 0, f < 0 \ (2.5)$$

Therefore, a negative *f* means a restoring force of moving back to the unstretched length, in other words, the polymer chain returns to its equilibrium of the unstretched state as the high entropy random coil configuration, after the external force is removed. Due to this mechanism, rubber elasticity is also called "entropy elasticity".

2.2 Industrial rubbers for sealing applications

The first "rubber" was obtained from a natural latex out of the tree Hevea brasiliensis, and is called natural rubber (NR). The more expressive term is "caoutchouc" from the Maya Indian words meaning "weeping wood". Originally, the word "rubber" was derived from the ability to remove marks on paper to erase (rub off) .This was named by the chemist John Priestley in 1770 [21]. Afterwards, In 1839, when the vulcanization was discovered by Charles Good year, the natural rubber was applied broadly to various industrial products.

However, currently, the term "rubber" is not restricted to the original NR, but is applied for all base rubber regardless of their chemical constitution. In the early 20th century, chemists have developed synthetic routes to synthesize materials whose properties imitate those of natural rubber. The remarkable progress in organic chemistry contributed to generate a large number of polymers with rubber elasticity. They are classified by their chemical structure according to DIN ISO 1629. The classification of the rubbers is shown in Table 2.1. These synthetic polymers in table have been important for the sealing applications because they have a high thermal stability and good chemical resistance.

Table2.1:Typical type of rubbers for sealing applications

Group	Type of rubber	Name
R Un-saturated backbone	BR	Butadiene rubber
	NR	Natural rubber
	SBR	Styrene-butadiene rubber
	NBR	Nitrile-butadiene rubber
	HNBR	Hydrogenated NBR rubber
	CR	Chloroprene rubber
	IIR	Butyl rubber
M Saturated back bone	EPM	Ethylene-propylene rubber
	EPDM	Ethylene-propylene-terpolymer
	ACM	Alkyl acrylate rubber
	FKM	Fluoroelastomers
U Back bone contains urethane functional group	EU	Urethane rubber
Q Backbone contains silicone	VMQ	Silicone rubber

2.3 EPDM (Ethylene-propylene-terpolymer)

2.3.1 Chemical structure

Ethylene-Propylene rubbers are a family of synthetic rubbers that are prepared by polymerization of ethylene, propylene and optionally, a diene. Unlike the majority of synthetic rubbers, these polymers contain a saturated back bone. Therefore, they are classified as type M (saturated backbone). Moreover, they are classed into two: Ethylene-Propylene copolymer (EPM) and Ethylene-Propylene-Diene terpolymer (EPDM). Originally, first synthesis of EPM was conducted by G. Natta in 1950s [22]. However, in order to obtain the adequate elastic properties, EPM needs to be crosslinked using peroxide. Peroxide crosslinking was not widely accepted in the rubber industry at that time. To enable the use of sulfur crosslinking, a diene was synthesized with ethylene and propylene as the third monomer. This functional monomer made it possible to vulcanize with sulfur. So EPDM consists of ethylene, propylene and diene monomers (Fig.2.2)
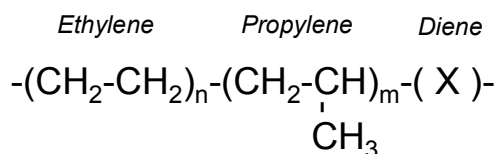
Ethylene   Propylene   Diene

$$-(CH_2\text{-}CH_2)_n\text{-}(CH_2\text{-}CH)_m\text{-}(\,X\,)\text{-}$$
$$CH_3$$

Fig.2.2: Chemical structure of EPDM and diene (ENB,VNB and DCPD)

As diene ter-monomers ENB (Ethylidene norbonene), VNB (Vinilidene norbonene) and DCPD (Dicyclopentadiene) are available in the market. In this research, ENB as the most common type of diene is chosen (Fig.2.3).

Ethylidene norbornene(ENB)   Vinylidene norbornene(VNB)   Dicyclopentadiene (DCPD)
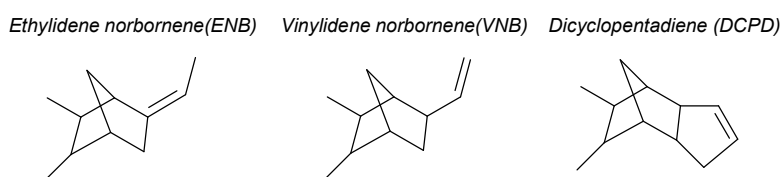
Fig.2.3: Chemical structure of diene (ENB,VNB and DCPD)

2.3.2 Physical properties

Until now, the development of EPDM polymer and improvement of resulting physical properties have been continuous demands by the automotive industry. The relationship between typical properties and structure is shown in Table 2.2 [22] [23].

Table 2.2. :Typical relationship between structure and properties

	Pros	Cons
Higher ethylene	Better physical property Higher resistance to thermal oxidation	Poorer low temperature behavior Poorer processability (higher viscosity)
Higher molecular weight	Better physical property	Poorer processability (higher viscosity)
Higher diene	Better physical property	

Normally the ethylene content of most grades are available range from 40 to 80wt%. At higher ethylene contents such as 60 to 70 wt.% of ethylene partial crystalline domains are formed.

The presence of the ethylene units increases the chain packing which leads to crystallinity. The partial crystalline domains form thermally reversible physical crosslinks as in thermoplastic elastomers. Above 85wt% of ethylene content leads to enough crystallinity to be treated as plastics. Higher ethylene contents have the advantage of higher tensile strength, tear strength, hardness, abrasion resistance and better thermal oxidation resistance due to fewer tertiary hydrogen of propylene which can be attacked by radicals (detail discussion is in chapter 4). Disadvantages are poor mixing at lower temperature and poor low temperature property (higher Tg).

The type of diene influences the speed and efficiency of crosslinking reactions. The VNB and ENB base EPDM have much faster cure rate in comparison with DCPD. An increase of the diene level results in higher efficient crosslinking, higher modulus, higher lower compression set. Moreover, the physical properties of EPDM are greatly affected by molecular weight and molecular distribution. For instance, higher molecular weight molecular provides higher hot green strength for extruding and shaping. Besides that, the properties of crosslinked rubber show higher tear and tensile strength both at room and elevated temperature and lower compression set [23]. However, there are disadvantages, for instance the poor processability due to the high viscosity. In order to improve processability, broad molecular weight distribution can be installed. Broader distribution provides better processability of EPDM but physical property gets worse. Therefore, in reality a fair compromise between processability and physical property is achieved. The control of chain branching could be another solution to balance the physical properties and the processability.

2.4 Crosslinking

As discussed in the previous section, crosslinking is necessary to obtain rubber elasticity. From the point of view of micro rubber structure, as a result of introducing chemical crosslinks, several types of the network junctions are generated as seen in Fig 2.4 :(1) Temporary entanglements, (2) Trapped entanglements, (3) Crosslinks (4) Free chain ends (5) Chain loops.

(1) Temporary entanglement

(4) Free chain end

(5) Chain loop

(3) Crosslink

(2) Trapped entanglement
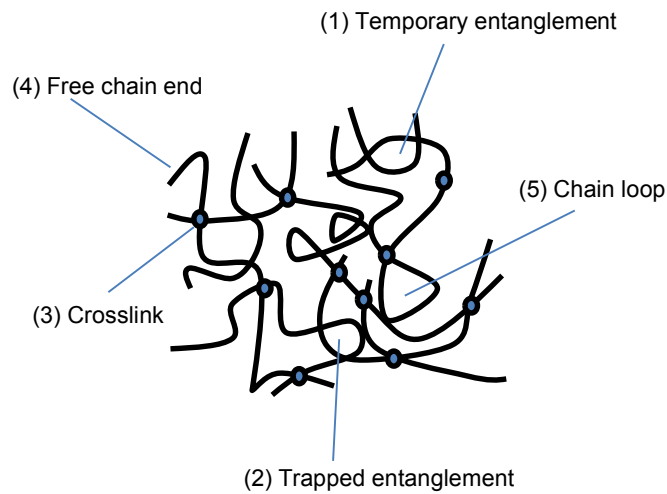
Fig.2.4: Assumed crosslinked network structure

In other words, the assumed rubber network can be divided into two categories. The category of network phase which contains temporary and trapped entanglements and chemical crosslink contributes to rubber elasticity. Conversely, the non-network phase which contains chain ends and chain loops does not contribute to the elasticity.

Crosslink provides significant improvement of physical property. As the one of the examples, Fig.2.5 shows the temperature dependency of relaxation modulus of uncrosslinked and crosslinked rubber.

Relaxation modulus

Glassy state

Glass transition

Rubbery state

C

A

B

Temperature

Fig.2.5: Relaxation modulus; A: Uncrosslinked rubber with low molecular weight, B:Uncrosslinked rubber with high molecular weight, C:Crosslinked rubber

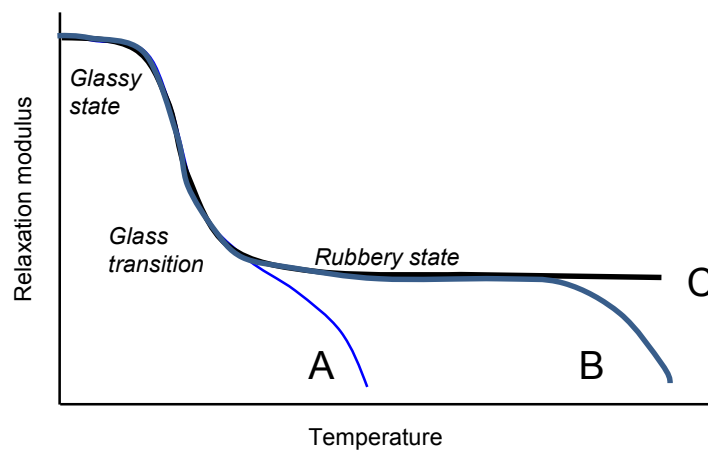When measuring the modulus of uncrosslinked rubber above Tg, the characteristic "rubbery plateau" can be observed. The length of this plateau depends on the number of entanglement. However, the modulus decreases at the certain high temperature because of flow of molecule. Vice versa, in a case of crosslinked rubber, flow of molecular doesn't occur. Because a crosslinked network will maintain its shape and prevent single molecule from slipping off one another (the flow or relaxation due to dentanglements).

In order to apply sealing materials in the field, seals are required to prevent from flow and maintain the shape under the wide range of temperature. From this reason as well as gaining rubber elasticity, crosslinking is important for sealing rubber materials.

Thus the crosslink property is the most critical on the sealing application and should be quantified with the appropriate index which is called "crosslink density". Saville described the correlation between two definitions of crosslink density and network structure [24]. For a rubber network, which has infinite molecular weight due to the chemical crosslinking, the moles of crosslinks per unit volume (mol/cm^3) can be directly associated with the number of network chains per unit volume (g/cm^3).

2.5 Sulfur crosslinking

Chemically, there are several additives available which are able to insert crosslinks in polymer networks. The first developed crosslinking system is the "sulfur crosslink", which is still important and in several cases irreplaceable with other crosslink systems. Sulfur can react with unsaturated double bonds of the polymer chain, such as NR, NBR, SBR and EPDM. The expected mechanism of Sulfur vulcanization of EPDM is shown in Fig.2.6 [25]
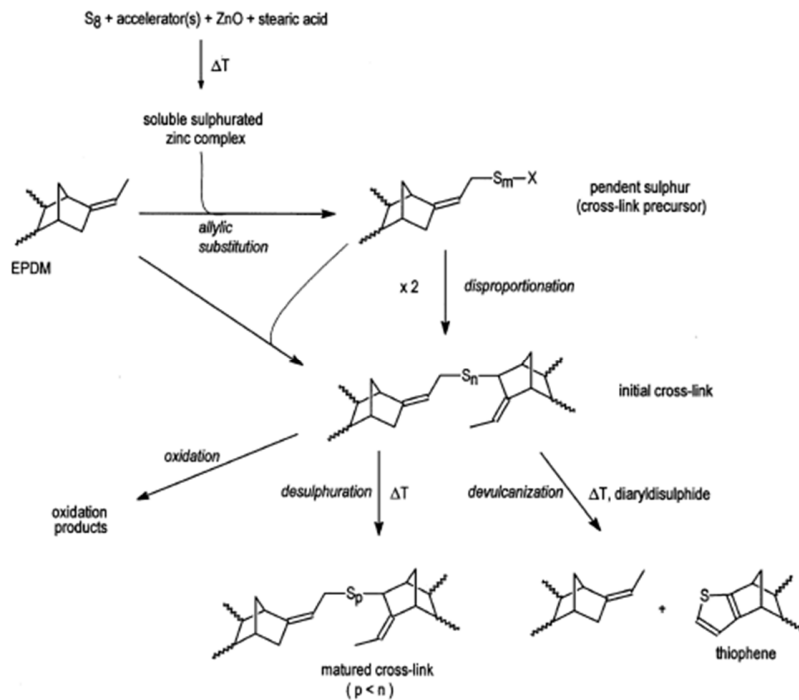
Fig.2.6: Mechanism of Sulfur crosslinking [25]

The reaction scheme consists of the following steps:

1) Sulfur vulcanization of elastomers starts in the presence of activators (ZnO and stearic acid) and accelerators such as MBT (2-Mercaptobenzothiazole), TMTD (Tetramethyl thiruam disulfide), ZDMC (Zinc dithiocarbamate) etc.
2) The substitution of the labile allylic H-atoms by sulfur bridges yields alkenyl sulfides.
3) The actual sulfur crosslinks are formed as initial crosslink. At the last of sulfur crosslinking reaction, the crosslink chain consists of a group of sulfur atoms. The type of sulfur chain can be predominated as the mono, di- and poly-sulfuric. In addition, In order to produce more efficient crosslink, accelerator can be adopted to the rubber formulation.

However, crosslinking with peroxides has been used for sealing applications more than crosslinking with sulfur. The reason lies in the lower stability of the C-S bond and S-S bond versus the C-C bonds as shown in Table 2.3 [26]. Therefore sulfur crosslinked materials have less heat resistance than peroxide crosslinked materials. For this reason, the long term properties like stress relaxation and compression set of peroxided materials are usually superior to that of sulfur crosslinked materials.

Table.2.3: Binding energy of chemical bonds [26]

Typr of chemical bond	Chemical formula	Bonding energy, kJ/mol
Polysulfidic	- C - S_x - C -(x > 3)	< 270
Disulfidic	- C - S_2 - C -	270
Monosulfidic	- C - S - C -	272
Carbon-Carbon	- C - C -	346

2.6 Peroxide crosslinking

Peroxides are a group of compounds with the structure R−O−O−R group. M. van Duin described the peroxide crosslinking reaction mechanism of EPDM polymer [25] as depicted in Fig.2.7.

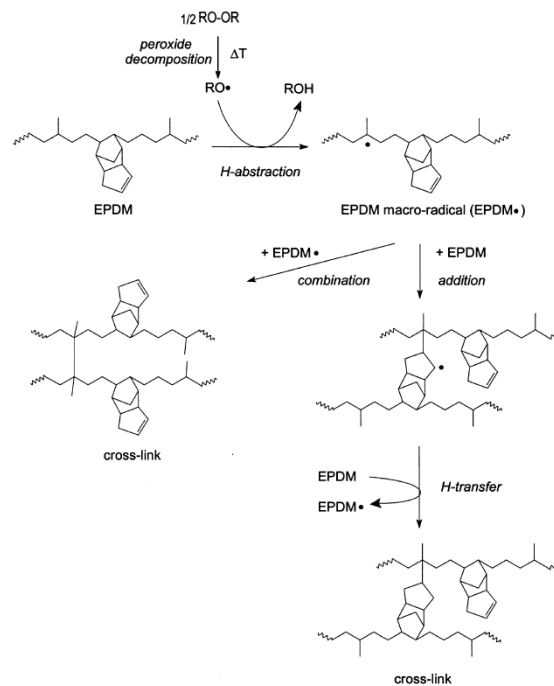Fig.2.7: Reaction scheme of peroxide crosslinking of EPDM [25]

The reaction scheme consists of the following steps:

1) Thermal decomposition of peroxides generates free radicals.
2) Free radicals abstract H-atoms from polymer chains and generate macro radicals.
3) Peroxides react with other polymer chains and abstract atoms from the carbon backbone of the polymer.

4) Two macro-radicals combine and form a crosslink. This crosslink consists of C-C bonds.

Theoretically, a peroxide molecule creates one crosslink; however, it is normally lower than theoretical expectation in practice due to the undesirable side reactions, which consume radicals [27]. For instance, if oxygen molecules are present during the crosslinking they can couple to the radical in the polymer backbone to yield a hydroperoxide radical, which leads to chain scissions instead of crosslinking. Because of this, peroxide crosslinking must always be performed in the absence of oxygen. Other non-productive, and therefore undesirable, side reactions that can occur to the polymer radical are chain scission as shown in Fig.2.8.
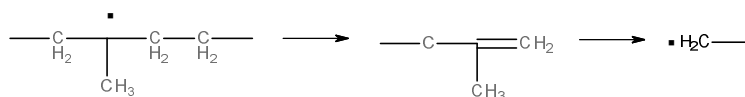

Fig.2.8: Chain scission reaction as side reaction of peroxide crosslinking

2.7 Co-agent

Co-agents are multi-functional organic molecules which are highly reactive towards free radicals [28]. They are used as reactive additives which can reduce boost peroxide crosslinking efficiency [29]

Co-agents can improve the peroxide crosslink efficiency by the reduction of inefficient side reactions to a large extent, like chain scission as reported in literature [27].

There are a lot of functional chemicals that have been used as co-agents for peroxide crosslink. Typical co-agents are shown in Fig.2.9. In this research the investigations are conducted using TAIC (Triallyl Isocyanurate) as one of major co-agents for peroxide crosslinked rubbers.
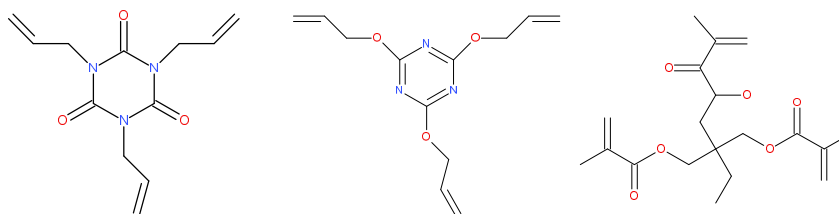
Fig.2.9: Typical co-agent ,Left: TAIC(Triallyl Isocyanurate),Center :TAC(Triallyl cyanurate), Right :TMTP (Trimethylol propane trimethacrylate)

In sum, since co-agent can reduce the chain scission as the side reaction of crosslinking, which leads a poor physical property, synergistic use of multifunctional co-agents with peroxide crosslink agent is efficient. Co-agent achieves an improvement of the rubber properties and avoiding the initiation of thermal oxidation with free radicals [30, 31].

Chapter 3

Theory of stress relaxation

3.1 Stress relaxation of seal

Tobolsky deduced following theoretical equation which describes the reaction force, $f_{(0)}$ of rubber as a function of the deformation with neo Hooke´s elastic model [32].

$$f_{(0)} = n_{(0)}RT\left[\alpha^2 - \left(\frac{1}{\alpha}\right)\right] \qquad (3.1)$$

Where $f_{(0)}$ is force, $n_{(0)}$ is the crosslink density, as moles of network chains per cubic centimeter of the original network, at time zero, T is temperature and α is the stretching ratio (stretched length/ unstretched length). As shown equation (3.1), the reaction force has a proportion to crosslink density.

On the other hand, static sealing mechanism of rubber can be described as shown in Fig.3.1.
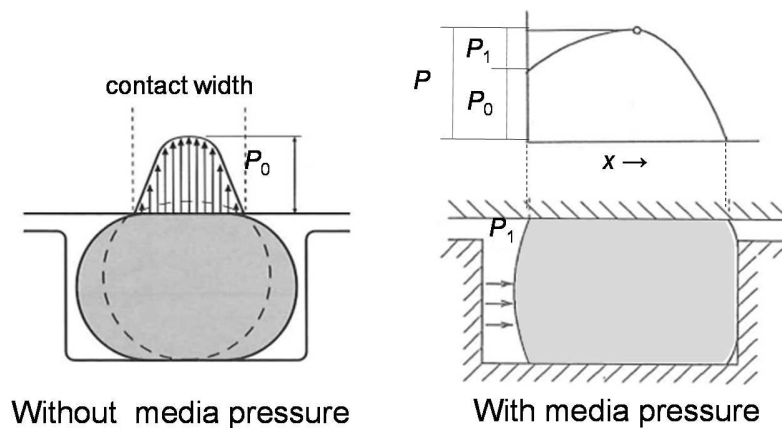

Fig.3.1: Schematic diagram of the sealing condition

Contact pressure of the material P_0 of static seals, based on the elasticity, generated by compression (as shown in Fig.3.1 left).

When the media pressure is applied (as shown in Fig.3.1 right). a seal is squeezed to a groove face due to the media pressure and sealing surface gains the additional pressure P_1. Contact

pressure with media becomes the sum of P $(P_0 + P_1)$. However, this contact pressure, P gradually decreases as a function of time due to stress relaxation.

There are physical as well as chemical causes for stress relaxation. Those are called "physical relaxation" and "chemical relaxation". In the practical situation, they can occur simultaneously and contribute to the complex aging process and can be difficult to divide. [33]

On the other hand, the mechanisms of stress relaxation of sealing materials can be explained by the change of the rubber structure. Fig.3.2. gives an overview of the stress relaxation and following permanent set of rubber, taking into special account chemical changes occurring in combination with mechanical stress and thermal oxidation.
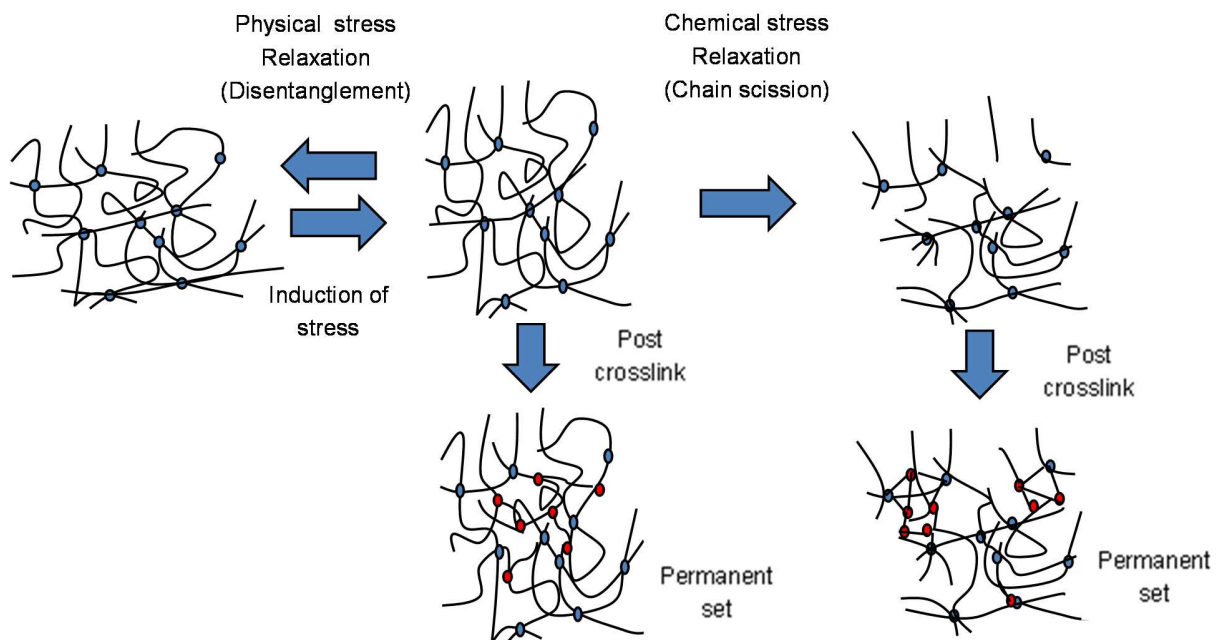
Fig.3.2:The rubber structural change during the aging process [34]

Physical relaxation takes place due to the deformation reversibly without any destruction of rubber network structure. However, in the practical condition, sever environmental parameters derives chemical relaxation with irreversible chemical changes in the rubber network structure. In particular, when rubber samples exposed to air (oxygen) experience at high temperatures, thermal decomposition or thermal oxidation can occur. Then upon removal of the stress the rubber specimen is incapable of returning to its initial state, and the phenomenon referred to as

"permanent set". This is due mainly to a change in the network structure during deformation. Tobolsky's two network theory describes the mechanism of permanent set taking into consideration structural changes [35, 36]. The original network structure is said to degenerate due to polymer chain scission, with new crosslink structures formed via radical reactions occurring during deformation.

3.2 Physical stress relaxation

The fundamental theory of "physical relaxation" was established by Eyring and Tobolsky [37] From their theory, if the network structure is not destroyed as a function of time, stress changes with the physical reasons such as chain disentanglement and the rearrangement of the chains of cross link and chain ends. Besides, this physical relaxation behavior is based on visco-elastic equation as below.

$$\frac{d\varepsilon}{dt} = \frac{1}{\gamma}\frac{dS}{dt} + A \sinh B\, S \quad (3.2)$$

Where t is time, ε is strain, S is stress and γ is elasticity of material. A and B are constants which are decided along rubber structure and temperature. Therefore, physical relaxation depends on time as well as the mobility of the polymer and has temperature dependent properties.

The mobility of polymer can be correlated to crosslink density of a rubber so that it determines the rate of physical relaxation. Normally, increasing crosslink density leads to a decreasing of the physical relaxation rate due to the reduction of temporary entanglements [38] as shown in Fig.2.4.

In addition, it is well known as an experimental fact that physical stress relaxation process can be described with the logarithmic decay as a function of time. [39, 40] Besides, K. Murakami delivered theoretically same equation from the equation (3.2) [41].

$$\frac{f_{(t)}}{f_{(0)}} = \alpha - \beta \log t \quad (3.3)$$

Where $f(t)$ is time at the certain time after a start of test, α and β are the constant which depends on the network structure (crosslink density) and temperature. This equation is based on the assumption that there is no destructive change of network as a function time. However, in the practical condition, a thermal oxidation can cause the network destruction such as chain

scissions. Therefore, chemical relaxation often predominated and physical relaxation can be observed in air within the short aging time, N_2 atmosphere or vacuum condition.

Furthermore, in terms of the filled material, filler gives an additional mechanism to associate with the breaking and rearrangement of bonds due to secondary valence forces between filler particles (filler network) or between polymer chains and filler particles (polymer-filler interaction). The stress relaxation mechanism of the filled materials is therefore more complicated to describe than that of unfilled rubber.

3.3 Chemical stress relaxation

At higher temperature and longer time with exposing air, chemical relaxation usually predominates over physical relaxation. As mentioned above, the main mechanisms which cause chemical relaxation are thermal decomposition or thermal oxidation. These aging processes can be attributed to the rubber structural change such as the scission of the polymer chains or thermal breakage of crosslinks and chains. As reaction force and crosslink density is in proportion as seen equation(3.1), Tobolsky described the relationship between relative force and crosslink density along time.

$$\frac{f_{(t)}}{f_{(0)}} = \frac{n_{(t)}}{n_{(0)}} \qquad (3.4)$$

Where $f(0)$ is the stress at time zero ,$f(t)$ is the stress at certain aging time, $n(t)$ is the moles of crosslink density (network chains per cubic centimeter) of the original network at the time t. Chain scissions decrease the density of the network and produce new dangling ends, while releasing force (chemical stress relaxation).

In addition, Tobolsky and Murakami describe this chemical stress relaxation with exponential equation as below.

$$\frac{f_{(t)}}{f_{(0)}} = \exp(-kt) \qquad (3.5)$$

Where k is the constant which represents chemical stress relaxation rate. This implies that measuring the stress relaxation enable to observe the change of crosslink density of original network due to chain scissions.

Moreover, this *k* can show a temperature dependence that complies with the Arrhenius equation [42].

$$k = A \, exp(-\frac{E_{act}}{RT}) \qquad (3.6)$$

Where *A* is the frequency factor, *R* is the gas constant, *T* is the absolute temperature and E_{act} is activation energy. Murakami shows the temperature dependency of stress relaxation of NR and showed activation energy [41]. Although stress relaxation is the simple physical test method, this activation energy provides quite useful information to estimate the mechanism of chemical degradation.

3.4 Separation technique between physical and chemical stress relaxation

As the discussion above, in the practical condition, the regression of the stress in air is determined by the physical and chemical relaxations which take place simultaneously. In order to distinguish physical and chemical relaxations, several approaches have been proposed [43, 44, 45, 46, 47]. For example, T. Kusano proposed an approach to fit the relaxation curve with the combination of exponential and logarithmic functions in order to resolve physical and chemical relaxations. [47]. Recently, S.Ronan introduced a unique separation technique of two relaxations which is derived from the numerical analysis [45].

In this research, an approach proposed by Murakami is adapted to separate physical and chemical relaxation [41]. An advantage of this method is the simple experiment to compare the stress relaxation curve in N_2 atmosphere with that in air (oxygen) [48]. The stress relaxation in N_2 can be interpreted as only physical relaxation due to chain disentanglement. Relaxation in air can be understood as a combination of chemical and physical relaxations. The additional chemical relaxation takes place due to the chain scissions of crosslink networks. The schematic diagram in Fig.3.3 shows this approach for distinguishing the different influences on stress relaxation.
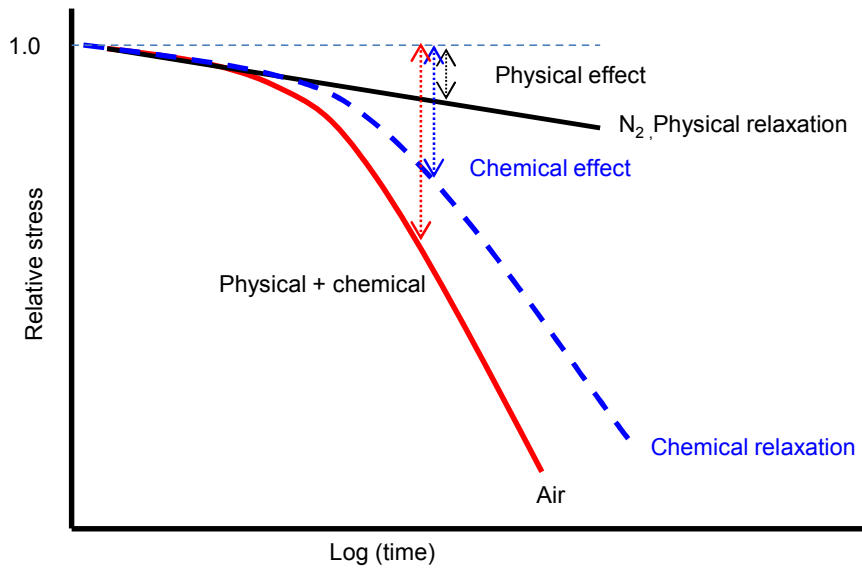
Fig.3.3: Schematic diagram for separating physical and chemical relaxation

Chapter 4

Theory of aging process of rubber

4.1 Influential factors on aging mechanism

Environmental factors as shown in Fig.4.1; such as high temperature, air, water, ozone and others cause irreversible structural changes of rubber network which results in physical and chemical stress relaxation. In this study, temperature, oxygen, and mechanical load were the considerable factors. Besides, the recipe of rubber material can influence on the stress relaxation behavior. The major influential parameters such as EPDM polymer composition (Ethylene content), carbon black filler, antioxidants and co-agent were considered. These factors were highly related to the thermal oxidation process and an understanding of these factors is essential to estimate the mechanism of stress relaxation.
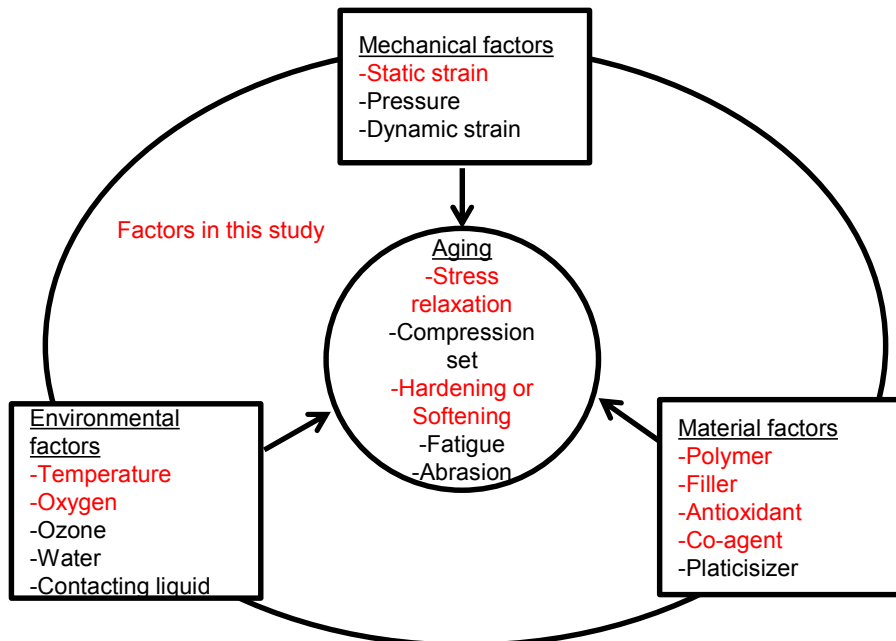

Fig.4.1: The influential factors of aging in this study

4.2 Thermal oxidation process

The thermal oxidation predominates in the mechanism of chemical relaxation because the sealing application operates usually at high temperature in air.

The thermal oxidation can be described as sequential chemical reactions called "auto-oxidation". In general, the contribution reactions can be divided into three stages: (1) initiation (2) propagation, and (3) termination [49, 50, 51, 52, 53, 54].

At the (1) initiation step environmental factors such as temperature, light, strain and chemical attack lead to the formation of free radicals.

The initiated free radical reacts with O_2 and produces a peroxylradical.

$$RH \rightarrow R\cdot \; + \; H\cdot$$
$$R\cdot \; + \; O_2 \; \rightarrow \; ROO\cdot$$
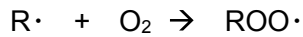
At the (2) propagation step, the peroxyl radical abstracts a hydrogen atom from another polymer chain and generates a hydroperoxide and free radical on a polymer chain.

$$ROO\cdot + R'H\cdot \rightarrow ROOH + R'\cdot$$
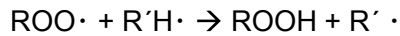
Single or double hydroperoxide decompose to radicals.

$$ROOH \; \rightarrow \; RO\cdot + \cdot OH$$
$$ROOH + R'OOH \rightarrow RO\cdot + R'OO\cdot + H_2O$$

Generated radicals react as below. This process is same as initiation step.

$$RO\cdot + R'H \rightarrow ROH + R'\cdot$$
$$R'\cdot + O_2 \rightarrow R'OO\cdot$$
$$R'OO\cdot + R'H \; \rightarrow R'OOH + R"\cdot$$
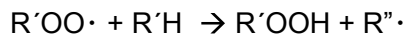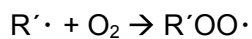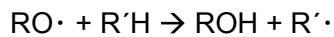
At (3) termination step (the reaction ends), free radicals combine their odd electrons to each other and a new bond is formed.

$$R\cdot + R'\cdot \rightarrow RR'$$
$$ROO\cdot + ROO\cdot \rightarrow ROOR + O_2$$
$$ROOR \rightarrow 2R=O$$
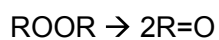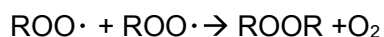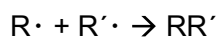
These reactions can be summarized as shown in Fig.4.2. This figure shows not only auto-oxidation, but also chemiluminescence processes (this will be discussed at Chapter 5)

Fig.4.2: Auto-oxidation and two major processes of chemiluminescence on the oxidation of polymer

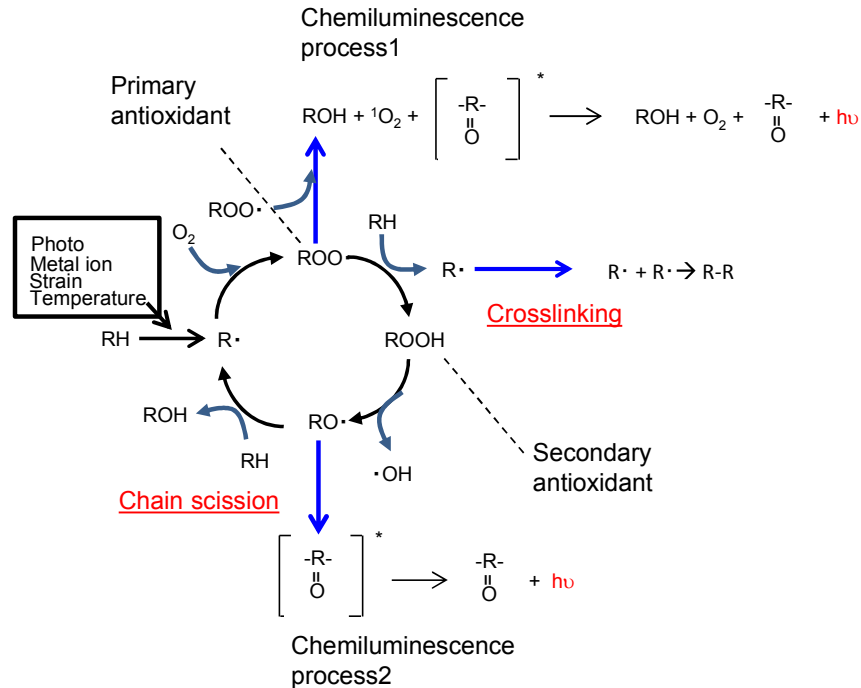The mechanism of the chemical stress relaxation and permanent set can be related to this auto-oxidation. The propagation leads chain scissions of network attributed to chemical stress relaxation. And termination reaction forms new bonds (crosslinking) attributed to permanent set.

The two reactions, chain scissions and crosslinking, compete with each other depending on the polymer structure and on the environmental parameters like oxygen, light, strain and temperature. Macroscopically the different reactions result in the rubber becoming brittle (in case that crosslinking dominates) or soft and sticky (in case that chain scission dominates).

4.3 Thermal oxidation under stress

As discussion above, temperature and oxygen are predominating factors of stress relaxation of seals. Since seals are always used in the deformed state and so it is necessary to consider the effect of the deformation as well. The general theory of thermal oxidation under the deformation was proposed by Zhukov [55]. He proposed that the activation energy decreases as

a result of the stress induced. The activation energy for chain scissions was the sum of the thermal and mechanical energy.

$$k = A \times \exp\left[-(E - a\sigma)/RT\right] \qquad (4.1)$$

Here σ is the stress and a is a structural coefficient which defines the actual stress level. Zhurkov claimed that the micro process of polymer fracture proceeds in three stages:

1) Deformation at covalent bonds decreases the necessary energy for covalent bond scission.

2) Scissions of the strained bonds generate chemically active free radicals

3) Nucleation of sub micro cracks occurs as a result of the scission of bonds.

Furthermore, his theory has been seriously disputed by Czerny, Kausch, Peterlin and others as Zhurkov overserved the creep of polymer to validate his theory [56, 57, 58, 59, 60]. For instance, Czerny studied the effect of tensile stress on thermos oxidation and photo oxidation of polypropylene. According to his conclusion, the oxidation rate is accelerated by tensile stress and this fact was validated by means of the weight loss, crack propagation and embrittlement time [60]. In contradiction with Zhurlov´s theory, Lemair et al concluded that the oxidation rate during thermos and photo doesn't depend on the mechanical stress [61]. Meanwhile, Calvert concluded the effect of stress on the local deformation of the bond and chain scission was not clear [62].

In order to get a better understanding, the direct observation method on thermal oxidation process is necessary to develop. Recently, some researchers have investigated to take into account of chemical reaction using chemiluminescence under strain. However, these investigations focused on the duromers and thermo-plastics such as polyamide, polypropylene and epoxy resin [63, 64]. This work validates the effect of stress in presence of oxygen on crosslinked EPDM rubber using chemiluminescence. This derives a further understanding the mechanism of stress relaxation with the rubber structural change due to thermal oxidation.

4.4 Influential material parameters

4.4.1 Ethylene propylene content of EPDM

EPDM has the outstanding resistance against weather, heat and ozone compared to BR, IR, and SBR. Because EPDM rubbers have no double bonds in the backbone of the polymer chains they are less sensitive to oxygen. Other excellent properties are high resistance against water, acid and alkali, non‐conductance of electricity. These are resulted by non-polar component monomers such as ethylene and propylene.

Considering the resistance of EPDM rubbers against thermal oxidation, it varies depending on the ethylene and propylene ratio, as well as on the amount and type of diene [65]. Especially, the composition variation of Ethylene/Polypropylene could greatly affect the degradation characteristics and aging speed [66, 67].

One of the systematic studies of the effects of composition and microstructure on the long-term properties was performed by C. Gamlina et al. [68]. They evaluated the activation energy of EPDM varying the content of Ethylene and propylene by means of TGA (Thermal Gravimetric Analysis). They concluded higher content of Ethylene led to higher activation energy against thermal oxidation.

This can be explained with the bonding energy of C-H which depends on the chemical structure. At the initiation step, as shown in Fig.4.2 free radicals generate form the polymer. The frequency of this reaction can be associated with the bonding energy of chemical structure as shown in Table 4.1.

Table.4.1: Bonding energy

Structure	Bonding energy, kJ/mol
H-CH$_3$	435
H-CH$_2$CH$_3$	410
CH$_3$ H-C-CH$_3$ H	401
CH$_3$ H-C-CH$_3$ CH$_3$	389

The propylene hydrogen is easier to abstract than ethylene hydrogen by thermal, light, strain and etc. This is the chemical reason for a higher ethylene amount delivering more stability against thermal oxidation of EPDM.

4.4.2 Effect of antioxidant on thermal oxidation

As described above, the thermal oxidation is based on radical reactions. Practically, antioxidants are often used as radical scavengers or inhibitors to extend the life time of rubbers. [69, 70] Usually, antioxidants can be categorized into two groups, which are called primary and secondary antioxidants as shown in Fig. 4.3 [71].

PH : Polymer of rubber, $A_{Pri}H$: Primary antioxidant, A_{Sec} : Secondary Antioxidant
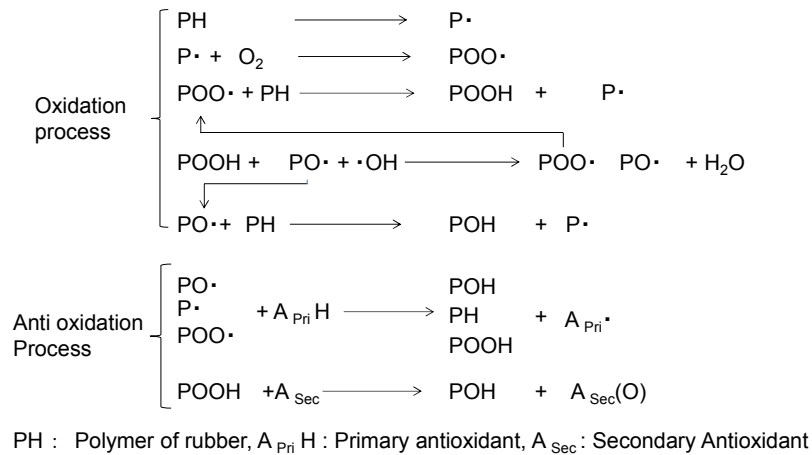
Fig. 4.3 :Scheme of oxidation reaction and anti-oxidation process [71]

The chemical structures of typical primary and secondary antioxidants are shown as in Fig.4.4. [72].
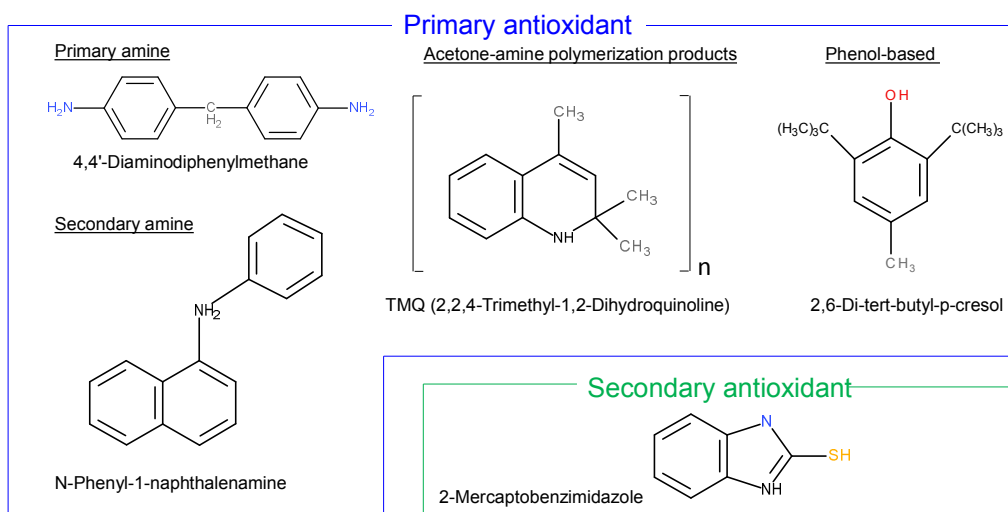
Fig.4.4: Chemical structure of antioxidant [72]

Primary antioxidants act as radical scavengers and stop the propagation of the reaction chain in oxidation of polymer. The principle is that the peroxylradical abstracts a hydrogen atom from antioxidant and results in a stable product instead of the abstraction of a hydrogen atom from a polymer chain [73, 74].

Secondary antioxidants like thioethers react directly to the decomposition of the hydroperoxide [75, 76]

Antioxidants provides a significant improvement of the stability against thermal oxidation and deaccelerate chemical relaxation. [77, 78]

However, peroxide crosslinking systems require special attention as to the selection of antioxidants. Several types of antioxidants detract crosslinking efficiency. Because free radicals produced by peroxides crosslink agent can react with antioxidants. In other words, antioxidant can scavenge free-radicals and therefore hinder peroxide crosslinking. This undesirable reaction can cause the lower crosslink density of materials below the expectation. In this research the investigations are conducted on TMQ (2,2,4-Trimethyl-1,2-Dihydroquinoline polymer) as one of the possible antioxidants in peroxide crosslinked rubbers [79].

4.4.3 Effect of carbon black

Carbon black is a generic term for an important family of products used principally for the reinforcement of rubber, as a black pigment, and for its electrically conductive properties [80]. It is a powder with extreme fineness and high surface area. Carbon black is one of the most stable

chemical products. In a general sense, it is the most widely used nano-material with its aggregate dimension ranging from tens to a few hundred nanometers (nm) .The structure of carbon black is schematically shown in Fig. 4.5.
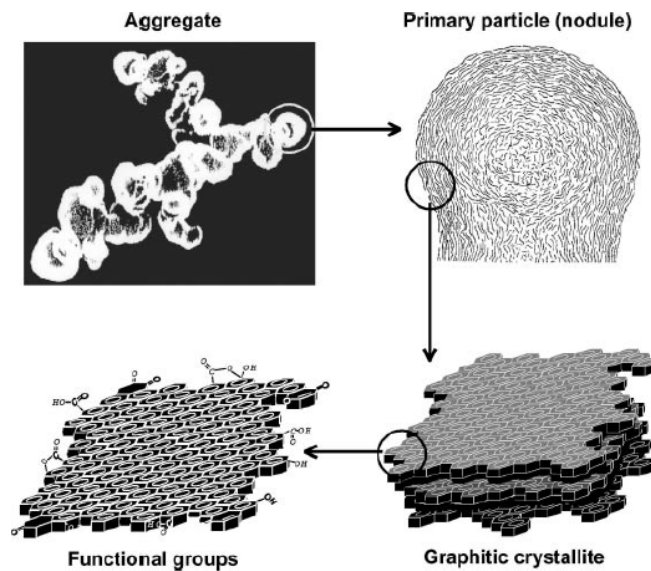

Fig.4.5 : Model of the morphology of CB [81]

The primary dispersible unit of carbon black is referred as an ''aggregate'' that is a discrete, rigid colloidal body. It is the functional unit in well-dispersed systems. The aggregate is composed of spheres that are gathered together for most carbon blacks. These gathered spheres are generally termed as primary ''particles''. These particles are composed of many tiny graphite-like stacks. Within the particles the stacks are oriented so that their z axis is normal to the sphere surface, at least near the particle surface. The surface functional groups that have been investigated are the oxygen complexes, i.e. carboxyl, carbonyl, phenol, hydroxyl, ethers, quinones, and lactones (Fig.4.6)
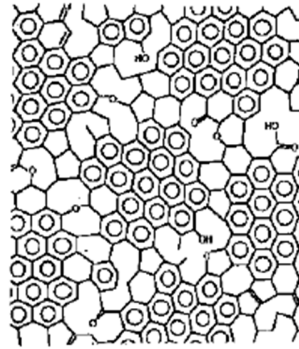
Fig.4.6: Surface functional groups of carbon black [80] [81]

This structure and functional groups attribute in reinforcement on physical property of rubber such as elasticity, tensile strength and tear strength [82]. In addition, the filler influence on not only for the property but also the resistance against the aging process. This influence will originate from the complex surface morphology, structure, and chemical functions as shown in Fig.4.5 and 4.6.

Despite broad discussions on the effect of carbon black on the aging process to date a comprehensive its theory has not yet been established. Several of the conclusions drawn are contradictory due to the complexity of the carbon surface morphology, as described below.

Hart et al. suggested that carbon black has the effect of promoting thermal oxidation in that its surface is capable of absorbing oxygen, which is then released into the rubber, subsequently accelerating the auto-oxidation of the polymer. What is more, a large specific carbon black surface area results in a higher rate of oxidation due to the higher oxygen absorption capacity [83] . On the other hand, M.-J. Wang et al describe an antioxidant effect of carbon black [81]. The mechanism can be attributed to the surface chemistry of carbon black. The chemical functional groups on the surface of the carbon black particle can be attributed with the process, condition or impurities in production. The presence of the oxygen complexes has been shown to affect the rate of crosslinking and stabilizing effect of the polymer radicals which are generated by thermal oxidation.

4.4.4 Effect of insufficient of crosslink

After reaction completion, a certain amount of peroxide crosslink agent can still remain in the crosslinked rubber due to insufficient crosslink reaction. The residual peroxide content

influences as a key factor on the thermal oxidative stability of rubbers [84] [85]. In order to prove this factor, U. Giese et al. evaluated the relationship between the residue of peroxide in rubber and Oxidation Induction Time (OIT) which represents the thermal oxidative stability [79]. They concluded that the OIT values decreased due to the insufficient crosslinking reaction. In other words, higher content of residual peroxide agent leads a poorer stability against thermal oxidation.

When the residual peroxide crosslink agent remains in the crosslinked rubber due to insufficient crosslinking, free radicals can be produced by the decomposition of peroxide radical initiator. Then auto-oxidation starts and leads to chain scission of rubber network.

Therefore, considering that EPDM is used for the industrial application, the reduction of residual peroxide is necessary. Low volatile peroxide chemicals can be vaporized by "Post cure". This means that there has already been a "press cure" as a preliminary processing in order to fix the rubber into its final shape and form the uncrosslinked compound is subjected to high temperature. After that, post curing, literally means "after cure" by definition, is conducted.

Chapter 5

Theory of methods

5.1 Theory of NMR (Nuclear Magnetic Resonance)

5.1.1 Low field NMR theory

NMR enables to characterize the crosslink structure of rubber. The basic theory is described in the following and illustrated in Fig.5.1
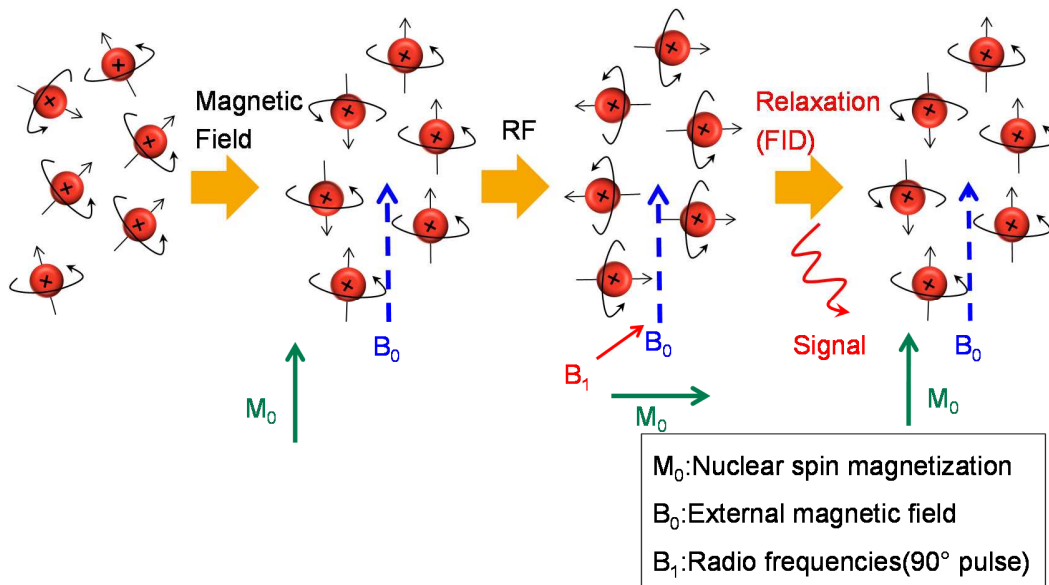

Fig.5.1: NMR principle

The hydrogen nucleus has unique nuclear spin, which can be regarded as a small magnet having a magnetic moment μ_i. All isotopes that contain an odd number of protons and/or neutrons have an intrinsic nuclear magnetic moment and angular momentum, while all nuclides with even numbers of both have a total spin of zero. The most commonly used nuclei are ^{1}H , ^{13}C , ^{19}F and ^{29}Si in order to investigate the rubber structure. In typical experiment hydrogens in sample are placed in a static magnetic field, B_o. The magnetic moments will adopt specific orientations relative to the field (It is oriented in the direction or the opposite direction). When the spins are in equilibrium state, their direction is determined according to the Boltzmann distribution. As the result of this distribution, more spins which orients up are aligned with the magnetic field. This

creates a mean magnetization (M_0) oriented with the field that is parallel to the z axis. In an NMR experiment, the M_0 direction of the sample is changed by applying a Radio frequencies (RF) pulse B_1 of a specific duration (pi/2 pulse) along the vertical direction of the magnetic field (x axis). The rotated magnetic moments will continue to spin around B_o producing an alternating current (the NMR signal) in the detection coil. The NMR signal generated is called a relaxation or free induction decay (FID) [86, 87, 88]

The NMR signal decays via two different processes. These are the longitudinal as called T_1 spin lattice and transversal as called T_2 spin-spin relaxation process. The T_1 spin-lattice relaxation can be described as the recovery of the magnetization in the B_o direction (Z axis) due to the energy transfer with the surroundings. The T_2 spin-spin relaxation occurs faster than the T_1. The spins exchange interacts with each other leading to a loss of synchronization. After a certain time, the spins of nuclear recover to the equilibrium state. This time is called "Spin-spin relaxation time or transverse relaxation time (T_2) ".The detail description is shown in the following section

5.1.2 Spin-spin relaxation and Hahn echo

T_2 is used to quantify the rate of the decay of the magnetization of the vertical of the B_o direction (within the x-y plane). After a 90° pulse the nuclear spins are aligned in one direction which can be also called phase coherent, but this arrangement is gradually lost because of magnetic field inhomogeneities and interactions between the spins without energy transfer to the lattice. Local magnetic field inhomogeneities on the micro and nanoscales release the energy of excited nuclear spins such interact with each other. Therefore some net signal will be lost due to interactions such as collisions and diffusion through heterogeneous space.

It is possible to be characterized by the spin–spin relaxation time, known as T_2, a time constant characterizing the signal decay. It is the time that it takes for the magnetic resonance signal to irreversibly decay to 37% (1/e) of its initial value after its generation by tipping the longitudinal magnetization towards the magnetic transverse plane ($x`y`$). The magnetization at time zero will decay to equilibrium state as following equation.

$$\mathrm{M}_{(t)} = \mathrm{M}_{(0)}\exp(-t/T_2) \qquad (5.1)$$

The relaxation of the transversal magnetization is measured by the well known Hahn-Echo-Sequence. The illustration of the behavior of the magnetic field is shown in Fig. 5.2.
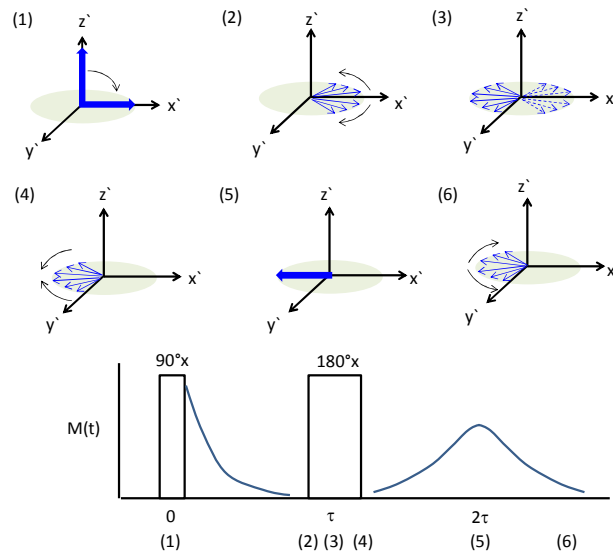
Fig.5.2 :Hahn echo method

This type of sequence cancels out effects of field inhomogeneities and chemical shifts. So the signal is mainly influenced by dipole-dipole-interactions. In the presence of a static magnetic field the Hahn-Echo-Sequence uses two high frequency pulses (90° and 180°) separated by the time interval τ after a time period $2*\tau$, the specimen responds with an echo that is detected via an antenna, amplified and digitized. The magnetization is plotted as function of time ($2*\tau$), Typically, the signal intensity decreases mono-, multi-exponentially, in accordance with a Gaussian-shaped function, or combinations thereof. The time constant determining the decay of the curve from spin-spin interaction is denoted as transverse T_2 -relaxation time, as described above. Basically, the smaller the T_2 value, the less mobile the polymer chain. Therefore, T_2 can have correlations with rubber crosslink density [89]. In sum, the analysis of the molecular dynamics is based on the measurement of the relaxation of the transversal magnetization caused by the spins of the ^{1}H nuclei that are part of the polymer chains. The relaxation properties are strongly influenced by the dipolar interaction of ^{1}H nuclei. The strength of this dipolar interaction depends on the molecular mobility.

Besides the spin echo sequence has the ability to refocus the distribution of spins due to magnetic field inhomogeneity. Since in this study not only unfilled polymers but also carbon black filled systems are investigated, the effect of the carbon black itself on the NMR signal has to be considered. The effect of these and their influence on the reliability of relaxation measurements have been critically discussed in several studies [13-18]. An important aspect in this respect is the

paramagnetic nature of carbon black acting as an additional magnetic field source and leading to inhomogeneities in the magnetic field. The following equation describes the relationship between theoretical T_2, experimentally determined T_{2*}, and the inhomogeneity of the field (ΔB_0), with γ gyromagnetic ratio. In reality, experimental decay is faster than theoretical computations would predict

$$\frac{1}{T_{2*}} = \frac{1}{T_2} + \frac{\gamma \Delta B_o}{2} \qquad (5.2)$$

This effect can, therefore, be said to get stronger with increasing relaxation time T_2. Nevertheless, most studies investigating carbon black filled systems have used free induction decay (FID) or solid echo pulse sequences. In the context these methods have a strong disadvantage against the Hahn-Echo-sequence used in this study. They do not allow refocusing of the spins in order to cancel out the effect of magnetic field inhomogeneities. Therefore the paramagnetic effect of carbon black gives rise to the modifications of relaxation times reported in literature. By applying the Hahn-Echo-sequence is able to ensure that carbon blacks' paramagnetic effect is not influencing the results presented here.

5.1.3 Conventional analysis of relaxation curves and issue using exponential fitting analysis

The conventional way to analyze the NMR signals for polymers showing only exponential relaxation in the investigated time frame is the multi-exponential approach. Mostly, the T_2 signal M(t) has been resolved into two exponentially decaying components in the previous studies [90, 91, 92]. For example a bi-exponential function was used by Folland et al. for crosslinked poly-isoprene [89, 93, 94, 95, 96].

$$M(t) = A_1 \exp\left[-\frac{t}{T_{2A}}\right] + A_2 \exp\left[-\frac{t}{T_{2B}}\right] \qquad (5.3)$$

In essence, instead of one T_2-value, several T_2 values resulting from the multi-exponential approach can be related to different rubber structures with different mobility as shown in Fig.5.3.
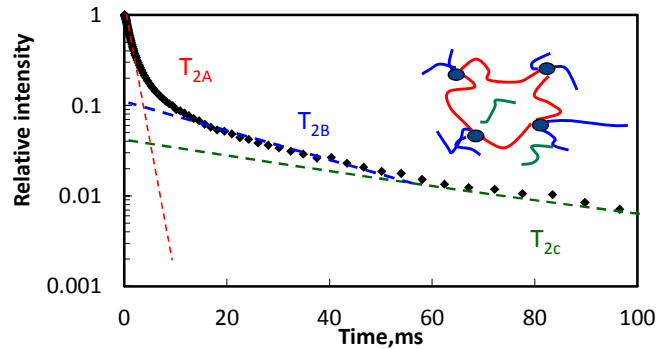
Fig.5.3: Crosslinked network structure model and schematic NMR relaxation

In the aforementioned studies [89, 93, 94, 95, 96], T_{2A} was attributed to the network phase, such as chemical crosslinks and physical entanglements. T_{2B} is associated with the non-network phase — chain ends, for instance. In the case of raw polymer, the molecular weight can influence chain mobility due to the presence of chain entanglements. In addition, the inverse of T_{2A} is closely related to the crosslink density (υ_e) determined by the swelling method according to the Flory-Rehner Equation [97, 98, 99, 100].

However, these results seem to be contradiction to the other studies. Some researchers didn't mention the non-network phase such as dangling chain ends. Besides they indicate the mono exponential function should be fitted to the crosslinked rubber [101, 102, 103].

On the other hand, the other researcher mentioned tri exponential function should be used to analyze unfilled crosslinked EPDM rubbers because they have inhomogeneous rubber structure [104]. These unconcluded results can be attributed by the unclearness of the analysis of using multi-exponential approach. The multi-exponential approach mentioned above has got some significant drawbacks. If the approach consists of more than two exponential terms the application of standard fit algorithms is critical since the results usually depend extremely on the starting conditions. For instance, a three-exponential approach consists at least of 6 fit parameters; however the NMR relaxation curve is just a simple shaped monotonically decreasing curve, so the fit results are usually not well-defined. For rubber, especially when analyzing the aging properties, at least three or four different structure types with different molecular mobility and different relaxation times as shown in Fig.5.4 have to be taken into account, so a bi-exponential approach is not adequate. Second, when applying a multi-exponential approach it has to be known in advance how many different structure types are contributing to the relaxation curves.

The following example illustrates these points. One set of experimental NMR relaxation data of crosslinked rubber was fitted with mono-, bi- and tri- exponential functions of relaxations using the following equations. The fitted curve and the experimental curve as well as the parameters which were obtained by the analysis are shown in Fig.5.4 and Table.5.1

$$M(t) = A \times \exp(-\frac{t}{T_{2a}}) \qquad (5.4)$$

$$M(t) = A \times \exp\left(-\frac{t}{T_{2a}}\right) + B \times \exp\left(-\frac{t}{T_{2b}}\right) \qquad (5.5)$$

$$M(t) = A \times \exp\left(-\frac{t}{T_{2a}}\right) + B \times \exp\left(-\frac{t}{T_{2b}}\right) + C \times \exp\left(-\frac{t}{T_{2c}}\right) \quad (5.6)$$
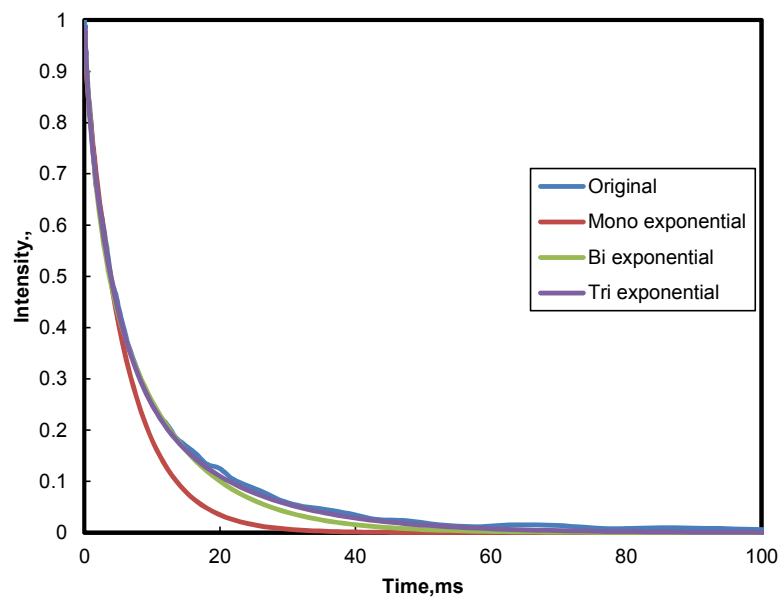
Fig.5.4 :Experimental and simulated relaxation curves

Table.5.1 Parameter obtained by exponential fitting

	Mono-exponential	Bi-exponential	Tri-exponential
R^2	0.99443	0.99956	0.99984
A	0.93148	0.33398	0.49747
T_{2a}	6.08591	1.7592	4.09002
B		0.64665	0.39664
T_{2b}		10.7357	15.20276
C			0.09963
T_{2c}			0.54302

It can be seen, bi- and tri- exponential functions yield closer fits to the experimental relaxation curve than mono - exponential function. The comparison between bi- and tri- exponential functions shows that the result of tri- exponential fit is slightly better than that of bi-exponential fit. In general. in order to determine the optimal function, the coefficient R^2 from least squares method can be compared (Table.5.1). However, all R^2 numbers show the closed to 1.0. In practice, it is difficult to determine the best suited fit function without uncertainties

## 5.2 Theory of chemiluminescence

5.2.1 Chemiluminescence

In terms of the chemical analysis to understand the aging process of rubber, several techniques are available: optical spectroscopy, high-resolution NMR, FT-IR and XPS and others. These spectroscopic methods can be used for the quantitative analysis of the chemical structure of crosslinks [105, 106, 107, 108].

Recently, the development of a photomultiplier tube with a highly sensitive detector progressed, the chemiluminescence has been able to be observed. This method shows the potential to investigate the thermal oxidation processes of polymer type and ingredients such as antioxidants.

As described in Fig.4.2, the thermal oxidation is the important process to correlate closely to the physical property change of polymers during the aging process. In association with the thermal oxidation of polymers, a high energetic triplet carbonyl species releases its energy and generates singlet carbonyl. Regarding this process, the reaction must be exothermic to produce sufficient energy form the excited state. And this energy releases as a photon emitting when these products return to the ground state. This phenomenon is called "chemi-luminescence" and can be applied to characterize the thermal oxidative reaction of polymer materials. There are several proposed mechanisms of Chemiluminescence emissions during aging of polymers. Two major mechanisms are known which can be detected via Chemiluminescence and are related to thermal oxidation (Fig.4.2). These mechanisms are summarized in the literature "Luminescence Techniques in solid state polymer research" Zlatkevich [109].

Process 1 Alkyl peroxyl radicals recombination (Russell's mechanism)

Only the reaction of primary or secondary peroxylradicals are highly exoenergetinc (460KJ/mol) and produce an excited carbonyl group directly through a six membered ring as an intermediate [110].
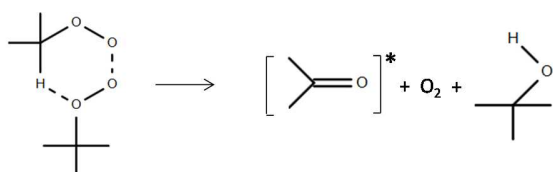
Process 2 Decomposition reaction of hydroperoxide radical

The direct decomposition of hydroperoxide yields an excited carbonyl and water. Vasilev showed that this reaction is exoenergetic by 315 kJ/mol and proceeds through a cage reaction after homolysis [111].

$$\text{---O---OH} \longrightarrow \left[\text{---CO} \cdot + \cdot \text{OH} \right] \longrightarrow \left[\text{C=O} \right]^{*} + H_2O$$
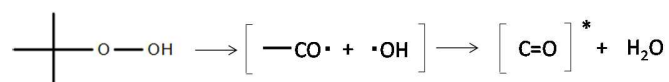
Considering EPDM, the emission of chemiluminescence can be highly correlated with above equation. This reaction causes the chain scission as shown in Fig.5.5. The mechanism of the emission of the chemiluminescence was proposed to occur when the carbonyl functional group is formed. The mechanism of the emission of the chemiluminescence is biradical. This transient biradical changes to the excited condition and emit the energy as the chemiluminescence to generate singlet carbonyl [112]
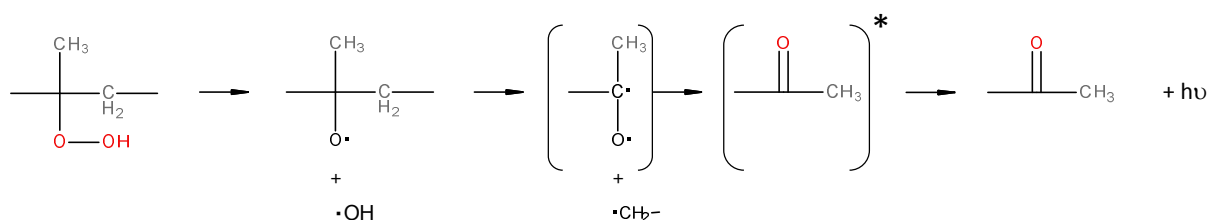
Fig.5.5: The reaction scheme of propylene site of EPDM [112]

In sum, the chemiluminescence process can be associated with the chain scission reaction. Therefore it will be useful to interpret the chemical relaxation due to the thermal oxidation. Fig 5.6 shows a typical curve obtained in isothermal chemiluminescence analysis.
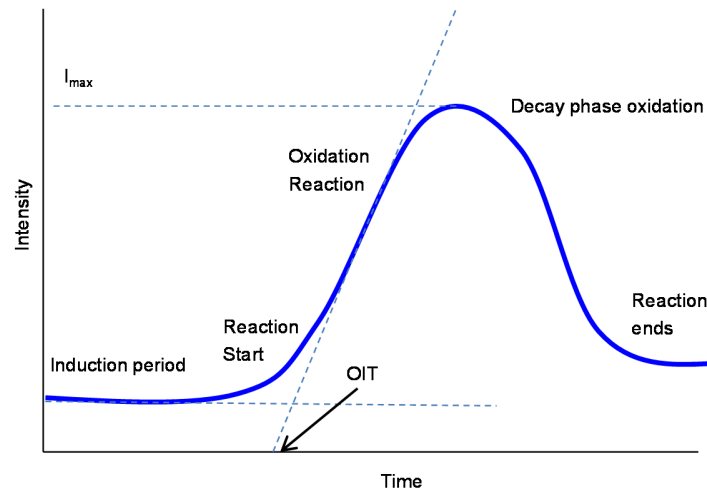
Fig.5.6: Typical curve of the chemiluminescence

At a given time the reaction begins and the chemiluminescence curve rises linearly until it reaches maximum intensity. The point at which the base line intersects with the linear curve upwards is referred to as the OIT, or the time at which the oxidation reaction begins.
The oxidation rate constant can be calculated from the reaction rate equation.

$$\frac{d[B]}{dt} = k[A] \times [B] \qquad (5.7)$$

Where A is the polymer and B is the hydroperoxide concentration , k is the kinetic oxidation reaction rate constant. The following equation is derived with initial concentration of A_0 ,B_0 and I_{max} from Chemiluminescence curve initial Chemiluminescence curves are derived from the reaction constant in the following equation [109]

$$\ln\left(\frac{I_t}{I_{max} - I_t}\right) = \ln(B_0 / A_0) + kA_0 t \qquad (5.8)$$

The plots of *ln It/(Imax-It)* and *t* at the increment area of the chemiluminescence curves show normally linear relationship. The gradient of this line is the value of the reaction constant *k*. Using the information of *k* at a different reaction temperature, the activation energy of the chemiluminescence reaction can be calculated according to the Arrhenius equation (3.6).

The temperature dependency of the kinetic constant of the chemical process can be described with the Arrhenius equation.

$$k = A \times \exp(-E/RT) \qquad (5.9)$$

Where k is the kinetic oxidation reaction rate constant, A is the frequency factor, R is the gas constant and T is the absolute temperature.

Chapter 6

Used materials and methods

6.1 Materials

Several types of EPDM raw polymer are selected for the investigation. Table 6.1. shows the structural properties of the investigated polymers. Weight-average molecular weight (Mw) and number-average molecular weight (Mn) are analyzed by GPC. Besides Mw/Mn is calculated as a representative value for the molecular weight distribution called PDI (polydispersity index)

Table 6.1: Structural properties of raw polymer

Polymer	EP-A	EP-B	EP-C	EP-D	EP-E	EP-F	EP-G	EP-H	EP-I	EP-J	EP-K	EP-O
Ethylene	56	45	51	51	56	58	55	47	41	65	70	48
ENB content	4.7	8.1	0	8.1	8.1	4.7	2.3	9.5	14	4.6	4.7	4.1
Mn,g/Mol	8750	19200	11500	11800	65100	65100	60100	38300	63300	2784	2759	3249
Mw, g/Mol	183750	192000	212750	158120	234360	188790	162270	222140	310170	1606	1523	1851
Mw/Mn[1]	21	10	18.5	13.4	3.6	2.9	2.7	5.8	4.9	1.73	1.81	1.76

1)PDI: polydispersity index

EPDM polymer EP-A is used for almost all the investigations of the crosslinked materials (if the other types of materials are used, there is remark). Dicumylperoxide, antioxidant, several types of carbon black and co-agent are mixed with the polymer on an open twin roll mill with by an open roll (diameter: 25 cm). Table 6.2. shows the recipes of the compounds. The compounds are press-crosslinked at 180°C for 6 minutes. Vulcanization behavior is characterized in a rheometer (ALHPA Technology RPA 2000). The rheometer curves show a conversion rate of more than 97% was reached in all cases.

Table 6.2: Compounds recipe

	EP1	EP3	EP5	EP3-CB-L	EP3-CB-M	EP3-CB-H	EP3-AO	EP3.6-E65	EP4.2-E70	EP3/Co3
Polymer(EP-A)	100	100	100	100	100	100	100			100
Polymer(EP-J)								100		
Polymer(EP-K)									100	
CB N990[1]			50							
CB N550[1]					50					
CB N343[1]						50				
Antioxidant (TMQ)[2]							1			
Cure agent (DCP)[3]	1	3	5	3	3	3	3	3.6	4.2	3
Co-agent (TAIC)[4]										3

1) N_2-adsorption number of used carbon blacks (CB):

  N990: 9 m^2/g (MT); N 550: 43 m^2/g (GSO); N 343: 99 m^2/g (IISAF)

2) 2,2,4-trimethyl-1,2-dihydroquinoline

3) DCP: Dicumylperoxide

4) TAIC:Triallyl isocyanurate

6.2 Continuous stress relaxation

Continues stress relaxation experiments were performed according to ISO 6914. Fig. 6.1 shows the cell used for the mechanical stress relaxation tests.
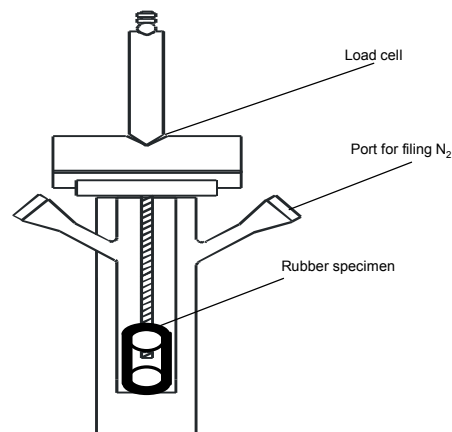
Fig.6.1: Glass cell for stress relaxation test

The test procedure is described as below and test conditions are shown in Table 6.3

1) In the case of measurements in a N_2 atmosphere, N_2 was filled into the cell at a flow rate of 200 ml/min during the first 5 minutes, then the flow rate is reduced to100 ml/min. In the case of measurements in air, the test produce starts with 2)

2) Vulcanized rubber test samples set in the cell were stored in the oven for 30minnutes at the desirable temperature without any stress being applied.

3) The vulcanized rubber test samples are stretched to a specific elongation ratio

4) Recording of counter force starts.

Table 6.3: The test condition of continuous stress relaxation

Parameter	Value
Elongation	20%
Atmosphere	Air or N_2
Temperature	150°C
Sample geometry	Ring-1mm thick$\times$52.6 mm diameter

6.3 Thermal oxidation

The thermal oxidation of rubber sheets (Geometry: 2 mm thick, 30mm length and 30 wide) were conducted in the oven at 150°C. Hardness, swelling, NMR and FTIR were measured on the aged samples.

6.4   Hardness measurement

Hardness was measured using the micro hardness tester. The test procedure was followed as ISO 48. The experiments were performed at room temperature on EPDM rubber samples before and after aging in order to characterize the chemical structure.

6.5 Swelling test

Crosslink density was measured using the swelling method. For the determination of crosslink density, swelling tests on the crosslinked rubber were performed in toluene in accordance to ISO 1817.

1) The crosslinked test pieces were weighed using an electrical balance

2) The weighed samples were swollen in toluene until equilibrium for 72 hours at room temperature.

3) The weight of the swollen samples were determined again.

4) These obtained values were used to calculate the crosslink density by applying the Flory-Rehner Equation [97, 98, 99, 100].

$$v = -\frac{1}{2V}\left[\frac{\ln(1-v_r)+v_r+xv_r{}^2}{v_r{}^{\frac{1}{3}}-\frac{1}{2}v_r}\right] \qquad (6.3)$$

Where v is the crosslink density moles per unit volume (mol/cm³), Vr is the Volume fraction of rubber in equilibrium swollen state vulcanized rubber sample is the ratio. V is Mole volume of used solvent at room temperature in cm³/mol (from molecular weight and density) , x is Flory-Huggins polymer-solvent interaction parameter (In this research, taken as 0.43 [113]).

6.6 Soxhlet extraction

In order to characterize the free low molecular structure in the crosslinked rubber before and after aging, GPC and FTIR were measured. For these measurements. The pretreatment was conducted as following procedure.

1) The samples were aged in the oven at 150°C for certain time.

2) The soxhlet extraction was done with the hexane and acetone (50vol%:50vol%) for 72hours at 80°C.

3) The swollen samples were dried under vacuum at room temperature.

4) The weight of dried samples was measured in order to quantify the weight loss by solvent extraction.

5) The extracted liquid was dried for the GPC or FTIR measurement.

6.7 Attenuated Total Reflectance-Fourier Transform Infrared Spectroscopy (ATR-FT-IR)

The instrument of the ATR-FTIR was Nicolet FTIR Nexus (Thermo scientific). The experiments were performed at room temperature on EPDM rubber samples before and after aging in order to characterize the chemical structure. The sample of the surface is set on the Ge Crystal and keep the contact between them during measurement. The spectral curves were

acquired at wavenumbers (see Table 6.4) of in the attenuated total reflection mode using a Ge crystal. The condition of measurement is shown as below.

Table.6.4: Measurement parameter of ATR-FTIR

Parameters	Values
Wave number	4000 cm^{-1} – 650 cm^{-1}
Scan number is	64
Crystal	Ge
Detector	TGS

6.8 Low field ^{1}H NMR relaxation

The NMR relaxation was performed using a Bruker Minispec mq 20 NMR time domain spectrometer at 19.2 MHz for protons (^{1}H) The Hahn echo experiment was used to measure the magnetical relaxation at the desirable temperature. The main parameters are shown in Table. 6.5.

There are two types of sample preparations. On one hand, the unaged and aged rubber specimen cut into apx. 1mm cubic and filled in a glass tube and measured (When there is no remark, the sample preparation was done with this way).

Table 6.5. The parameters of NMR measurement

Parameter	Value
Equipment	Bruker Minispec mq 20 NMR time domain spectrometer
Resonance frequency	19.2 MHz
Pulse sequence	Hahn Echo
Temperature T in °C	100
Scans	40
Recycle delay in ms	1.0

On the other hand, in order to estimate the effect of strain on the rubber structural change during thermal oxidation, crosslinked rubber are set to the PTFE rod as shown in Fig.6.2.
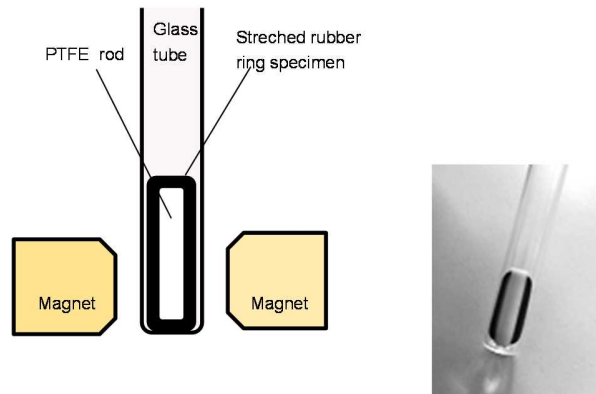
Fig.6.2: Elongation device for NMR measurement

The crosslinked rubber was prepared as following. The 2 mm thick vulcanized sheet was cut into 1 mm thick rings. Rubber ring specimens are stretched using the PTFE rod at room temperature from 0 up to 40% elongation ratio. PTFE doesn't disturb NMR measurement because it does not have the signal of proton.

6.9 NMR relaxation spectra

As discussed above, multi-exponential approach has several issues, a powerful alternative to the multi-exponential approach is the Inverse Laplace Transformation (ILT). This evaluation delivers the T_2 distribution as a measure for the frequency or number of specific chain nobilities [114, 115, 116, 117, 118] .

$$M(t) = \int_0^{\infty} L(\tau)F(t,\tau)d\tau \qquad (6.1)$$

Here M(t) stands for the experimental NMR data, L(τ) for the distribution function, which has to be determined, and F(t, τ) for the kernel function, in the case

$$F(t,\tau) = e^{-\frac{t}{\tau}} \quad (6.2)$$

The integral shown above is a Fredholm integral of the first kind. Unfortunately the inversion of this integral in order to determine $L(T_2)$ is a so called ill-posed mathematical problem, so usually there is not one unique solution for $L(T_2)$. In addition measurement noise can also have a big influence on the solution. In order to invert the Fredholm integral the CONTIN algorithm was

applied [119, 120]. This algorithm was developed especially for inverting integral equations with noisy measurement data.

6.10 Chemiluminescence

The results of chemiluminescence were attained by using a chemiluminescence analyzer (Atlas CL400). Fig.6.3 shows the schematic of the chemiluminescence device. An isothermal mode was operated at the desirable temperature which was maintained by a constant flow of air.

1) The cells are heated up to a desirable temperature in nitrogen.
2) The atmosphere was switched to oxygen and the light intensity was logged.
3) A lens above the sample focused light emission during ageing.
4) The analysis was carried out under a high flow oxygen atmosphere (gas pressure: 6.9 ± 2.0 kPa) in a desirable temperature range.
5) The light emission was detected by a highly-sensitive photomultiplier tube (PMT). When the oxidation reaction begins, the increase in light intensity is detected by the CL signal.
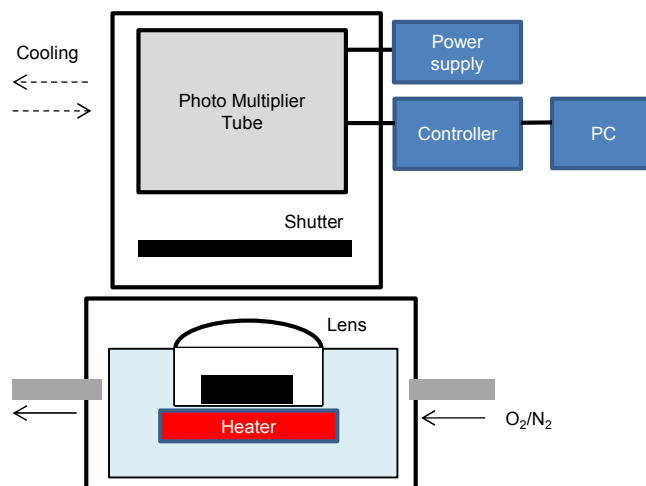
Fig.6.3: Scheme of the chemiluminescence equipment

In addition, in order to quantify the effect of strain on the thermal oxidation, a 1 mm thick and 3 mm wide rectangular sample was fixed in an elongated state with the device shown in (Fig.6.4).
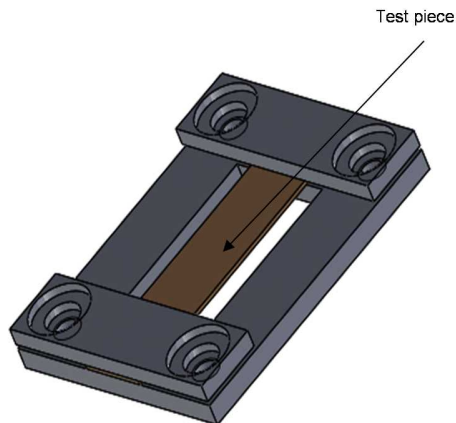
Fig.6.4: Test device for elongation in the chemiluminescence chamber

This stretched sample with the device was set in the chemiluminescence chamber as shown in Fig.6.5.
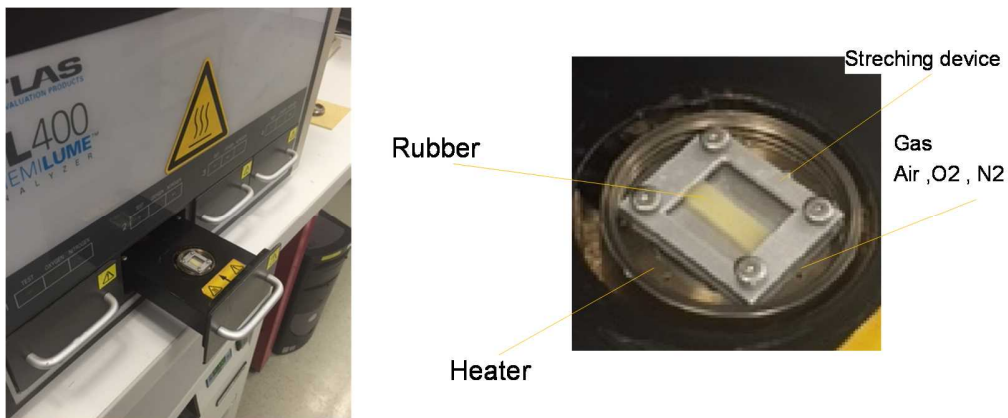
Fig.6.5: Device for stretching rubber and chemiluminescence chamber

6.11 GPC (Gel permeation chromatography)

The instrument used for GPC measurement is Agilent 1100 and the parameters are shown in Table6.6. Two types of molecular weight were calculated from the chromatogram named the number average of molecular weight (Mn) and the weight average of molecular weight (Mw). Besides, for the characterization of the distribution of molecular weight distribution, polydispersity index (PDI) was calculated as Mw/Mn.

Table.6.6: Measurement parameter of GPC

Parameters	Values
Solvent	THF
Temperature	50°C
Colum, L/I.D.	Polystyrene divinyl benzone(300 ×7.5)
Pressure, bar	60
Detector	RI (Reflective index)
Flow rate, ml	1.0

6.12 DSC (Differential scanning calorimetry)

The instrument of DSC is Mettle Toledo DSC1 and parameters are shown in Table 6.7.The melting temperature of partial crystalline in crosslinked EPDM rubber was observed with this method.

Table .6.7: Measurement parameter of DSC

Parameters	Values
Temperature sequence	-100°C→200°C
Rate	10°C/min
Sample size	10mg

Chapter 7

Experimental results

7.1 Validation of NMR-ILT

      For validation purposes, several trials were performed using simulated data to determine the accuracy of the ILT method. The first trial was to produce spectra which contain three relaxation processes with ideal noiseless tri-exponential functions.

$$M(t) = A \times \exp\left(-\frac{t}{T_{2a}}\right) + B \times \exp\left(-\frac{t}{T_{2b}}\right) + C \times \exp\left(-\frac{t}{T_{2c}}\right) \qquad (7.1)$$

      The original artificial relaxation curve was formed by fitting one of the experimental data as shown in Fig.7.1.
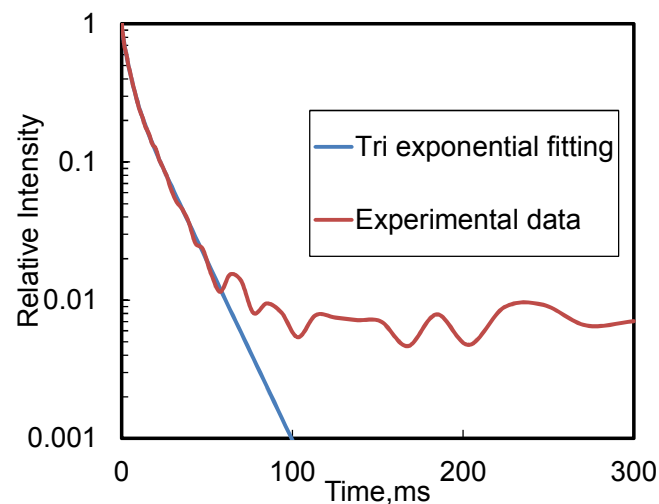
Fig.7.1 : Comparison between experimental and simulated data

      The ideal relaxation curve was produced with the relaxation times T_{2a}, T_{2b} and T_{2c} equal to 0.36 ms , 4.0 ms and 16.7 ms. A , B and C equal to 0.093 ,0.53 and 0.36. Fig.7.2 shows the relaxation spectra using ILT.
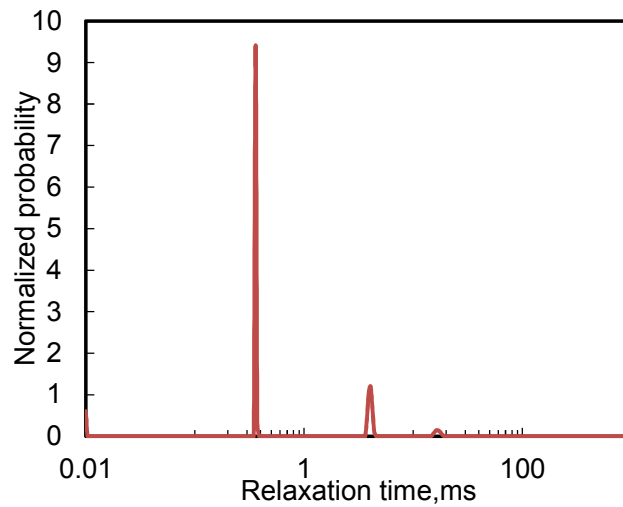
Fig.7.2 :Relaxation spectra obtained by tri-exponential fitting data

CONTIN algorithm calculated the relaxation spectrum showing from the artificial relaxation and three peaks at 0.36 ms, 4.05 ms 16.7 ms. The area of peaks are equal to 0.1, 0,53 and 0.36 are observed and total area of all peaks equal to 1.0, in other words, the normalization is done by algorithm. Table 7.1 shows the summary of the parameters which obtained by fitting exponential functions and ILT. This result confirms the programs ability to separate relaxation processes.

Table 7.1 : Tri exponential fitting and ILT

	Tri exponetinal	ILT
T2a:	0.36	0.36
T2b:	4.03	4.05
T2c	16.7	16.2
A	0.093	0.1
B:	0.53	0.53
C:	0.36	0.36

During a NMR relaxation test, several factors can affect the accuracy of a relaxation curve. For instance, a large change in the external environment temperature or noise from electrical devices, thus slightly varies the output. Therefore, an investigation was conducted into the effect of a scattered relaxation curve on the resulting relaxation spectrum. Fig.7.3 (left) shows the original data with and without noise. Noise is generated by a random number. The

number such as 0.001, 0.005 and 0.1 describe the maximum intensity of the noise. A larger range of scatter intensity resulted in an increase of peak width and, consequently, a reduction in spectrum height as shown Fig.7.3 (right).
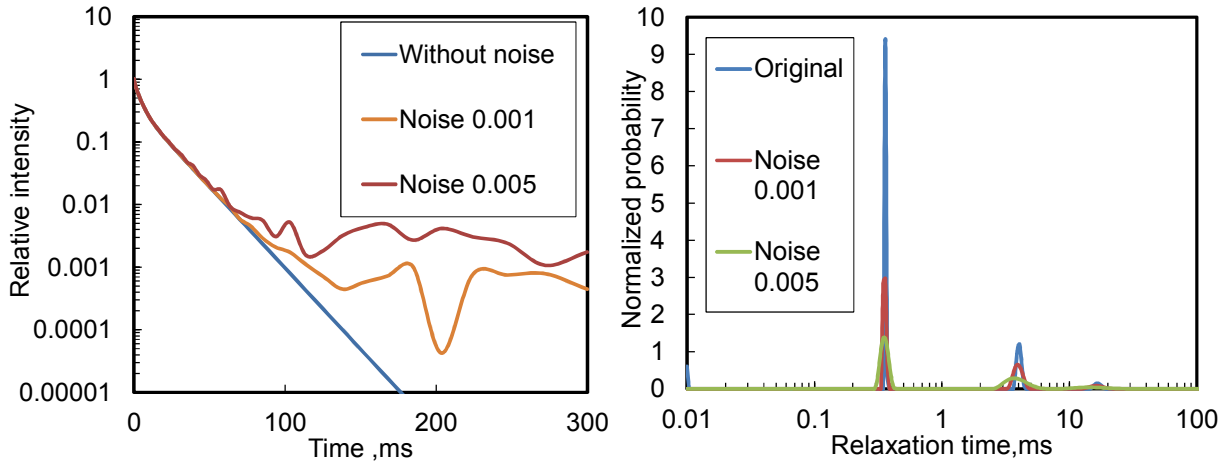
Fig.7.3: Simulated scattered NMR relaxation curves (left) and NMR spectra (right)

The area of the spectra v.s. noise level is shown in Fig.7.4.
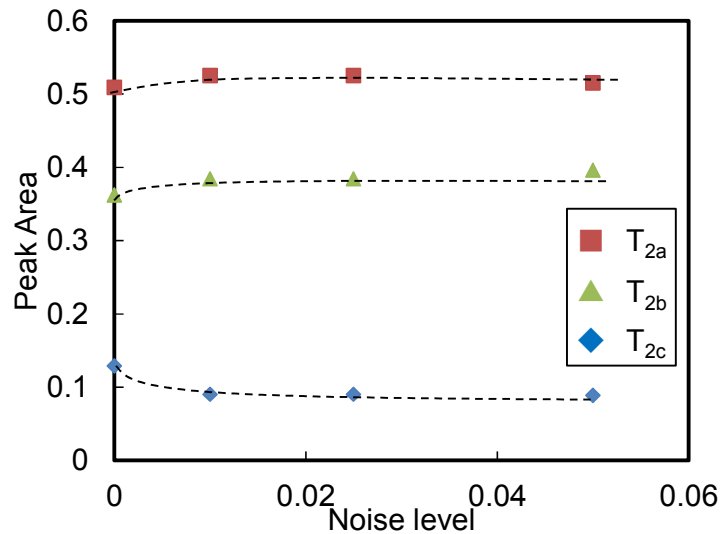
Fig.7.4 :Peak areas of the peaks which obtained with different levels of noise

In all cases, peak area was stable even if the data had included a certain amount of noise. It was concluded that a smoother relaxation curve resulted in a more accurate spectrum with more well-defined peaks.

The purpose of the next analysis was to study how the relaxation time spectrum affects when insufficient relaxation data was available. To verify the effect of differentiating with a reduced intensity range, the artificial NMR relaxation data was used.

The cut off curves data for the investigation were chosen at 90% ,95%,97.5% 99% of original intensity. Fig.7.5 (left) shows all cut off and original NMR relaxation curves. Regarding the peak maximum time, all cut spectrums produced a peak maximum time similar to the complete original data in Fig.7.5 (right).
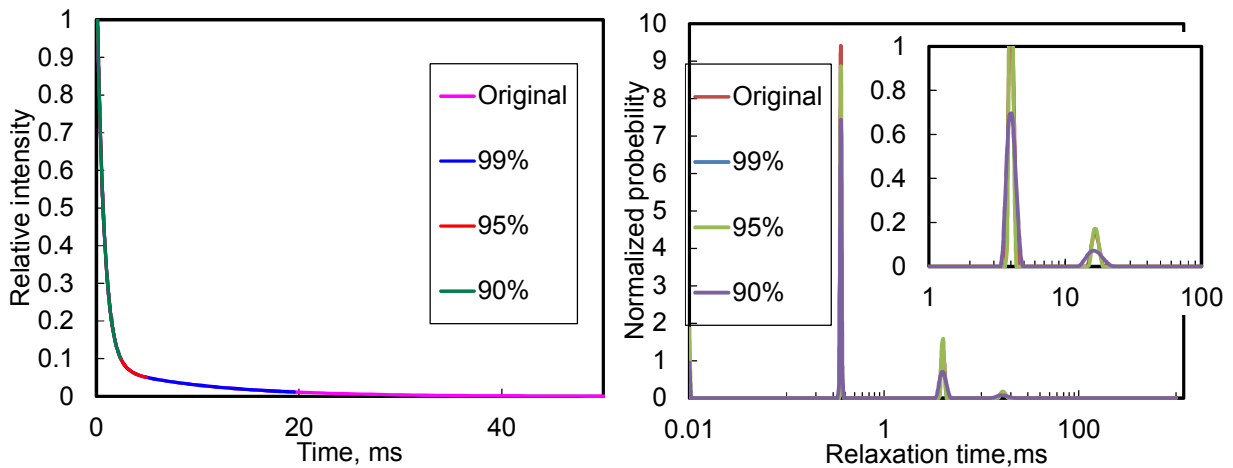
Fig.7.5: Reduced NMR relaxation curves(left), NMR relaxation spectra with reduced data(right)

Additionally, the area of the peaks changed slightly. However, the cut off curves produced wider peaks as well as scattered relaxation data. In addition, the height was reduced considerably and the width got broader while the peak area remained constant as shown in Fig.7.6. From this investigation it can be concluded that it is necessary to produce sufficient (complete) relaxation data for accurate spectra analysis.
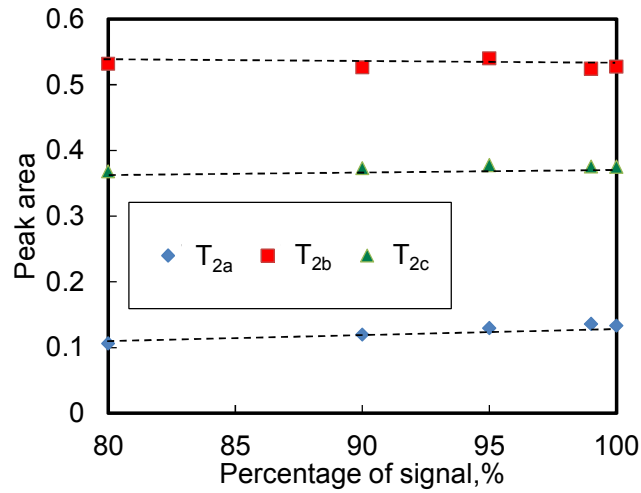
Fig.7.6: Peak area which obtained by complete and insufficient relaxation.

Thus peak width is influenced by several factors not from the only materials but also from data quality. However, although an ideal tri-exponential data set was used, the ILT gives broad peaks, especially at longer relaxation times. For further understanding the effect of the used algorithm on peak width, three types of mono- exponential functional data sets were created. Fig.7.7 shows the relaxation curves.
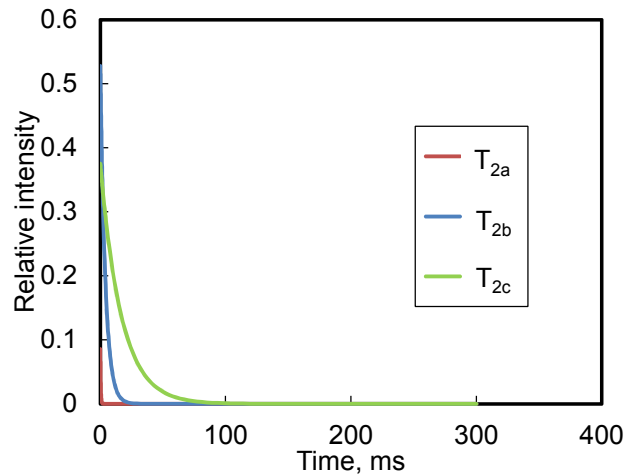
Fig.7.7: Three types of exponential decays

Fig.7.8 shows the relaxation time spectra resulting from Fig.7.7 by using ILT.
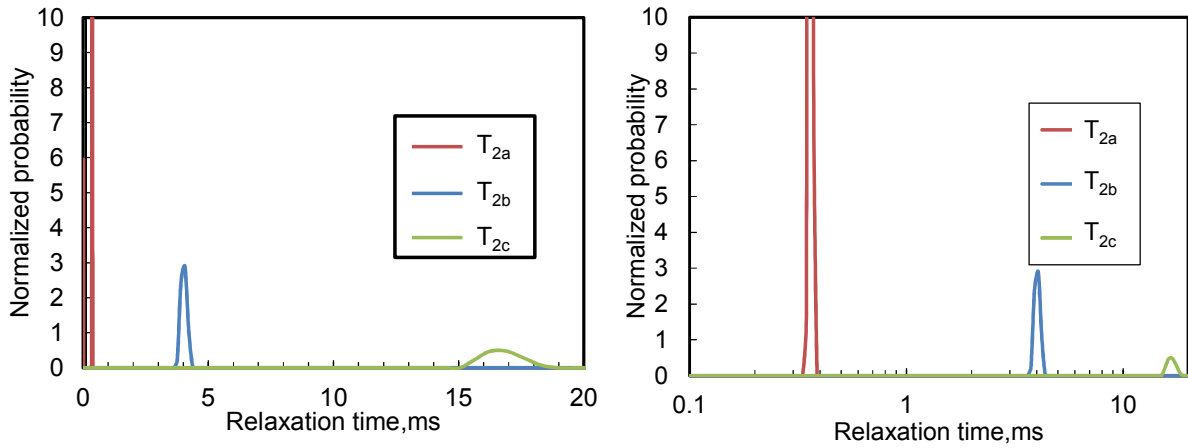
Fig.7.8: ILT spectra resulting from Fig.7.7 with linear scale(light) ,ILT spectra with logarithmic scale (right)

Peak width increased as the relaxation time increased. Although the main purpose of conducting relaxation time spectra is to show the T_2 distribution referring the chain mobility, it is necessary to understand the broadness due to the width originating from the algorithm. However, when the relaxation time (x axis) was looked at logarithmic scale, each peak width had the similar value. The peak width (full width at half maximum) on logarithmic and linear scale is shown in Fig.7.9.
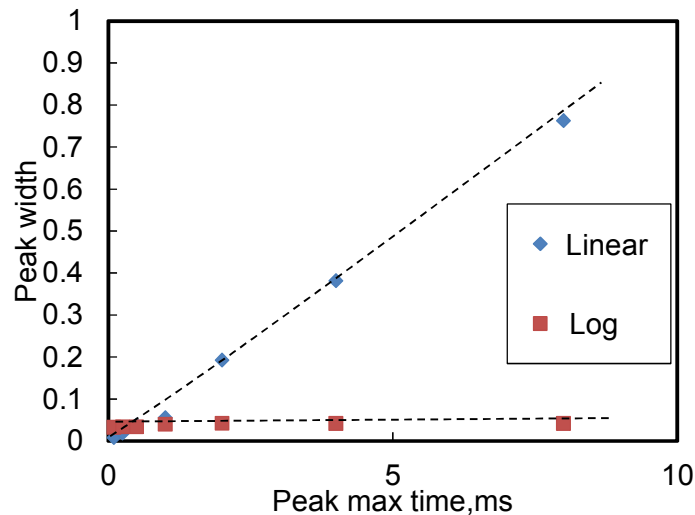
Fig.7.9: The half maximum on linear and logarithmic scale

When the peak position was similar, or full width at half maximum calculated on the logarithmic scale, it is possible to compare the peak width on the different peak position.

7.2 Influence of raw polymer molecular weight on the chain mobility

Before starting the discussion on the crosslinked EPDM rubber, the NMR techniques were applied to the raw EPDM polymers. It is important to find out, how the influence of chain length on the chain mobility delivered by NMR relaxation is.

The different NMR curves correspond to samples with varying molecular weight (Mn: number-average molecular weight g/mol) which was analyzed by GPC. Fig.7.10 (Left) shows the NMR relaxation curves of the several raw EPDM polymers with varying molecular weight.Fig.7.10 (Right) shows the relaxation spectra obtained using ILT method.
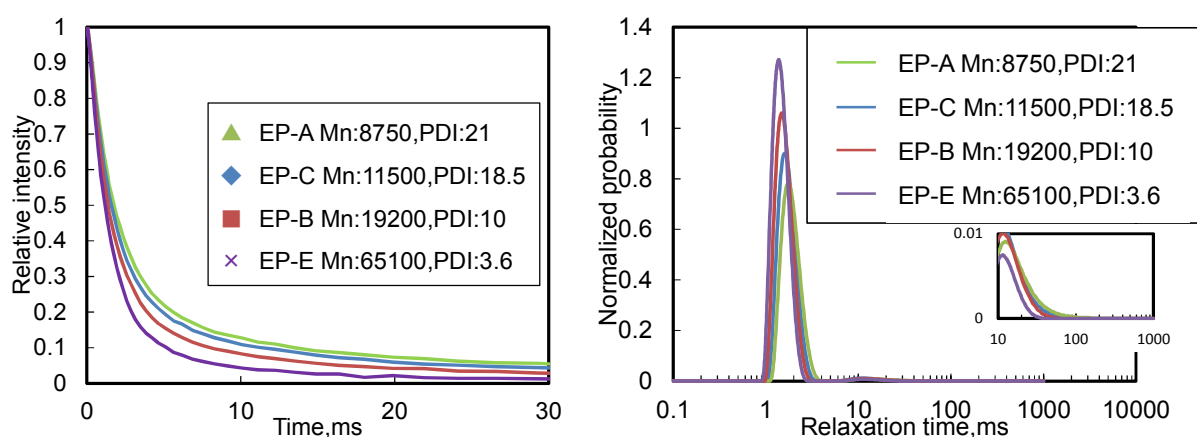
Fig.7.10: NMR relaxation curve of EPDM raw polymer with varying Mn (left),NMR relaxation spectra(right)

The relaxation became faster as the molecular weight increased and the PDI (polymer dispersity index) decreased. PDI is a polymer chain length distribution index and shows a correlation with NMR relaxation behavior.

For a further correlations, the peak max times (Fig.7.11 left) and areas (Fig.7.11 right) of spectra were plotted as a function of molecular weight (Mn) from GPC .
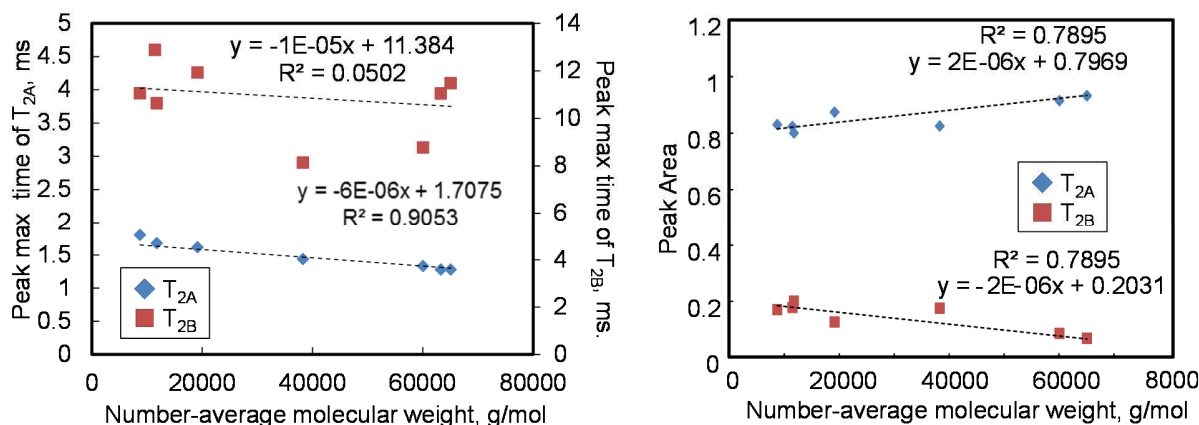
Fig.7.11: Peak max time (left) and peak area (right) of T_{2A} and T_{2B} vs. Number-average molecular weight (Mn) from GPC.

The peak max time of T_{2A} decreased with increasing Mn as shown in Fig.7.11. Whereas the peak area of T_{2A} increased with increasing Mn.

This indicated that higher molecular weight polymer shows higher number of entanglements which resulted in decreased chain mobility due to a restriction of chain movement. In other words, the peak maximum time of T_{2A} correlates with the chain mobility, which is determined by entanglements, whereas the peak area of T_{2A} shows the amount of entanglement. These results are in the good agreement with Folland descriptions [121, 122].

However the peak max time of T_{2B}, which can be associated with dangling chain ends, sees more scattering than the peak max of T_{2A}, as shown in Fig.7.12.
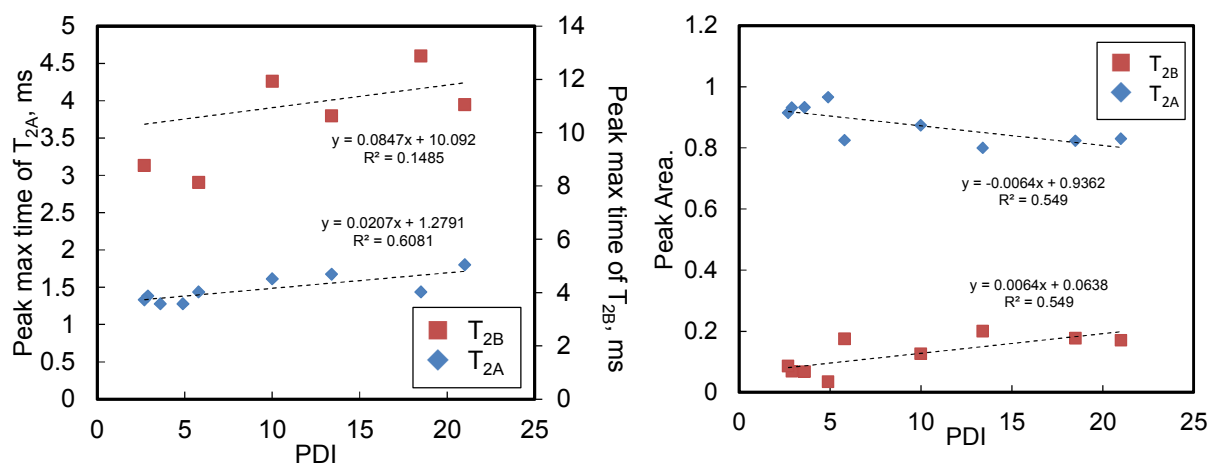
Fig.7.12: PDI from GPC vs. peak maximum time (left) and area (right) of NMR relaxation spectra

This might be resulted from the shape of the chains or their degree of branching because of different microstructures which are from commercially available EPDM polymers used. In other words, even if the molecular weight is same, the degree of branch (and also chain mobility) might be different.

In addition, PDI made a correlation with the peak maximum time, the peak area and the peak width (full peak width at half maximum) of T_{2A} and T_{2B} are shown in Fig.7.13.
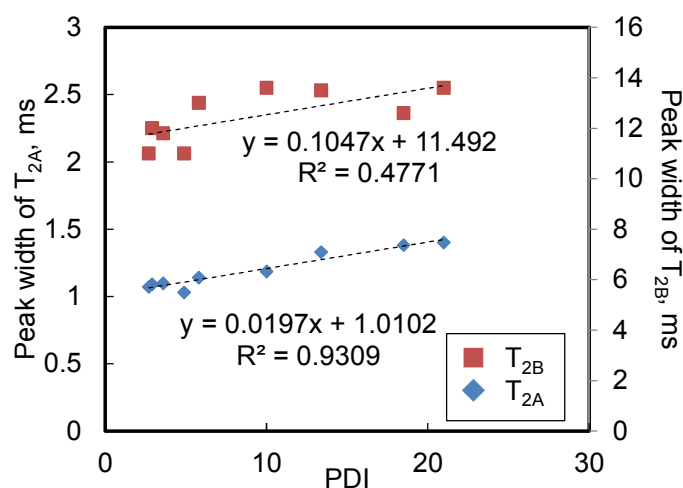
Fig.7.13: PDI from GPC vs. peak width at half maximum of T_{2A} and T_{2B} from NMR relaxation spectra

The peak max time and area did not show a good correlation with PDI from GPC but the peak width of T_{2A} from NMR relaxation spectra correlated well with PDI. These results indicate that the peak width of T_{2A} can represent the distribution of entanglement length since the number of polymer entanglements have a positive relationship with the molecular weight.

However, T_{2B} did not show a good correlation with PDI. This could have the same reason as discussed above. The EPDM polymers are commercial grade materials and vary in the shape of chain ends. Further characterization of chain end shape is needed to able to make a better correlation with the chain mobility. This extends the scope of this work and is addressed in the outlook.

7.3 Influence of crosslinking on chain mobility

7.3.1 NMR relaxation spectra of crosslinked EPDM

So far the discussion was focused on the uncrosslinked polymer structure. This section moves on to the crosslinked structural analysis.

The NMR relaxation curves of EPDM crosslinked rubber are shown in Fig.7.14 (left). The different curves correspond to samples with varying amount of curing agents. The relaxation became faster as the amount of curing agent was increased. Fig.7.14 (right) shows the NMR relaxation spectra by using ILT method. There were two or three peaks in all measurements.
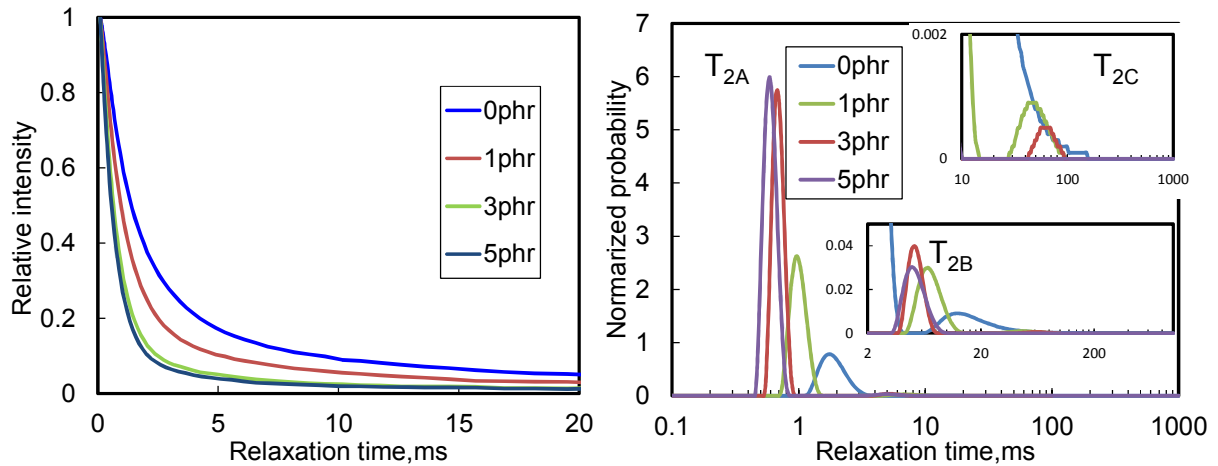
Fig.7.14: NMR relaxation curves of crosslinked EP-A with varying amount of cure agent (left). NMR relaxation spectra with varying amount of cure agent (right).

7.3.2 Characterization of chemical crosslinks

As seen in the discussion above, T_{2A} can be associated with the physical entanglements. In addition, chemical crosslinks, induced during the chemical crosslinking, increased the intensity of T_{2A} as shown in Fig.7.14. This means that T_{2A} can also be influenced by the chemical crosslinks. In other words, T_{2A} represents the sum of entanglements and chemical crosslinks.

The relationship between the T_{2A} peak max of the spectra and crosslink density obtained with the swelling method is plotted in Fig.7.15.
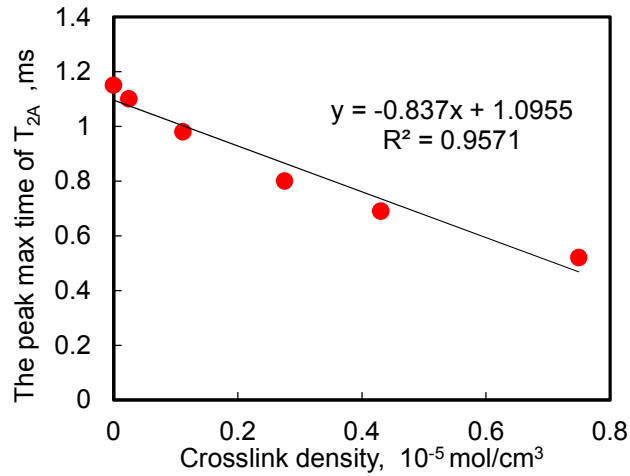
Fig.7.15: T_{2A} obtained by NMR relaxation spectra vs. crosslink density by swelling for crosslinked EPDM

The peak max time of T_{2A} shows a nearly linear relationship to the crosslink density which was obtained using the swelling method. This result is the essential experimental proof that the time of T_{2A} can be an index of the crosslink density and chain length in between crosslinks.

Besides the peak width (full width at half maximum) of T_{2A} was also calculated and plotted vs. crosslink density in Fig.7.16.
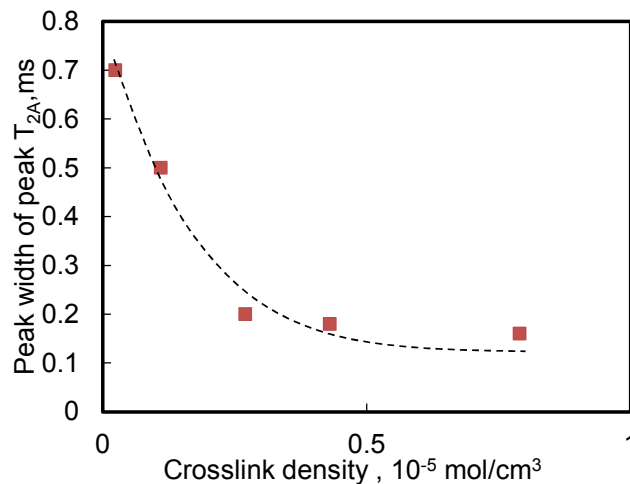
Fig.7.16: Crosslink density by swelling vs. half width at half maximum of T_{2A}

As crosslink density increased, the peak width of T_{2A} decreased. This result can be explained with the crosslink structural change.

In the uncrosslinked state, the relaxation time (T_2) distribution was broad because the chain entanglements have a wide distribution of chain mobility. But by inducing chemical crosslinks, the network changed from physical entanglement to chemical crosslink. This led to reduced chain mobility and a more narrow distribution of chain mobility. This distribution information cannot be obtained from classical exponential fitting of NMR data. Therefore Inverse Laplace transform has a significant advantage.

7.3.3 Characterization of low molecular weight molecules in the crosslinked rubber matrix

Raw polymers have two peaks T_{2A} which is associated with entanglement and T_{2B} which is associated with dangling chain end. However, after crosslinking, a new peak T_{2C} was generated as shown in Fig.7.14 (magnification of graph at right side).

In order to validate the relationship of T_{2C} with the molecular structure, soxhlet extraction of crosslinked EPDM (EP3) was conducted to get rid of the free chains and the extracted material were dried in vacuum and measured using NMR relaxation with ILT.

The NMR spectra before and after extraction are shown in Fig.7.17.
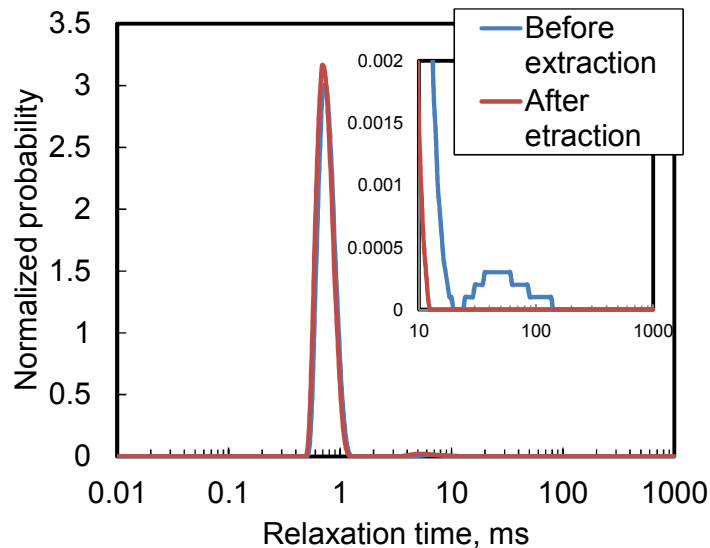
Fig.7.17 : NMR relaxation spectra before and after extraction

After extraction, the T_{2C} peak disappeared. Besides, GPC analysis showed that the polymer originally has apx.183700 g/mol as weight average molecular weight but the extracted polymer has 5800 g/mol as that.

These results indicate that T_{2C} can be attributed from the low molecular weight polymer which is not binding in the crosslink matrix. Therefore T_{2C} positions at higher relaxation time which represents high chain mobility. These free low molecular chain fragments were generated by the chain scission reaction as a side reaction of crosslinking via peroxide. The reaction scheme is shown in Fig.2.8 [123].

Besides, the ratio of the areas of the three peaks is shown in Fig.7.18. The peak area of T_{2A} increased with an increase of crosslink but the peak areas of T_{2B} and T_{2C} decreased. This can be explained with the crosslink structural changes, as described in the next section.
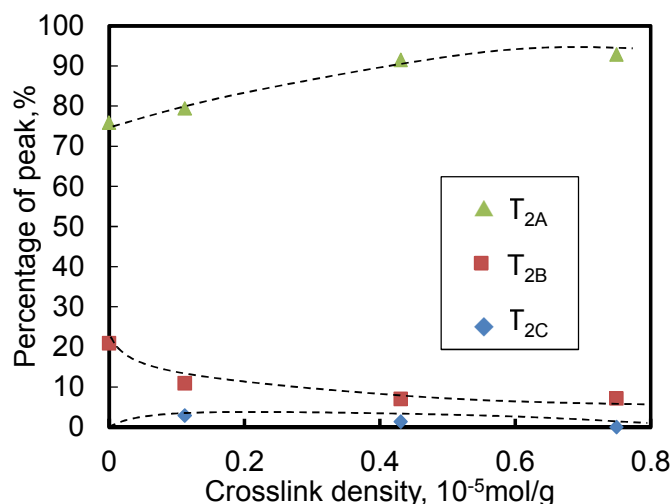
Fig.7.18: Percentage of T_2 peak areas, $T_{2x}/(T_{2A}+T_{2B}+T_{2C})$ as a function of crosslink density

7.3.4 Summary

In summary of this discussion, NMR-ILT enables to describe precisely how crosslink structure is built up during the crosslink reaction .The model of crosslink structure is shown in Fig.7.19.
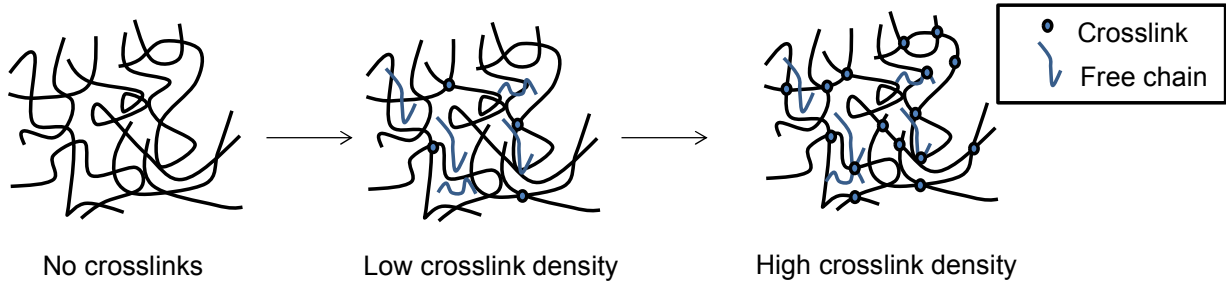
Fig.7.19: Crosslinked network model

1) Raw polymer has chain entanglement (T_{2A}) and chain end(T_{2B}).

2) Peroxide crosslink induced the chemical crosslinks (T_{2A}) and decreased the dangling chain end (T_{2B}).

3) Besides, chain scission, as the side reaction of crosslink reaction with peroxide, led to the formation of free low molecular weight polymer fragments (T_{2C})

4) The more chemical crosslinks were built, the lower number of fragments (T_{2C}). Because these fragments were taken up by the chemical crosslinking.

As the discussion above, NMR-ILT is quite a highly powerful method to analyze the rubber network structure of un-crosslinked and crosslinked elastomer. In addition, by using conventional exponential fitting techniques, the distribution of chain mobility cannot be obtained. Both aspects lead to a significant advantage of the relaxation spectra using ILT. The relationship between rubber structure and peaks, obtained by NMR relaxation with ILT, is summarized below.

Table 7.2: Peak information on rubber structure

Component	Relaxation time, ms	Rubber structure
T_{2A}	Apx. 0.5-2	Chain entanglement
		Crosslink
T_{2B}	Apx. 5-15	dangling chain end
T_{2C}	Apx. 30-200	Low molecular weight free chain

7.4 Rubber structural changes during thermal oxidation

7.4.1 Changes of physical properties during thermal oxidation

As shown above, the results were obtained by NMR relaxation time spectra can describe the unaged rubber structure precisely. In this section, the discussion moves on to the rubber structural change induced by thermal oxidation.

Fig.7.20 shows the crosslink density of unfilled materials determined by the swelling method. The left figure shows the unaged materials with varying amount of crosslink agent. The right figure shows the crosslink density during thermal oxidation at 150°.
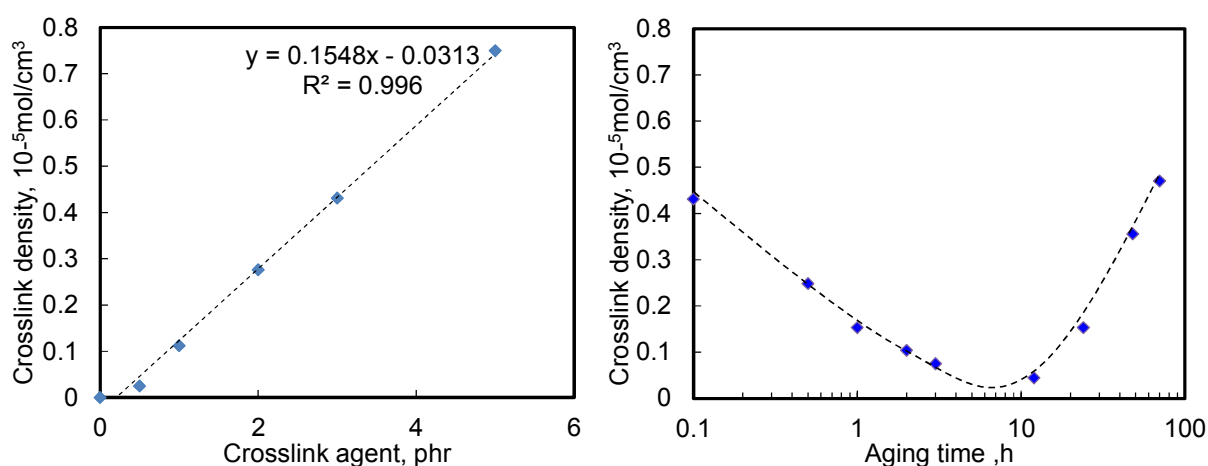
Fig.7.20: Crosslink density varying with crosslink agent (left, basic polymer is EP-A) and cross link density determined by swelling as a function of aging time for EP3.

Even if the crosslink density from the swelling tests between unaged and aged samples show equal value, the actual crosslink structure, structural distribution and partial structural change should be different. This information cannot be obtained by the standard swelling method. Thus the swelling method is a suitable method but has as drawback that the distribution of crosslink structural information cannot be assured.

As additional remark, a careful interpretation is necessary for the aging study regarding the crosslink density using swelling method. Because the degree of swelling depends on the crosslink but also on the polarity of the network. During thermal oxidation, the polarity of the polymer is changed. This might lead to an over or under estimation of crosslink density using constant x parameter in the Flory-Renner equation (6.3).

Therefore, the real crosslink density cannot be observed by the swelling method during the thermal oxidation process. Also in the case of the NMR method, the interaction of proton spins can be influenced by polar groups such as carbonyl functional groups, which evolve during thermal oxidation.

The hardness results during aging are in the good correspondence with the swelling results (Fig.7.20) as shown in Fig.7.21.
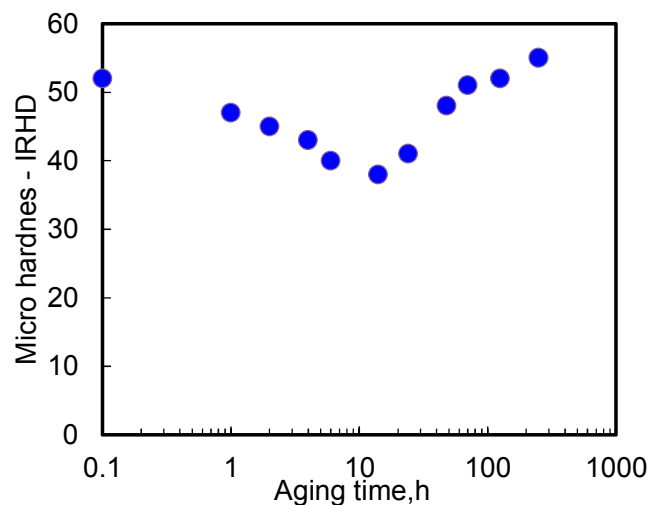

Fig.7.21: Hardness at 150°C as a function of aging time

Initially the hardness decreased and increased later on. This is related to the aging mechanism of thermal oxidation of EPDM polymer. Firstly, chain scission took place and after a certain aging time, the recombination reaction predominated. The formation of new crosslinks led to an increasing hardness. Additional effects can originate from DLO (Diffusion limited oxidation) effect. This means that the results of Micro hardness IRHD can overrate the information of the surface over that of the inside of the material. In an extreme case, the inside of the material can still be in in the original state because no oxygen reaches the core of the material.

In order to deeper understand the changes in crosslink structure during aging process, a powerful alternative state of art to the physical tests approach can be the Inverse Laplace Transformation (ILT).

7.4.2 Changes in crosslink structure during thermal oxidation

As explained in the previous section, apparently when EPDM polymer was crosslinked by peroxide, no changes of the crosslinks could be expected during aging especially due to the high bonding energy of the C-C-bonds. But clearly there was a time dependent change in the radical mechanism of chain scission and further crosslinking by macro radical addition reactions as shown in Fig.4.2 [124].

Chain scission and crosslinking led a decrease and then an increase in hardness. In order to obtain a deeper understanding of the aging mechanism, NMR-ILT technique was applied to crosslinked EPDM (EP3) during aging.

The relaxation time spectra and the corresponding peak times and areas are shown in Fig.7.22, 23 and 24. During the thermal oxidation of EPDM (EP3) for 72 hours, maximum 4 peaks (T_{2A}, T_{2B}, T_{2C} and T_{2D}) can be observed. The relationship between the change of peak max time, area and rubber structural change are described as follows.
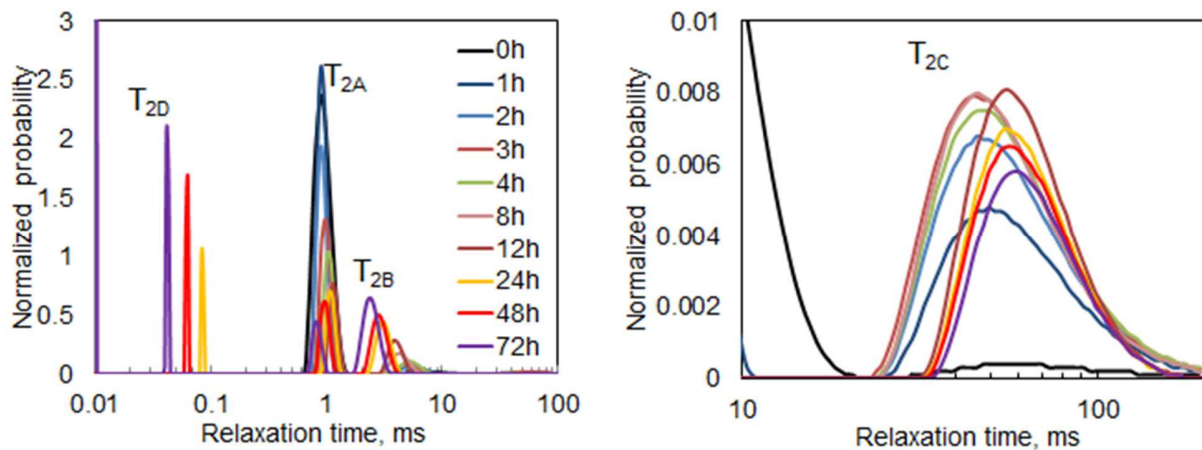
Fig.7.22: NMR relaxation spectra as a function of the aging time (left) and magnification of higher relaxation time (right).
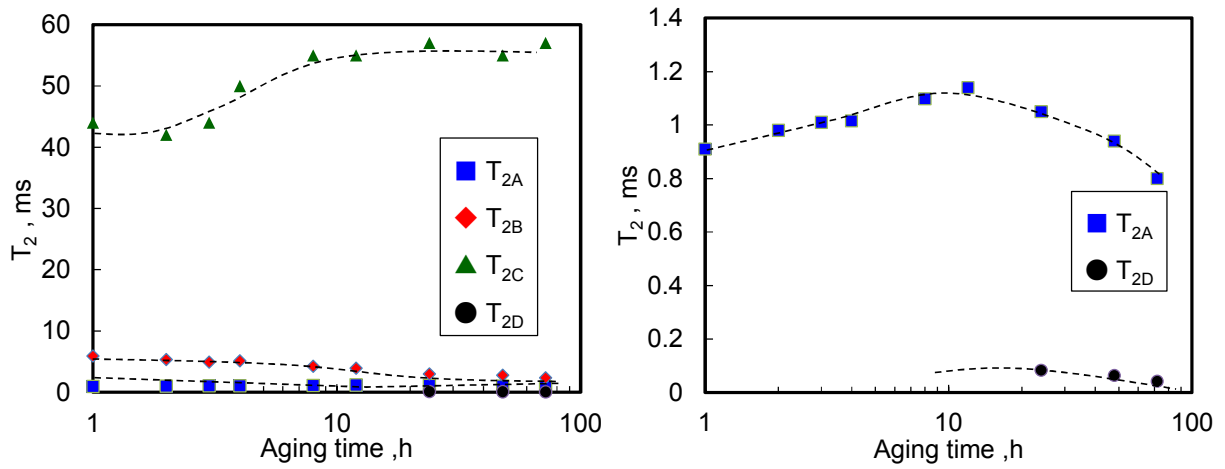
Fig.7.23: Peak max time, after aging for a certain time (left), Magnification around T_{2A} and T_{2D} (right).
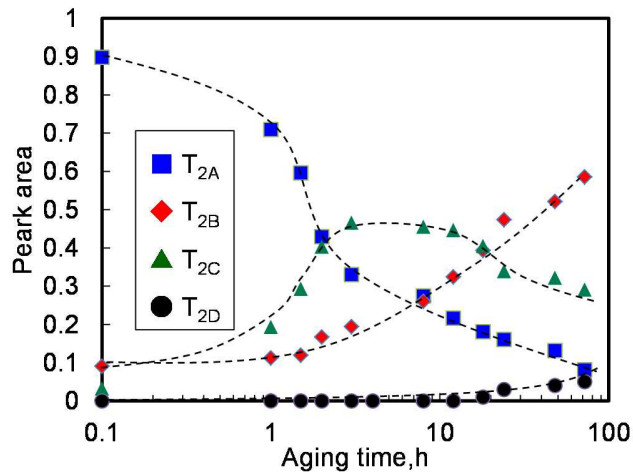
Fig.7.24 :The area of peak after aging for a certain time

For a better understanding of these spectra results, the model structure is introduced as shown in Fig.7.25.
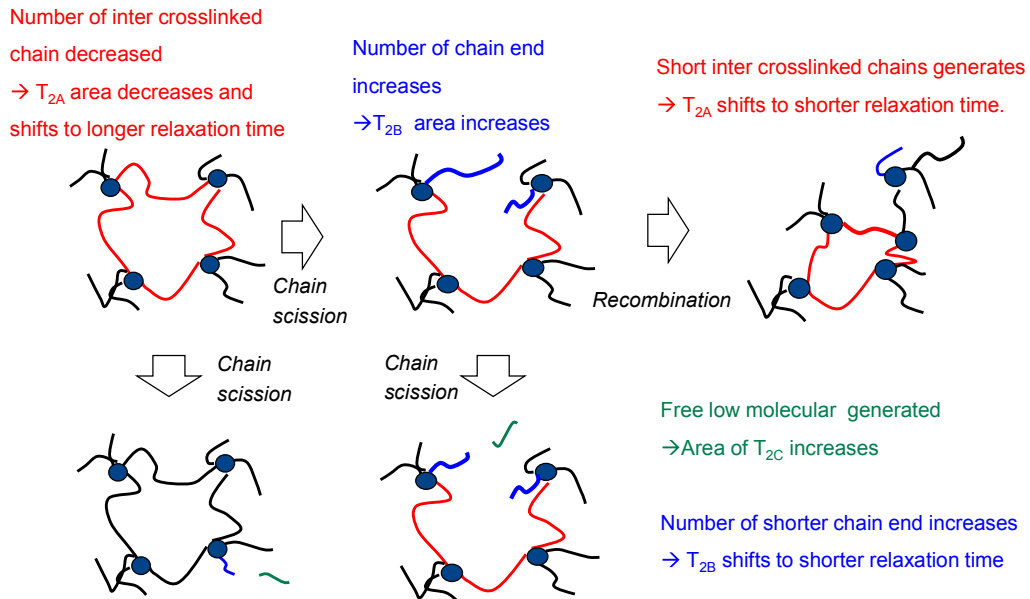
Number of inter crosslinked chain decreased
→ T_{2A} area decreases and shifts to longer relaxation time

Number of chain end increases
→T_{2B} area increases

Short inter crosslinked chains generates
→ T_{2A} shifts to shorter relaxation time.

Chain scission

Recombination

Chain scission

Chain scission

Free low molecular generated
→Area of T_{2C} increases

Number of shorter chain end increases
→ T_{2B} shifts to shorter relaxation time

Fig.7.25 :Schematic model crosslink structural change during thermal oxidation

During aging, the relaxation time of the main peak (T_{2A}), firstly increased and later decreased as shown in Fig.7.23 (right). The shift of the peak maximum time is corresponding to the network structural change such as chain scission followed by post crosslinking. The first increase of the chain mobility (T_{2A} increase) can be associated with chain scission and later decrease of chain mobility (T_{2A} decrease) can be explained by post crosslinking. Besides, the area of T_{2A} continuously decreased as shown in Fig.7.24. The change of T_{2A} area indicate that the initial network irreversibly changed to the several types of structure such as low molecular weight free chain or dangling chain ends because of chain scission reaction.

The relaxation time represented by peak T_{2B} which is associated with chain ends decreased continuously and the area of T_{2B} continuously increased. This can be explained by the fact that shorter chains are generated by the chain scission reaction. Short chain ends are less mobile than longer chain ends and this results in a shorter relaxation time. In addition, apparently the number of the chain ends increased by the chain scission.

The peak max time of T_{2C} increased continuously. This indicates that the chain scission constantly generated the smaller molecular chains as a function of aging time. However T_{2C} area firstly increased and after around 8 hours, the area decreased. The explanation can be that after a certain amount of chains scissions, the small chain fragments might vaporize (thermal desorption) and decrease the amount of T_{2C}.

7.4.3 Free low molecular weight chain fragments induced by aging

In order to validate the assumption of a generation of free chain fragments and correlate T_{2C}. The aged samples were extracted with solvent soxhlet extraction method. The procedure is described in 6.6 soxhlet extraction.
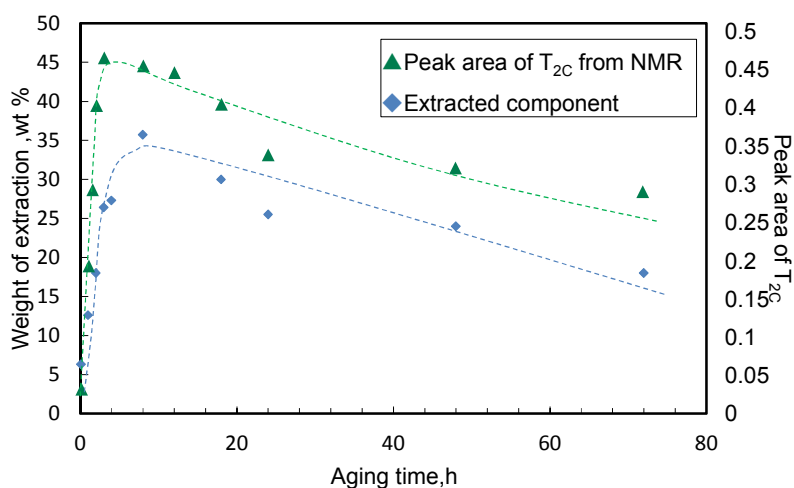

Fig.7.26: Weight loss by extraction and. peak area of T_{2C} from NMR relaxation spectra as a function of aging time.

Both the weight loss and the change of T_{2C} area are in the good agreement. This result indicates at T_{2C} consists of "free" molecules without binding within crosslink network because it is possible to extract by solvent. In addition, the extracted component was measured by GPC and FTIR in order to determine the chemical structure. Fig.7.27 shows GPC chromatograph, RI signal v.s. retention time before and after thermal oxidation. After aging for 128h, the longer retention time was available shorter than 0h.
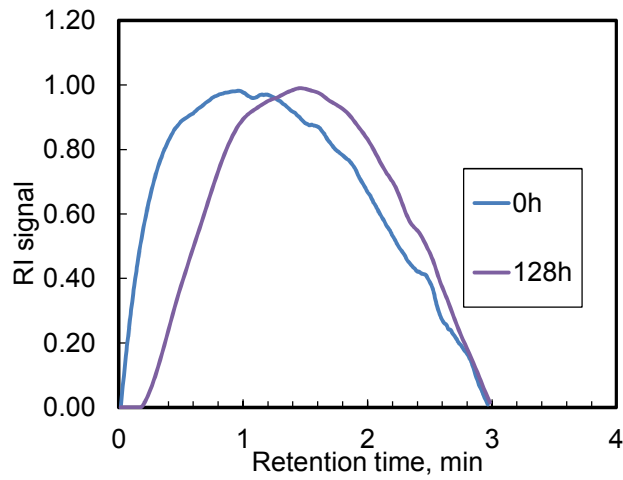
Fig.7.27: GPC chromatograph of extracted components by extraction

Furthermore, Fig.7.28 shows the average molecular weight, of the extracted polymer as a function of aging time. It is seen that the average molecular decreases during aging, indicating that chain scission created smaller length of polymer chain.
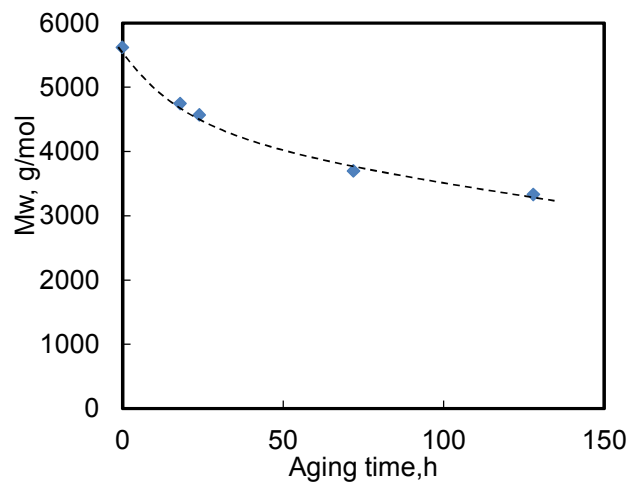
Fig.7.28: Weight average molecular weight (Mw) of extracted polymer from unaged and aged EPDM

Besides, the extracted components were analyzed using FTIR as shown in Fig.7.29.
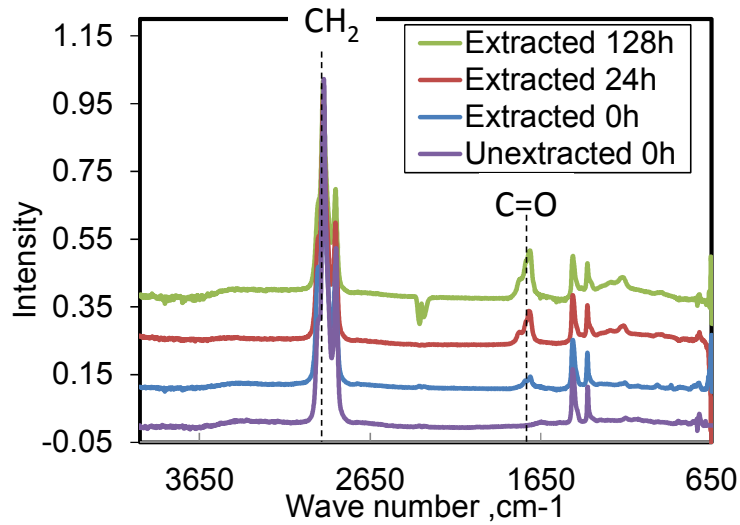
Fig.7.29 : FTIR spectra before and after extraction

Interestingly, the unextracted polymer without aging (see unextracted 0h) did not show carbonyl peak at 1720cm⁻¹ but the extracted polymer from virgin sample show carbonyl peak (see extracted 0h). This could originate from chain scission reaction as a side reaction of peroxide crosslink. In order to interpret the oxidation degree of extracted polymer, Fig.7.30 shows the peak ratio of C=O (1720cm⁻¹)/ CH$_2$ (2920cm⁻¹) of extracted components.
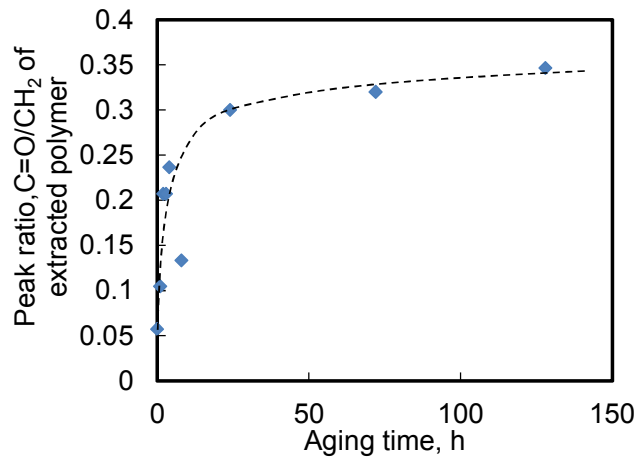
Fig.7.30 : Peak ratio of C=O(1720cm⁻¹)/ CH$_2$(2920cm⁻¹) of extracted polymer as a function of aging time

The extracted polymer could be identified as oxidated chain fragments of the EPDM polymer and the degree of thermal oxidation increased as a function of aging time. This can be led by the chain scission reaction due to the thermal oxidation (Fig.4.2).

These results can strongly support that T_{2C} can be attributed to free short polymer chain fragments which were generated by the chain scission reaction during aging(thermal oxidation) as well as the side reaction of peroxide crosslinking.

7.4.4 New crosslink network induced by aging

At the end of the aging process, another new peak (T_{2D}) appeared in the fast relaxation time regime. This peak can be associated with a new network which is called the secondary network. Several researchers indicated the existence of a new crosslink network with higher crosslinking due to a recombination following the chain scission. Previously, Oikawa demonstrated the existence of an inhomogeneous crosslink network in the aged rubber by means of melting point depression of toluene in the swollen rubber [125, 126]. In addition Fukumori proved the existence of higher crosslinked regions after aging using NMR relaxation with Solid echo pulse program [127]. They both concluded that aged rubber has partial highly crosslinked regions. In other word, although average crosslink density show the same, crosslink density distribution (inhomogeneity of network) can be different due to chain scission and following post crosslink.

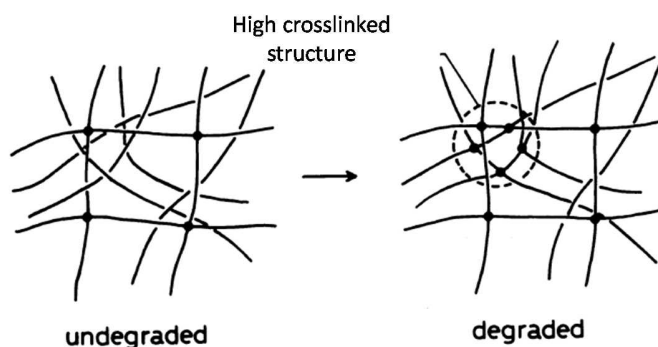A sketch of those highly crosslinked regions is shown in Fig.7.31 [127].

Fig.7.31 : Model picture of chemical structure by Fukushima [127]

The results of T_{2D} are in the good agreement with their results. T_{2D} represents crosslinks with lower chain mobility than that of initial crosslinks.

7.4.5 Activation energy

As discussed, the decreasing area of T_{2A} represented the chain scission of crosslinks, due to the thermal oxidation. So the slope of T_{2A} peak area can be correlated with chain scission speed k by the following equation.

$$\frac{Peak\ area\ of\ T_{2A(t)}}{Peak\ area\ of\ T_{2A(0)}} = \exp(-kt) + A \quad , \quad (7.2)$$

Fig.7.32 (left) shows the relative peak area of T_{2A} at three different temperatures, the activation energy was calculated as 124 kJ/mol from the slope of the plot in Fig.7.32 (right).

Where Peak area of $T_{2A\ (t)}$ is peak area of T_{2A} at aging time t, peak area of $T_{2A\ (0)}$ is the peak area at the initial state. A is a constant value, k is the reaction constant.
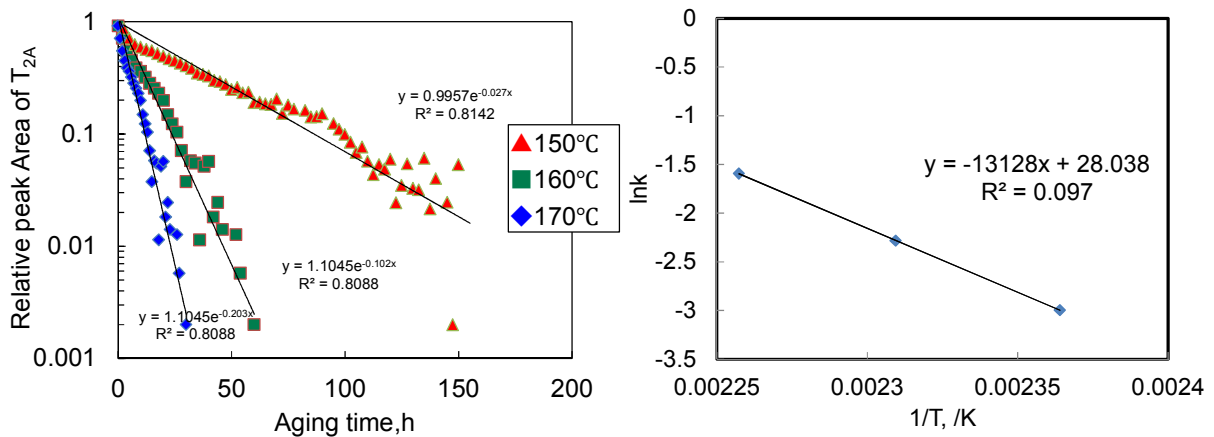
Fig.7.32: Temperature dependency and Arrhenius plot and Arrhenius plot

7.4.6 Summary

These NMR results are in good correspondence to the physical tests such as hardness measurements and swelling tests. Furthermore NMR yields more precise information of the crosslink structure. The results of NMR relaxation indicate the partial structural change of the rubber network during the aging process as visualized in the model shown Fig.7.33.
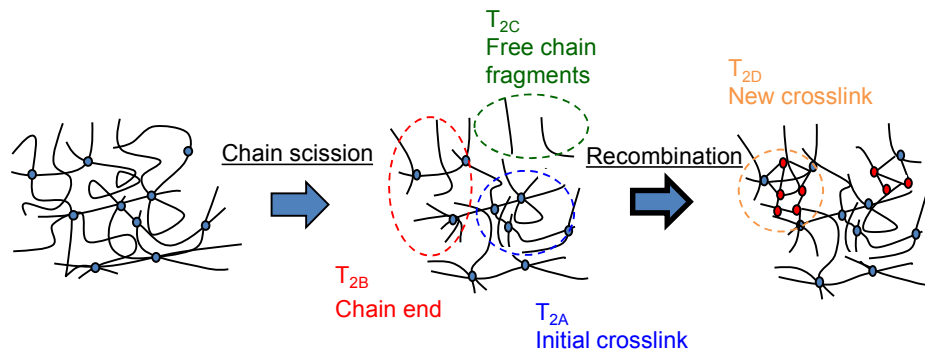
Fig.7.33: Relationship between aging model and peaks of NMR spectra.

7.5. Effect of carbon black fillers on stress relaxation

As described, the crosslink structure changed during the aging process in a complex way. Although the aging process of unfilled material is complex, industrial rubber materials often contain carbon black and carbon black affects the aging mechanism chemically and physically.

The two main targets if this section:

- Understand the crosslink structural change during the stress relaxation in N_2 and air atmosphere.
- Understand the effect of carbon black on the aging process.

7.5.1 Physical stress relaxation of crosslinked and filled EPDM-materials under N_2 atmosphere (anaerobe)

As mentioned above, during stress relaxation in N_2-atmosphere physical relaxation is the dominating process due to the absence or at least reduced concentration of oxygen and therefore negligible amount of chemical relaxation processes. It is true that for short measurement times, at low temperatures or for measurements under specific conditions (such as in N_2 atmosphere or a vacuum [without oxygen]), the relaxation observed closely approximates a logarithmic function of time [43, 128]. All measured data could be approximated by logarithmic regressions. The related force curves (F(t)/F(0)) were fitted with following equation to reveal the speed of stress relaxation.

$$\frac{F(t)}{F(0)} = -k log\left(\frac{t}{h}\right) + A \qquad\qquad (7.3)$$

with the slope k the representative value for the physical relaxation rate, t/h is the experiment time measured in hours and A is a constant value. Fig.7.34 shows the results of mechanical stress relaxation measurements on the EPDM vulcanized samples for varying carbon blacks types (shown in Chapter 6, see above). Besides, k by approximated by fitted results shows in Fig.7.35.
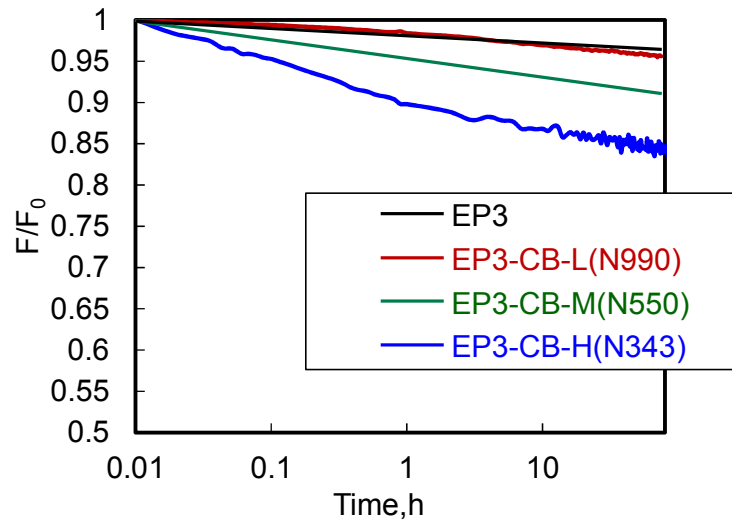

Fig.7.34: Stress relaxation of crosslinked EPDM with varying types of carbon black in N_2 – atmosphere and 150 °C , (F_0=stress at t=0; F= stress at time t)
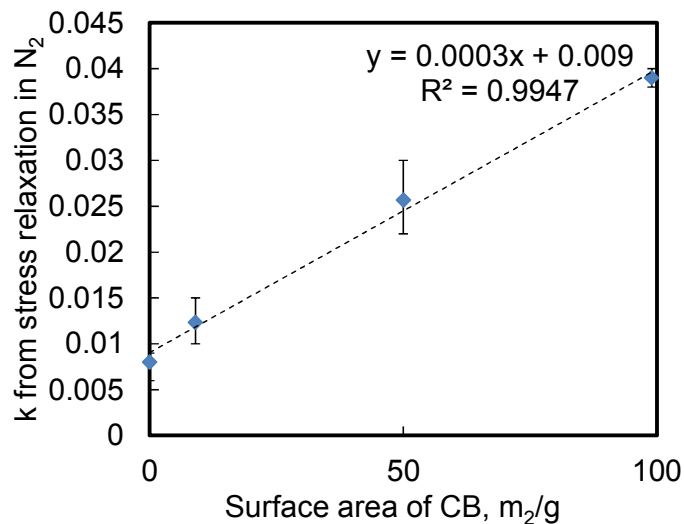
Fig.7.35: Relationship between specific surface of carbon blacks (CB) and k from equation (7.3)

The value of k increases with increasing carbon black surface area in the rubber compound. This result could be attributed to either the chemical network or to the filler network. Due to the inhibitor effect of carbon black on the crosslinking reaction the quantity of polymer entanglements and chemical crosslinks which dominate physical relaxation might therefore decrease regardless of the same crosslinking agent amount and the conditions of vulcanization.. In addition the type of filler is strongly influencing the filler-filler- or polymer-filler interactions. If the material maintains a certain force, however, the filler-filler or filler-polymer bonds would gradually be destroyed, and the counterforce would drop as a function of time

7.5.2 Effect of filler on uncrosslinked materials using low field NMR

The effects out of stress relaxation experiments can be investigated deeper by low field NMR investigations. Since NMR is sensitive to polymer chain mobility which can be changed due to chemical crosslinking, but as well for filled systems by physical or chemical adsorption of chains onto the filler surface, the two effects have to be separated first. Since crosslink density has an enormous effect on NMR resultsthe interaction between filler and polymer was investigated using uncrosslinked material. Fig.7.36 shows the NMR relaxation curve and NMR relaxation spectra. It can be seen that relaxation accelerates very slightly with increasing carbon black surface area. This can be explained by the restricted mobility of polymer chains adsorbed on the filler surface.
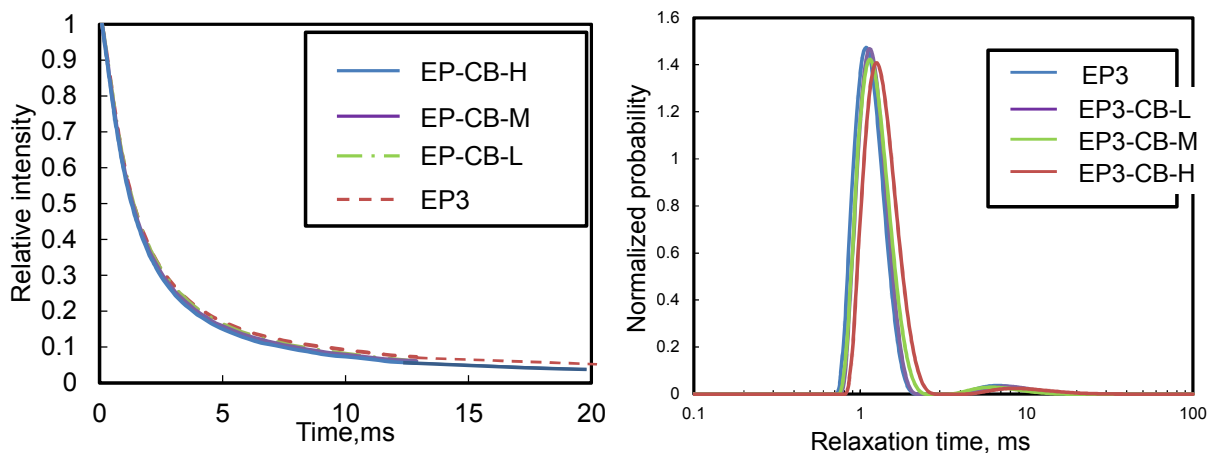

Fig.7.36 :NMR relaxation(left) and NMR spectra (right) of uncrosslinked materials varying type of carbon black(H:N343, M:550, L:N990) crosslinked

In sum, the differences of filler and specific filler surface in uncrosslinked EPDM are much smaller than in comparison to the filled crosslinked materials (see next section). With increasing specific surface of the carbon black, chain mobility nonetheless shows a downward trend.

7.5.3 Effect of fillers on the chain mobility of crosslinked materials measured by NMR

As described in the previous section, the rate of physical relaxation during the stress relaxation experiment is generally determined by the quantity of polymer entanglements. It could be reduced by increasing chemical crosslink density. To arrive at an understanding of the relationship between physical relaxation (disentanglements) / chemical relaxation (chain scissions) rate and crosslink structure, the NMR with the ILT technique was applied to unfilled and filled crosslinked EPDM. Fig.7.37 (left) shows the magnetic decay curves of EPDM compounds with different carbon black types. NMR relaxation becomes slower as the carbon black surface increases. Fig.7.37 (right) shows the NMR relaxation spectra calculated from the curves.
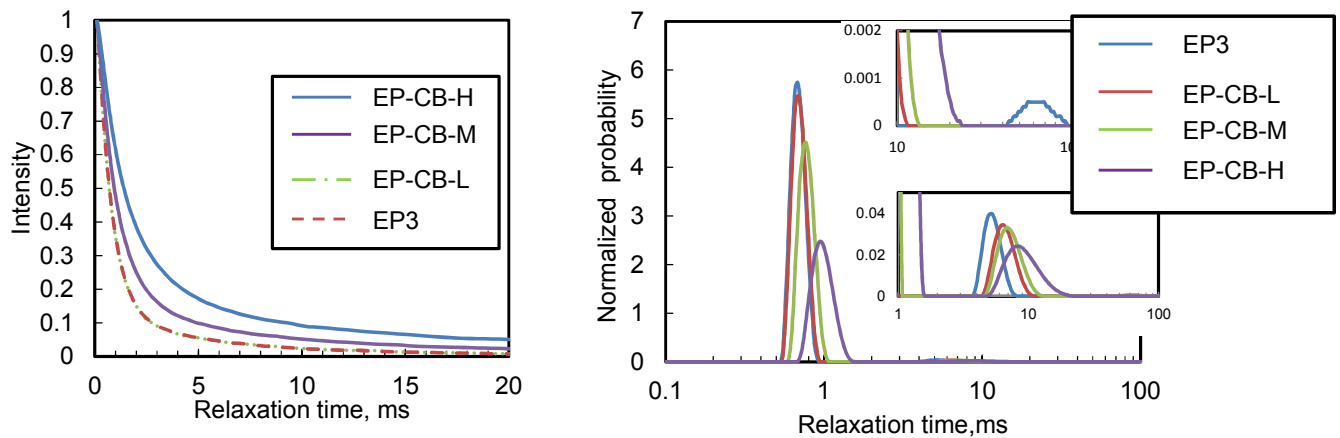
Fig.7.37: NMR relaxation(Left) and NMR relaxation spectra(Right) varying with different types of carbon black(H:N343,M:550,L:N990)

Each sample shows two or three peaks. The relaxation time is estimated from the peak maximum and leads to an T_{2A} of approx. 1ms and T_{2B} of approx. 10 ms. In the case of the unfilled material, an additional small peak T_{2C} at approx. 80 ms can be observed. This results from the curing reaction using peroxide, where the side reaction induces a ß-redistribution with chain scission and formation of a radical of the polymer with smaller molar mass as the

discussion above. T_{2C} was not observed, however, in the case of the filled materials. This may be connected to carbon black's inhibitor effect on chain scission.

Fig.7.38 shows the peak maximum time and area to be a function of the carbon black surface area.
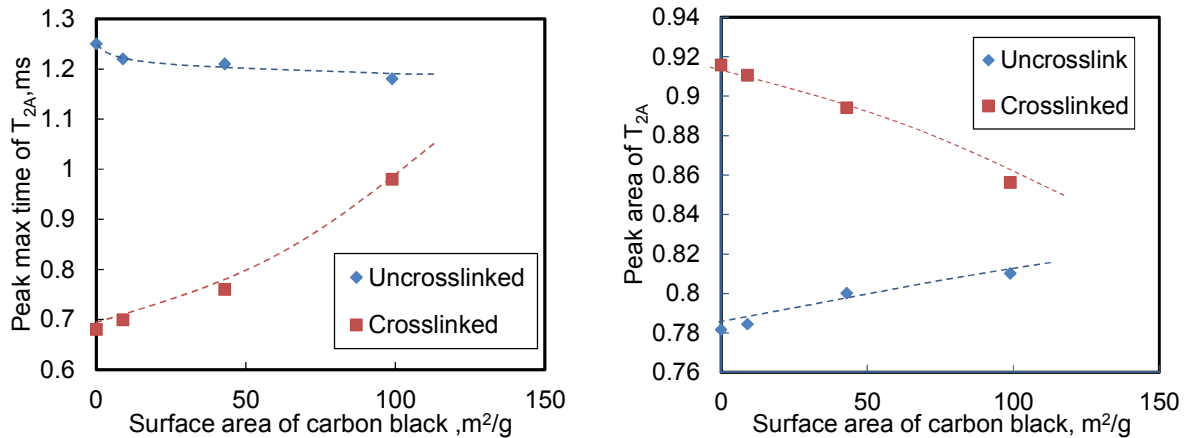

Fig.7.38: Relationship of peak max time(Left) and peak area (Right) of T_{2A} and surface area of carbon black for crosslinked and uncrosslinked EPDM

In the case of the uncrosslinked material, the peak maximum gradually decreases (chain mobility decreases) and the T_{2A} area increases as a function of carbon black surface area due to filler and polymer interaction and absorption of free chain ends on the filler surface. The T_{2A} area represents the immobile phase. In the case of crosslinked materials, on the other hand, an increase in the carbon black surface area correlates with an increase in T_{2A} peak maximum time (an increase in chain mobility) and a decrease in T_{2A} area. One reason for this is the inhibitor effect carbon black has on crosslinking due to of adsorption of crosslinking chemicals or the filler particles acting as spacers between the polymer chains.

7.5.4   Chemical stress relaxation in air on crosslinked EPDM

When performing stress relaxation experiments in air at 150°C, a logarithmic decay of the stress is observed only at the very beginning of the test (< approx.1h). Later on the shape of the decay curve changes and undergoes a sharp decrease as shown in Fig.7.39.
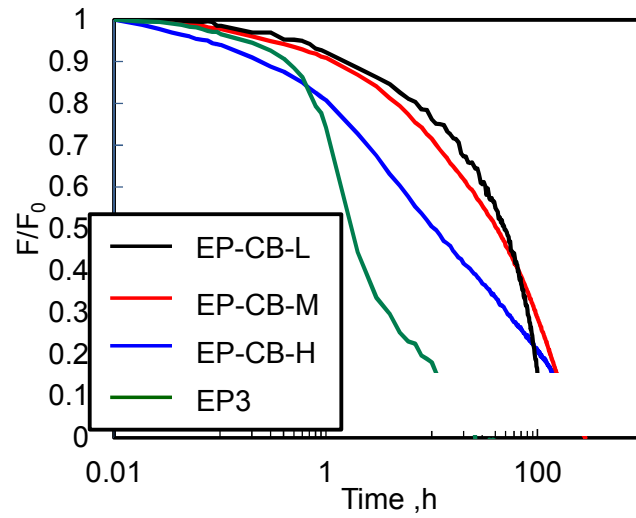
Fig.7.39: Stress relaxation of crosslinked EPDM depending on the type of carbon black in air at 150 °C(H:N343,M:550,L:N990)

To determine only the amount of chemical relaxation, the contribution of physical relaxation as determined by stress relaxation experiments in N_2, has been subtracted from the original experimental data in air resulting in the chemical relaxation curves depicted in Fig.7.40.
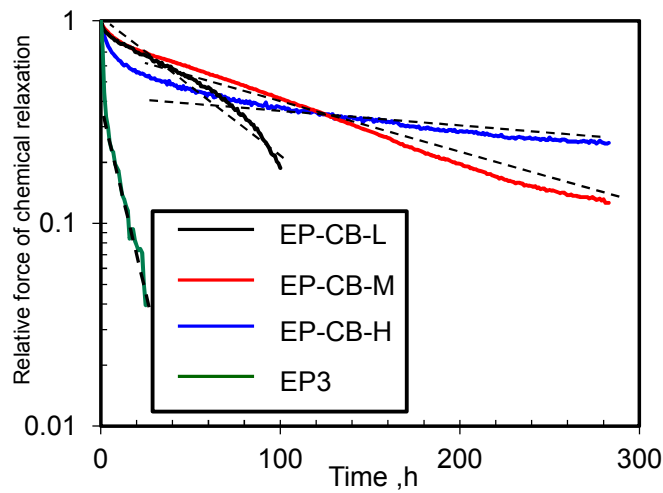

Fig.7.40: Chemical relaxation curves calculated by subtracting the stress relaxation in N_2-atmosphere from the stress relaxation in air (H:N343, M:550, L:N990)

In order to compare the chemical relaxation speed, the characteristic aging time constant can be defined as an exponentially decreasing variable dropping from an initial force .The characteristic aging time constant $\tau_{aging\,CSR}$ can be estimated by fitting with the following function.

$$\frac{F(t)}{F(0)} = \exp\left(-\frac{t}{\tau\,aging\,CSR}\right) + A$$
           (7.4)   (CSR: Chemical stress relaxation)

with *F(t)* the force at aging time, *F(0)* the initial force, t the experiment time and *A* a constant value. According to Tobolsky, the rate of chain scission can additionally be determined via the slopes of the chemical stress relaxation curves (linear part at short times) [32, 129, 130]

Fig.7.41 shows the influence that the surface area of carbon black has on $\tau_{aging\,CSR}$ resulting from equation (7.4).
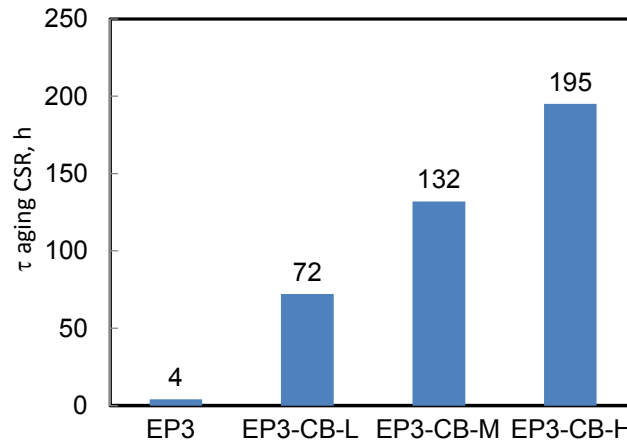
Fig.7.41: Relationship between the surface area of carbon black (H:N343,M:550,L:N990)and $\tau_{aging\,CSR}$, from equation (7.4)

$\tau_{aging\,CSR}$ increases with increasing carbon black surface area. In other words, high active carbon black inhibits the degradation of the polymer.

7.5.5   Correlation between chain mobility evaluated by ILT (Inverse Laplace Transformation) from low field NMR measurements and aging

The evaluation of the NMR relaxation data by ILT technique was applied to EPDM compounds during aging in air. All the results were obtained using the same samples as described in the previous section without any stress or deformation and aged only in air at

150 °C. Fig.7.42, 7.43 and 7.44 show NMR relaxation using ILT for unfilled, middle active (EP3-CB-M) and high active (EP3-CB-H) filled materials during aging in air.
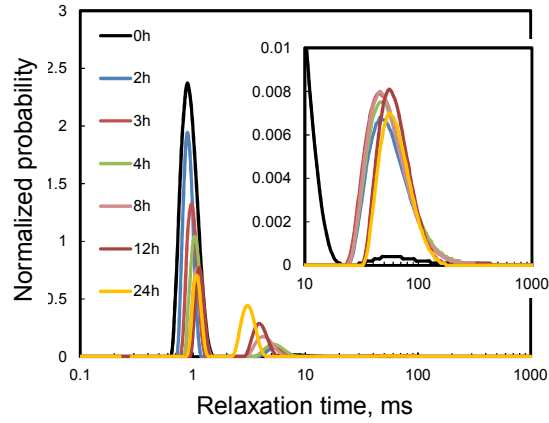

Fig.7.42: NMR relaxation time spectra of EP3 (unfilled crosslinked EPDM) aged at 150°C in air
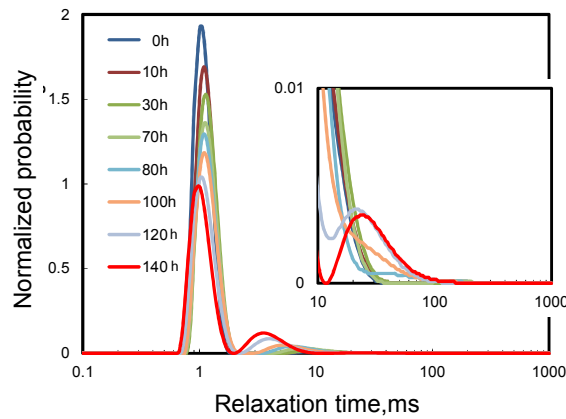

Fig.7.43: NMR relaxation spectra of EP3-CB-M (filled crosslinked EPDM with N550) aged at 150°C in air.
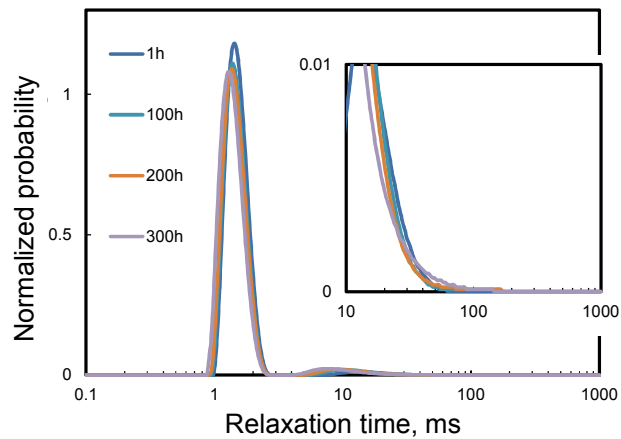
Fig.7.44: NMR relaxation time spectra of EP3-CB-H (filled crosslinked EPDM with N345) stored at 150°C under air.

All materials show a decreasing maximum of the T_{2A} – peak during aging. The T_{2B}_peak behaves vice versa. Besides that, in the case of the unfilled material, the T_{2C} –peak around 80ms was observed and increased as a function of aging time as shown the magnification of the spectra in Fig.7.42, 43 and 44. This means that the initial crosslink part (T_{2A}) is changed irreversibly into several types of structure, such as short chains (T_{2B}) or free chains (T_{2C}) due to the chain scission caused by thermal oxidation as mentioned above section.Fig.7.45 shows the peak area corresponding to T_{2A} as a function of aging time for unfilled and filled EPDM .
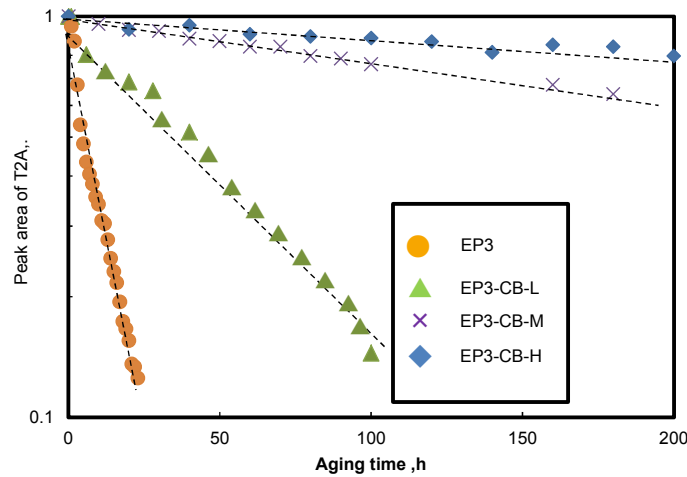

Fig.7.45: Peak area T_{2A} depending on the type of carbon black type v.s. aging time at 150 °C

In all cases the peak area is decreasing with aging time. The more active the carbon black the smaller is the effect. Besides that, the area changes approximately in an exponential way. So a characteristic aging time constant $\tau_{aging\ NMR}$ can be attributed as shown in equation (7.5) using the same approach as in the analysis of the chemical stress relaxation results in the previous section.

$$\frac{Peak\ area\ of\ T_{2A(t)}}{Peak\ area\ of\ T_{2A(0)}} = \exp\left(-\frac{t}{\tau_{aging\ NMR}}\right) + A \quad (7.5)$$

with *peak area of $T_{2A}(t)$* is the peak area of T_{2A} at experimental time t, peak area of $T_{2A(0)}$ is the initial peak area, and *A* is a constant value. The characteristic aging time constant $\tau_{\text{aging NMR}}$ is shown in Fig.7.46.
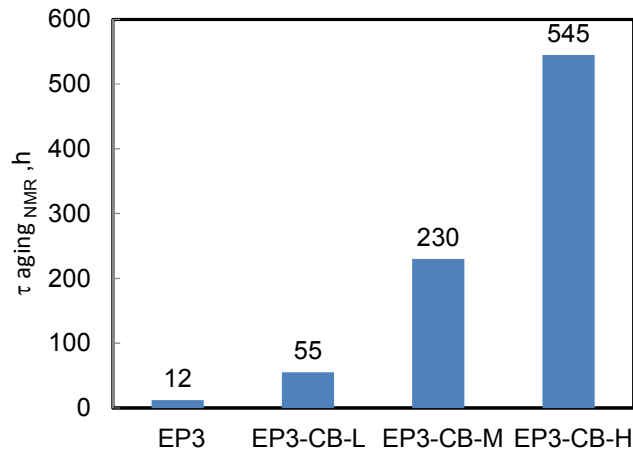

Fig.7.46: Characteristic aging time constant $\tau_{\text{aging NMR}}$ resulting from equation (7.5) for different types of carbon black

Fig.7.47 shows the correlation of the characteristic aging time constant delivered by NMR and chemical stress relaxation.
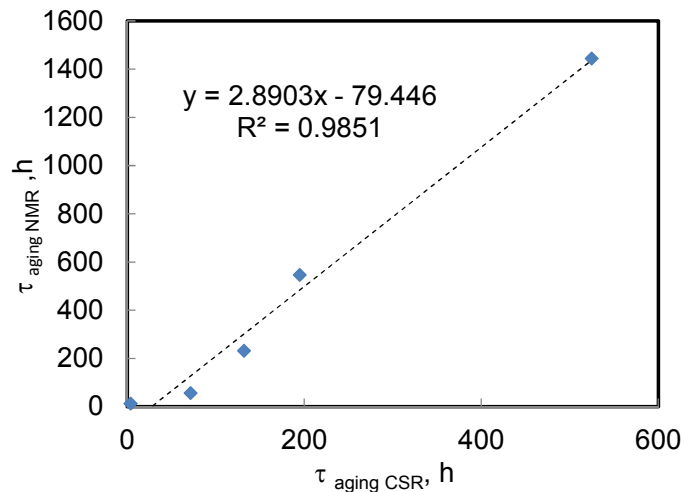

Fig.7.47: Correlation of relaxation time from chemical stress relaxation and from NMR

Obviously there is a good correlation between both methods. However, the absolute values of characteristic aging time constant from the two methods differ. This could be caused by the

geometry of sample or aging condition (exposure of air) For this point to clarify, further investigation is necessary.

Additionally to the peak area also the position of the peak maximum can be analyzed in more detail. In Fig.7.48, the peak maximum time for T_{2A} is plotted vs. the aging time for the different filled and unfilled samples.
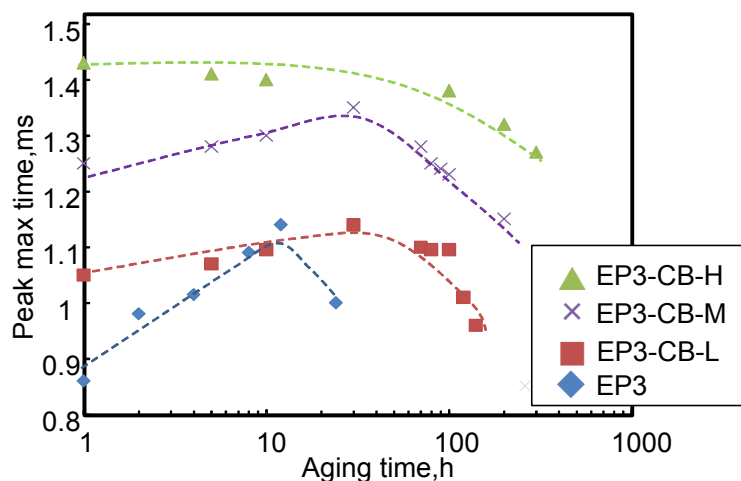

Fig.7.48: Peak maximum time of T_{2A} for various types of carbon black vs. aging time at 150 °C

As can be seen the dependencies depend to high extend on the type of filler. For the unfilled and filled materials with low active or middle active(EP3-CB-M) carbon black there is an increase in the peak maximum time of T_{2A} at shorter time from the stat of test, which is resulted by chain scission. At longer times a decrease of the peak maximum time of T_{2A} sets in which might be due to post-crosslinking. Apparently, two competitive effects are observed: chain degradation and aging induced cross linking. The type of carbon black has an influence on the kinetics of both processes. The time where the change in the behavior is taking place seems to be filler type dependent but is not increasing with the filler surface area. In addition, in the case of the high active carbon black, the peak maximum shifts directly to shorter times. The reason is not clear up to now and gives rise to future research.

7.5.6   Summary

Low field ^{1}H NMR with inverse Laplace transform and stress relaxation both provide suitable methods for examining the aging process of EPDM. This NMR technique contributes to a better

understanding of the results of stress relaxation. The characteristic aging time constant estimated on the basis of the results of stress relaxation and NMR correlate closely, both showing an increase in relaxation times with increasing carbon black filler surface area.

What is more, the surface area of carbon black has a strong influence on the stress relaxation mechanism. By means of low field NMR measurements, it could be observed that carbon black works to inhibit thermal oxidation. NMR can thus be helpful in understanding the degradation mechanism and in predicting the lifetime of seals.

7.6. Effect of ethylene - propylene ratio of EPDM polymer on stress relaxation

7.6.1 Partial crystallinity of EPDM rubber

The main topic in this section is the investigation of the effect of the ethylene –propylene content of EPDM on the stress relaxation and the characterization of the rubber structural change during aging using NMR-ILT.

The partial crystallinity of in the rubber matrix should also be an important influential factor on aging. A high ethylene content (e.g.70%) of EPDM polymer leads the partial crystalline.

A. Kömmling et al concluded that a higher ethylene content resulted in an increase of the aging resistance of EPDM. This improvement was attributed to both a higher crystallinity that inhibits oxygen diffusion as well as a smaller number of chain scissions which occur in the propylene units [131].However, the investigation focus is on the chemical stability against thermal oxidation. The diffusion effect of oxygen is absolutely important for the aging process but it exceeds the scope of this work (refer to the outlook). Therefore, the melting point of partial crystalline of EPDM was measured using DSC (Differential scanning calorimetry) and the aging temperature was chosen to be above the melting point of the crystalline of EPDM to get rid of the crystalline effect. At the aging temperature 150°C, the crystalline was solved and the rubber structure could be considered as amorphous. DSC curves are shown in Fig.7.49.
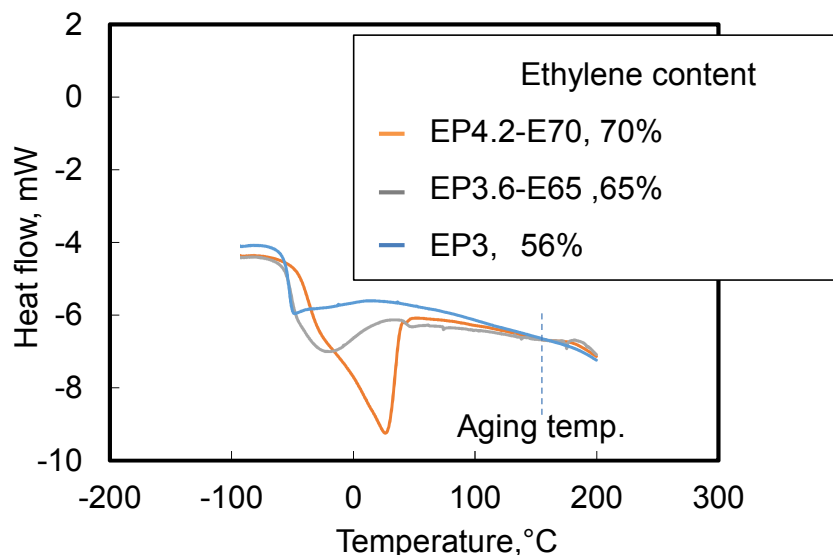

Fig.7.49: DSC curves of EPDM rubber with varying different amount of ethylene /propylene ratio

7.6.2 Effect of ethylene content on stress relaxation

When the ethylene-propylene content of EPDM polymer is changed, the different crosslink densities of materials should vary since propylene has higher reactivity with peroxide crosslink agent than ethylene. Therefore, in order to obtain the same crosslink density among samples which have different ethylene propylene content, calibration line of crosslink density was created as follows. The raw polymers are incorporated with different amount of peroxide crosslink agent and vulcanized. Fig.7.50 gives the crosslink densities of the samples measured using the swelling method.
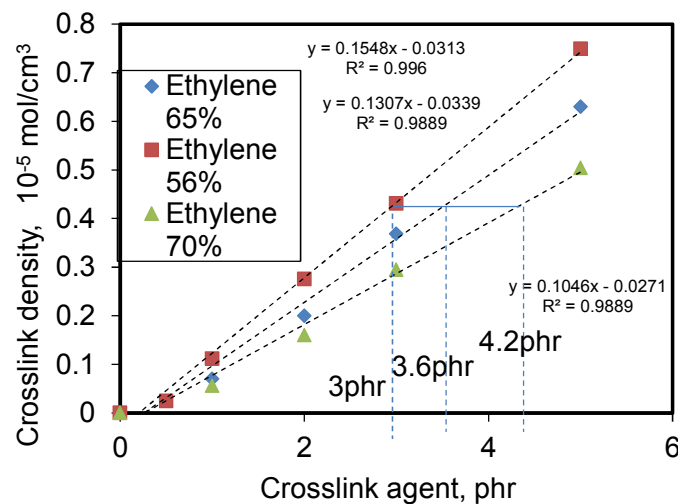
Fig.7.50: Crosslink agent concentration v.s.crosslink density of EPDM which different ethylene Content

So the amount of crosslink agent could be optimized to provide the same crosslink density (apx 9.0×10^{-5} mol/cm^3). When the crosslink agent amount of 3phr for ethylene 56%(This is the standard material EP3) is used, 3.6phr for ethylene 65%(EP3.6-E65) and 4.2phr for ethylene 70%(EP4.2-E70) ,the crosslink density of each materials can be considered as same. These materials were used for the following experiments.

Fig.7.51 shows the stress relaxation test in air at 150°C. An increase of the ethylene content shows a slower relaxation in air.
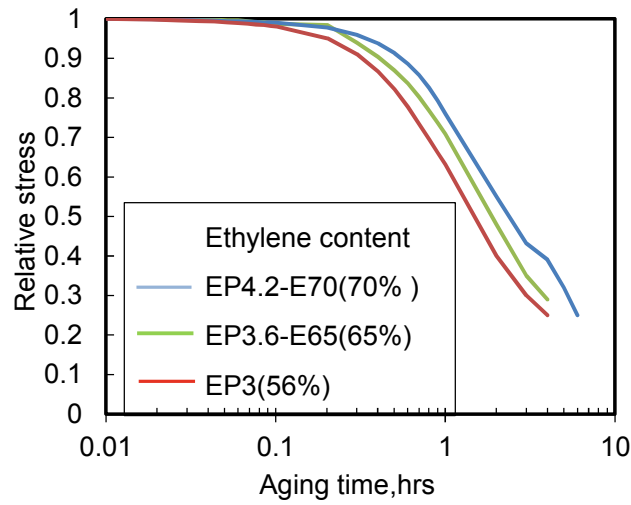
Fig.7.51: Stress relaxation of EPDM with varying ethylene content in air at 150°C

Besides, the characteristic aging constant can be calculated with the equation (7.5) using the same approach as in the previous section and results show Fig.7.52.
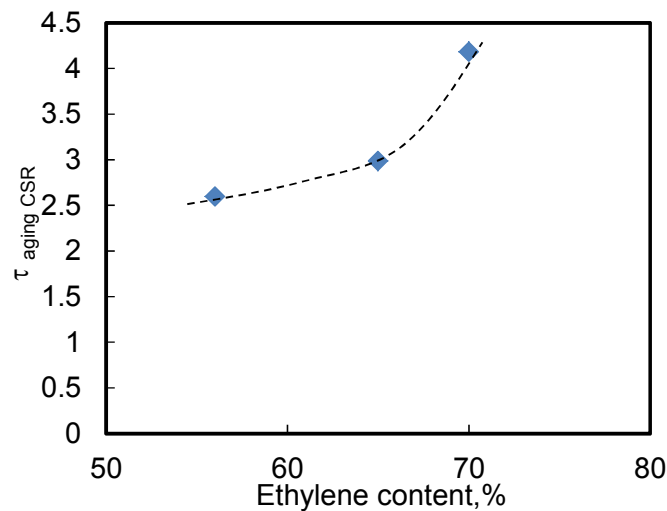

Fig.7.52: Characteristic aging constant (τ) from stress relaxation

In this case, the subtraction of physical relaxation was not applied (see previous section). Because in this case the effect of physical relaxation on the test results was significantly smaller than that of chemical relaxation.

In general, thermal oxidation of poly olefins such as polyethylene , polypropylene and EPDM can be described as a radical chain reaction which degrades the polymer chains and generates different short chain segments [132]. This process is common for both polymers polyethylene and polypropylene. However, normally the rate of the oxidation of polypropylene is higher than of polyethylene. This is a result of the different chemical reactivity. The radical stability of a polyolefin increases in the order methyl < primary < secondary < tertiary. This means that the tertiary carbons of polypropylene can react more easily with radicals than the secondary carbons of polyethylene. As a result, the activation energy of the thermal oxidation of polypropylene (92kJ/mol) is lower than that of polyethylene (117-145 kJ/mol, depending on the degree of crystalline of the materials) [133]. This explanation is in good agreement with stress relaxation results.

7.6.3 Effect of ethylene content on crosslink structural changes during the thermal oxidation

For a better understanding of the stress relaxation results, NMR relaxation with the ILT technique was applied to the EPDM compounds with varying ethylene and propylene contents, during aging. Fig.7.53 gives the NMR relaxation with ILT magnifying the peak of T_{2A}.
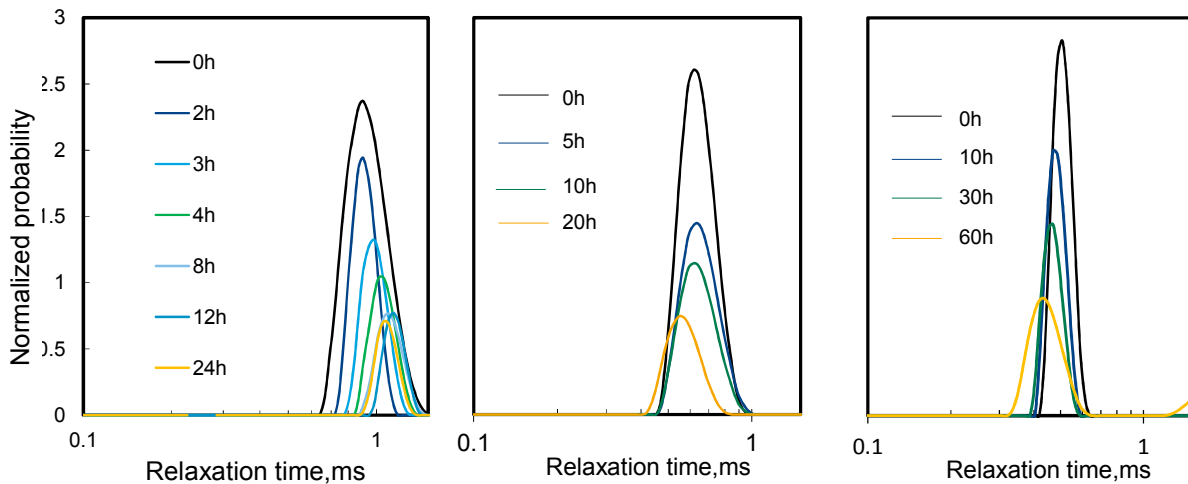

Fig.7.53: NMR relaxation spectra of T_{2A} (left: EP3 Ethylene 56%, middle EP3-65 Ethylene 65%, right: EP3-70 Ethylene 70%)

Besides, the T_{2A} area was plotted logarithmically against the aging time as shown in Fig.7.54.
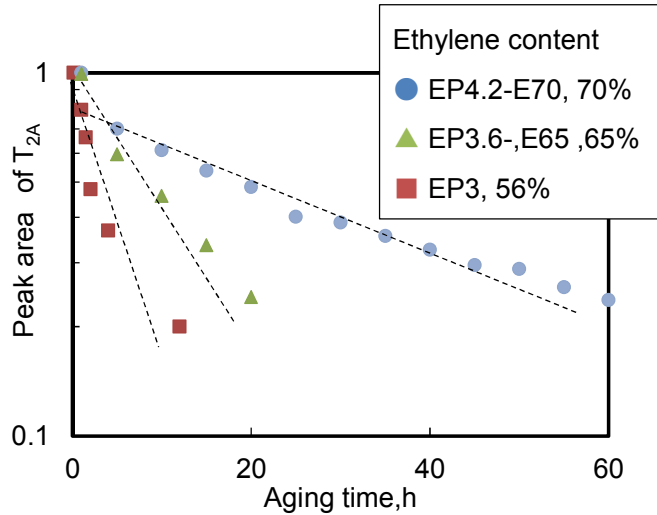

Fig.7.54: Peak area of T_{2A} as a function of aging time

In order to determine the characteristic aging constant, equation (7.5) was used and the results are shown in Fig.7.55 (left) and the relationship of characteristic aging constant between two methods is shown in Fig.7.55 (right).
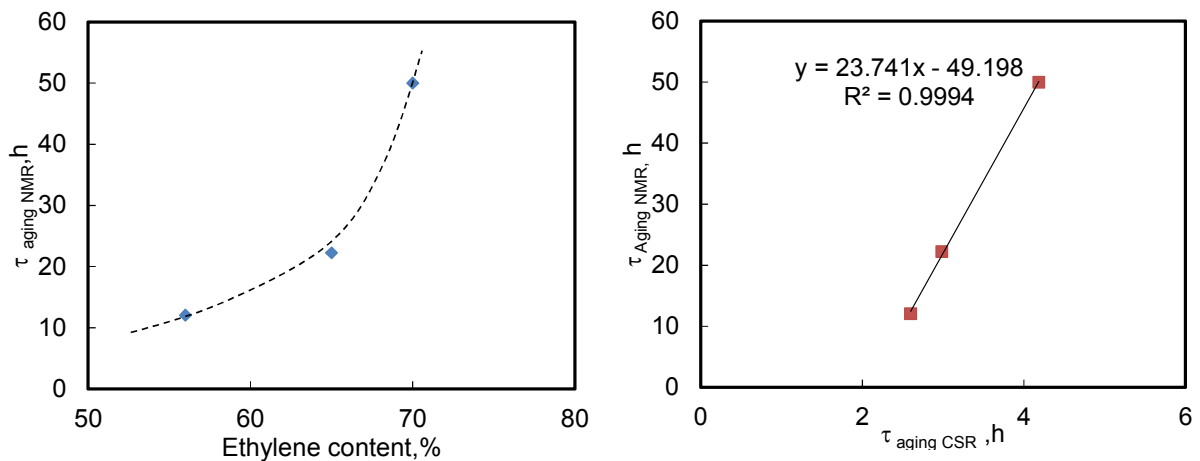

Fig.7.55 : Ethylene content vs. τ aging NMR from NMR (left),Characteristic aging time constant τ

from NMR and continuous stress relaxation (CSR) (right):

The results showed that a decrease of the ethylene content (increase of polypropylene) led to a higher speed of degradation of the crosslinks, (lower resistance against thermal oxidation). Besides, the characteristic aging time constant τ from NMR and continuous stress relaxation are in a good agreement as being discussed in the previous section. The influence of an increase in ethylene content can be explained by differing the radical stabilities of the propylene and ethylene as discussed above.

7.6.4 Summary

Form the results of both stress relaxation and NMR-ILT, it is concluded that a higher ethylene content leads to a higher stability of EPDM rubber against thermal oxidation. The findings are in good agreement with the different chemical relativities of the ethylene and propylene with oxygen.

7.7 Effect of crosslinking on stress relaxation

The main topics in this section are:

- The effect of insufficient crosslinking in, e.g. the influence of residual peroxide crosslink agent on the stress relaxation and rubber structural change due to aging.
- The effect of co-agent on the stress relaxation and rubber structural change due to aging.

7.7.1 Insufficient crosslinking

A certain amount of peroxide crosslink agent sometimes remains in the crosslinked rubber due to insufficient crosslink reaction or overloaded crosslink agent. The residual peroxide content has a key influence on the thermal oxidative stability of elastomers. In order to evaluate the effect of residual peroxide in the crosslinked rubber, several materials varying the degree of crosslink, using the same compound recipe of EP3 were prepared. The insufficient crosslinked samples were created by stopping the crosslink reaction at t80, t90 and t97 (Following sample names are EP3-80%,EP3-90% and EP3).A rheometer curve is shown in Fig.7.56. Moreover, the sample containing antioxidant was evaluated as reference (EP3-AO).
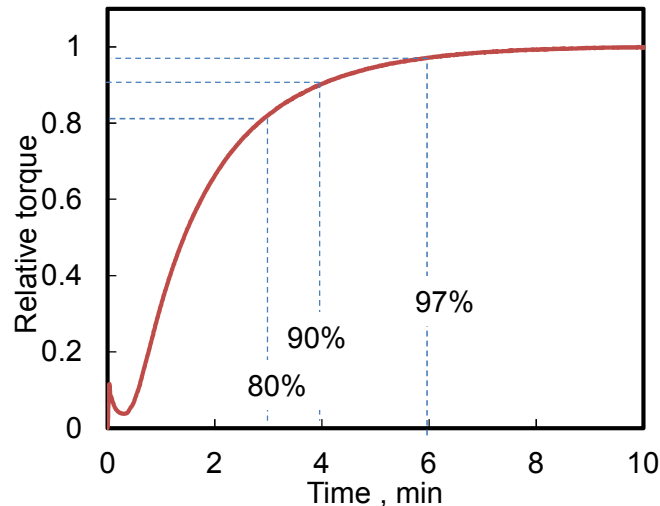

Fig.7.56: Rheometer curve of EP3

The insufficiently crosslinked materials showed faster regression of stress relaxation while the material with antioxidant (EP3-AO) showed the slower regression as shown in Fig.7.57.
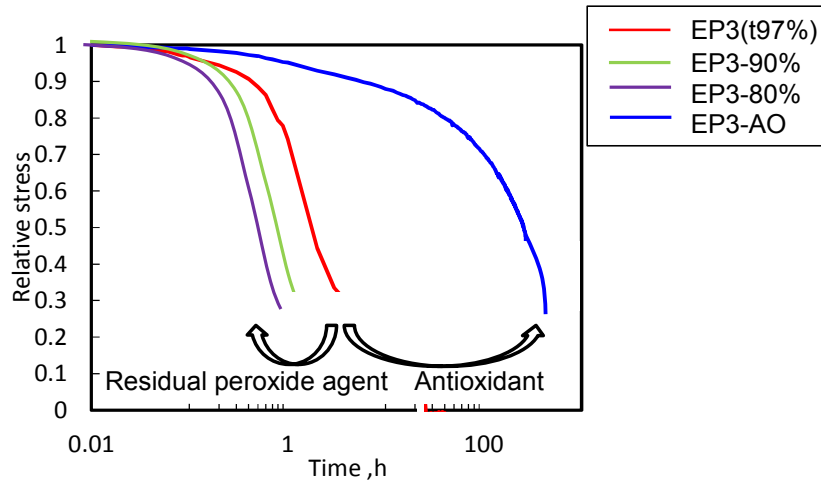
Fig.7.57: Stress relaxation of EPDM materials with and without antioxidant at different cure states.

Insufficient crosslinking could induce faster physical relaxation due to a larger amount of physical entanglement and faster chemical relaxation due to the larger amount of residual peroxide agent. Therefore, the speed of stress relaxation could be associated with both speed of physical and chemical relaxation. On the contrary, antioxidant has the capability of protection of the crosslink structure against oxidation reaction which causes scissions of the polymer chains.

In order to further analyze the mechanism of stress relaxation, the peak area of T_{2A} from the NMR-ILT is shown in Fig.7.58 with the approximation using equation (7.5) and the characteristic aging time constant is shown in Fig.7.59.
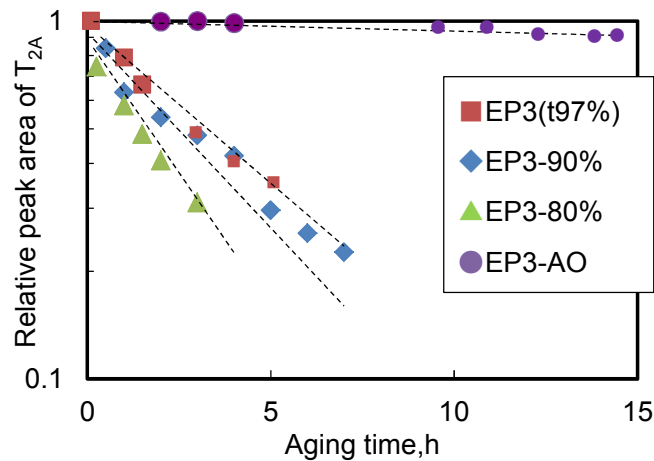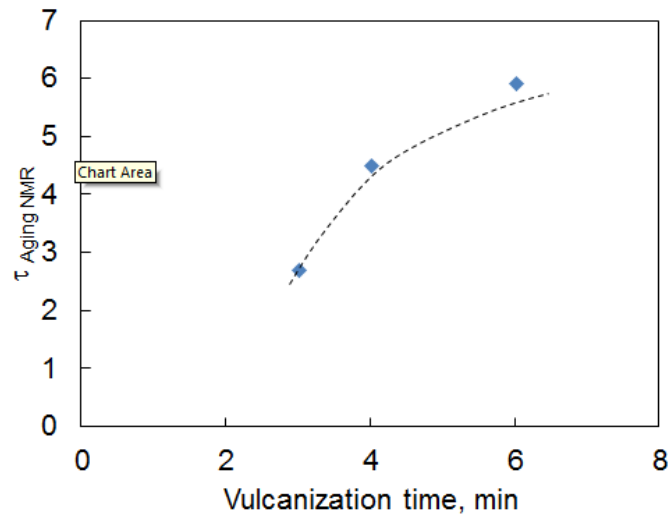

Fig.7.58: T_{2A} peak area vs. aging time

Fig.7.59: Characteristic relaxation time τ of EPDM materials with different crosslinking degree

This result shows that insufficient vulcanization leads to a higher decomposition rate of the crosslink structure. For a more detailed understanding, chemiluminescence was performed at 150°C to evaluate the chemical stability against thermal oxidation. Chemiluminescence curves are shown in Fig.7.60.
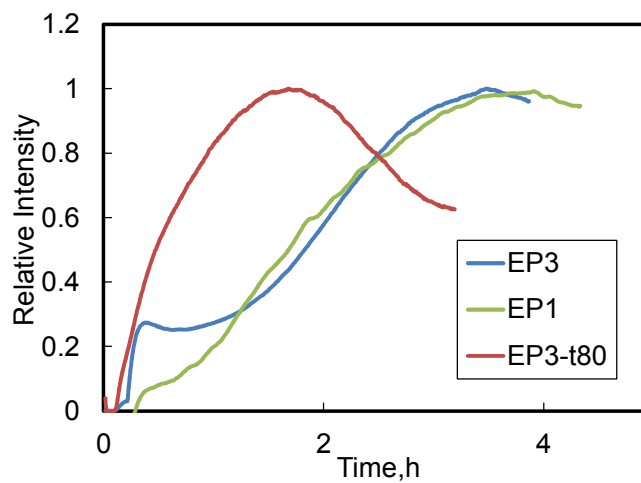

Fig.7.60: Chemiluminescence curve

The peak max time of EP3-t80% was lower than that of EP3. But EP1 (DCP 1phr, lower crosslink density) and EP3 (DCP 3phr, higher crosslink density) show similar peak positions. Besides, the reaction constant k calculated from the slope of the chemiluminescence curve using equation (5.8) is shown in Fig.7.61.Although EP3 has higher crosslink density than EP1, the degree of crosslink has less sensitivity on the thermal stability. This indicates that the

thermal oxidative stability was highly dominated by the residual amount of peroxide which led the initiation of auto-oxidation and not by the initial crosslink density. EP3-t80 shows a higher k value than EP3 and EP1 as shown in Fig.7.61. This supports the assumption that the residual peroxide can speed up the thermal oxidation reaction.
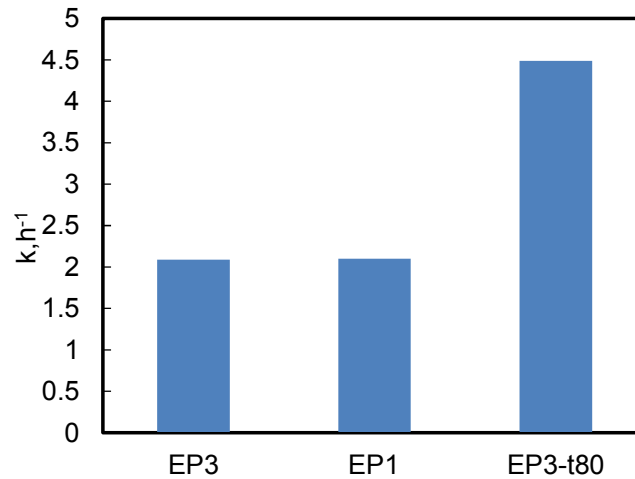

Fig.7.61: Reaction constant, k

7.7.2   Effect of co-agent

7.7.2.1 Co-agent and crosslink structure

The co-agent effect on crosslink structure was investigated in this section. Fig.7.62 shows the relationship between the amount of crosslink agent (DCP) and the crosslink density with /without co-agent determined by swelling method.
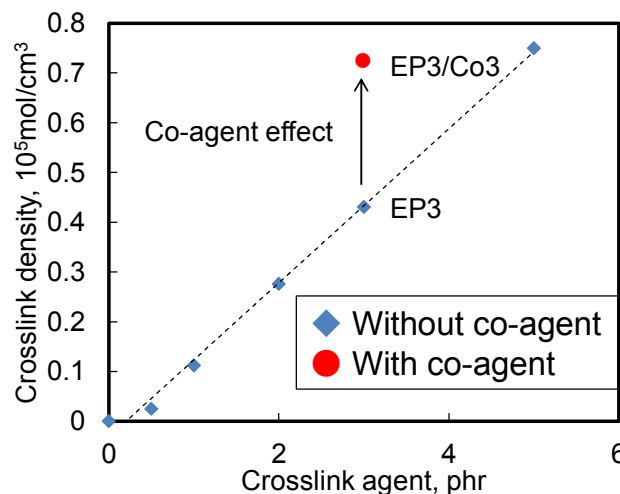

Fig.7.62: Crosslink density comparison of EP3 with and without co-agent

As a result, 5phr crosslink agent and the combination of 3phr crosslink agent and 3phr co-agent (TAIC) led almost same value of crosslink density as determined by the swelling method. Therefore, the two materials without co-agent (EP5) and with co-agent (EP3/Co3) were taken for the aging study to understand the effect of co-agent.

The modification effect on crosslink structure by incorporating co-agent was investigated by NMR. Although the crosslink density from swelling shows that EP5 has a slightly higher crosslink density than EP3/Co3, NMR relaxation of EP3/Co3 shows faster decay than that of EP5 as shown in Fig.7.63.
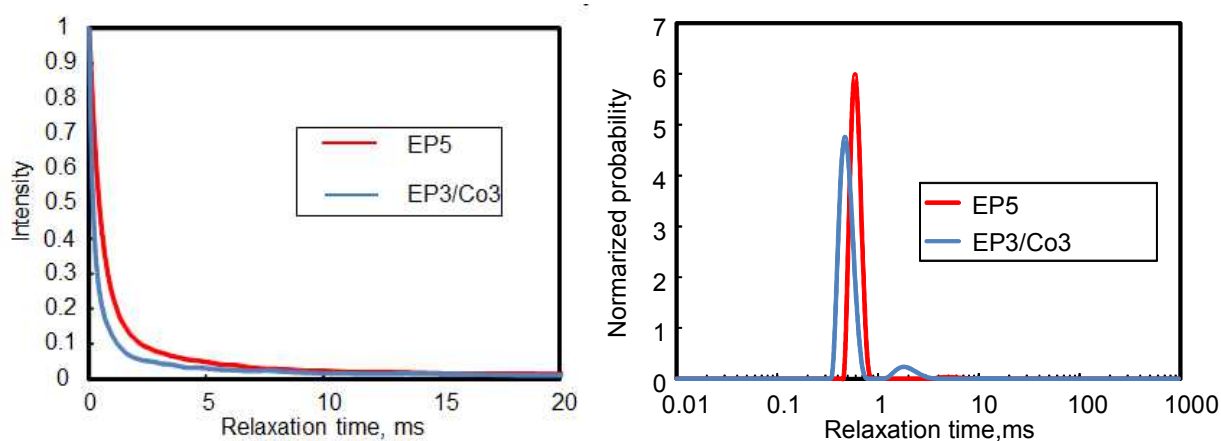

Fig.7.63: NMR curves with co-agent(EP5) and without co-agent(EP3/Co3) (Left) and NMR-ILT spectra with and without co-agent(Right)

This indicates that the incorporation of a co-agent creates a different crosslink structure, even if the swelling levels of the samples with and without co-agent are equal.

Fig.7.64 shows that the relative peak area ratios with and without co-agent.
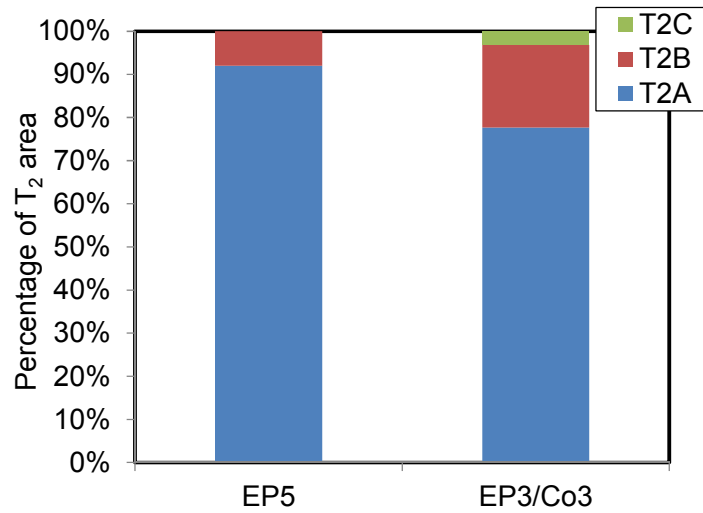
Fig.7.64: Peak area ratio of $T_{2A,B}$ and $_C$ with and without co-agent

All peak positions shifted to shorter relaxation times when by co-agent was used. This means that the co-agent created chain connections with highly restricted mobility. However, the area of T_{2A} which represents the amount of crosslinks and entanglements decreased. In contrast, T_{2C} and T_{2B} which represent the amount of chain ends and free chains increased. This result could be interpreted by assuming that co-agent leads to shorter lengths of intermolecular chains in the crosslink structure. At first glance, the results of peak position and area seems to be contradicting .But considering the inhomogeneity of the network, it is possible to interpret this result.

In a previous study, Steven K. et al suggested that a peroxide crosslink structure with co-agent as shown in Fig.7.65 [134]
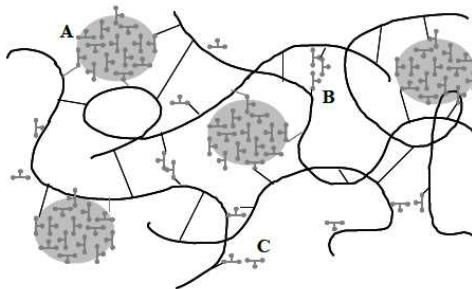

Fig.7.65: Idealized network derived from a poorly soluble co-agent with co-agent domains grafted to the network(A), co-agent forming effective crosslinks(B) pendant co-agent grafted to the network without effective crosslinks(C) [134]

Steven K. mentioned that the poor solubility of co-agent can produce phase-separated domains which all cause high local concentrations of crosslink density (A). As the peroxides for crosslinking agent have polar functions, it is likely that a disproportionate amount of the radicals formed are partitioned in the co-agent domains as well. In case of TAIC used in this study, which is considered as being soluble in the EPDM elastomeric matrix, the difference in solubility parameters could be much less pronounced. Therefore Steven et al concluded that domain formation of crosslink is typically not exhibited when using TAIC. However this results show the possibility of the existence of a phase separated (inhomogeneous) network because of using TAIC.

The model structure in Fig.7.65, the results of NMR-ILT can be explained as follows. The domains grafted to network (A) and the effective network (B) contributed to a shorter relaxation time of T_{2A}. However, the amount of T_{2A} decreased because pendant co-agent could grafted to the network without effective crosslinking (C) and this could lead to an increase of T_{2B} and T_{2C} area.

However the results shows that the co-agent TAIC also has the possibility to build co-agent domains (inhomogeneous network).

As an outlook of further work, it can be interesting to investigate the influence co-agent solubility to the network structure.

7.7.2.2 Effect of co-agent on aging

Stress relaxation in air at 150°C was measured for EP5 and EP3/Co3 as shown in Fig.7.66.
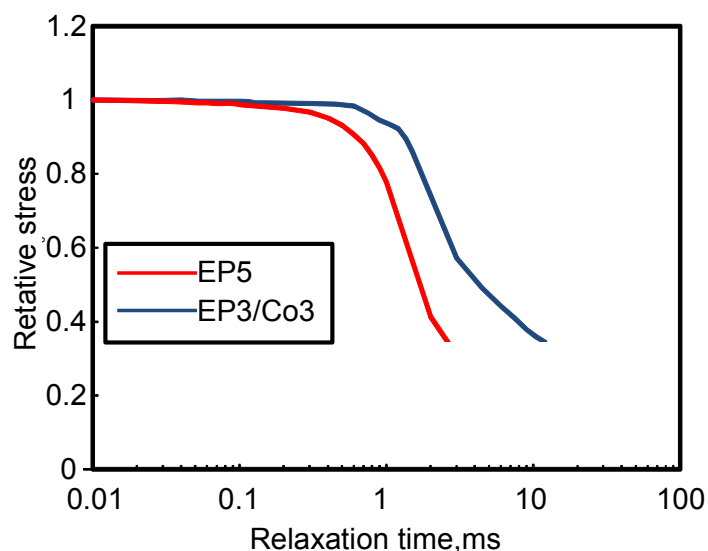
Fig.7.66: Stress relaxation with co-agent (EP3/Co3) and without co-agent (EP5)

Although these two materials have a similar crosslink density, the stress relaxation of EP5 was faster than EP3/Co3.

For understanding these stress relaxation test results, these materials were aged at 150°C and NMR was measured. Fig.7.67 shows the relative T_{2A} peak area ($P_{(t)}/P_{(0)}$) as a function of aging time.
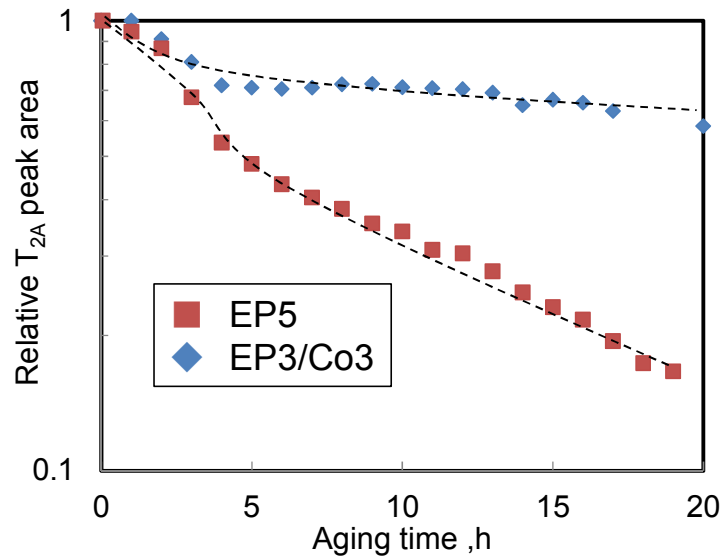

Fig.7.67: Decay of T_{2A} peak area due to aging at 150°C in air for the EPDM rubber with and without co-agent(EP5 and EP3/EPco3)

As shown by the graph of EP3/Co3, the change of T_{2A} peak area at first dropped sharply but after certain time, the slope became less steep. This can be related to the amount of residual peroxide. The residual peroxide worked as accelerator for the thermal oxidation of crosslinks at, the start, but after a certain time, all residual peroxide was consumed and the degradation speed became slower because of the stabilized crosslink structure due to co-agent crosslink. In other words ,this results showed that the co-agent contributes to the stabilizing effect of the crosslink structure against thermal oxidation. This mechanism could contribute better physical properties results during the aging process when using co-agent.

7.7.3 Summary

Crosslink density has a minor influence on the stability against thermal oxidation. However, insufficient crosslink can leads to the poor sensitivity on the stability due to residual

peroxide. Co-agent leads to a higher oxidation stability because of introducing multifunctional stable crosslink.

7.8 Effect of strain on chain mobility and crosslink structural change

In this section, the effect of strain on chain mobility is discussed using the original device for stretching rubber specimen within the NMR tube. There are two main targets to be addressed in this section.

- To describe the effect of strain on chain mobility.
- To understand the crosslink structural change during aging under the deformation.

7.8.1 Effect of strain on chain mobility

Fig.7.68 shows the NMR relaxation spectra with and without stretching of unfilled (EP3) and middle active filled material (EP3-CB-M).
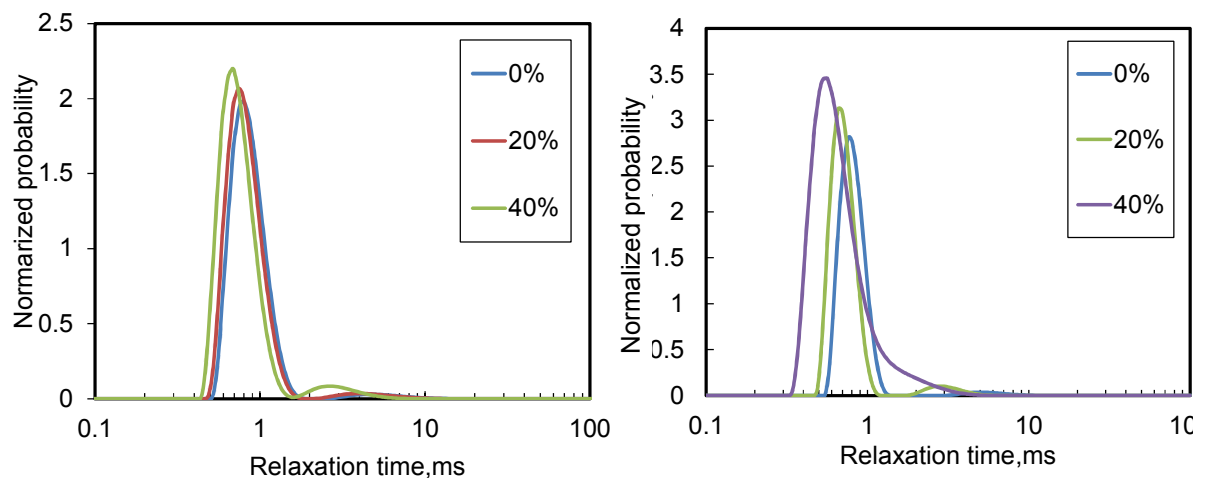

Fig.7.68: The NMR relaxation spectra of EP3 (left) and EP3-CB-M (right) with stretching from 0% to 40%. The peak max times are shown in Fig.7.69.
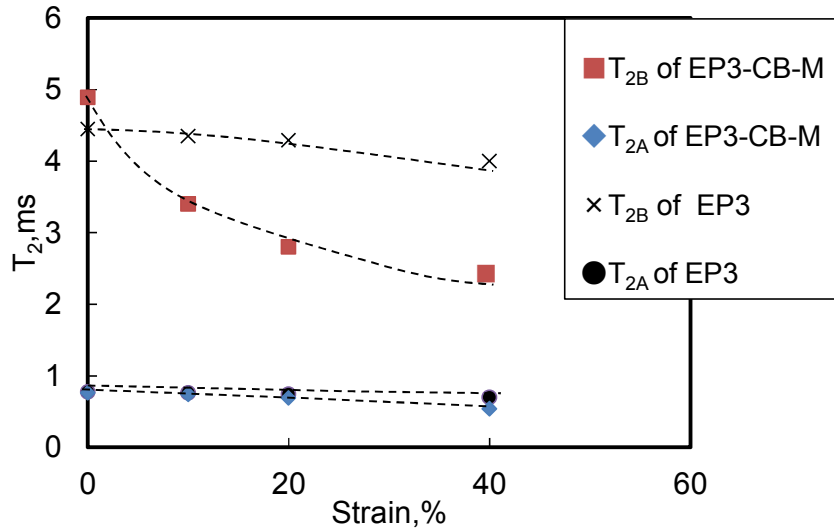
Fig.7.69: Peak max time of T_2 as a function of elongation ratio

The T_2 relaxation shows that the chain mobility was restricted by increasing the stretching ratio. From the micro structural view, the mobility of chain molecules on the strained sample is restricted and their mobility is therefore reduced. All peaks shift to shorter relaxation time in the deformed state. There are several hypotheses for this phenomenon which were discussed in literature [135, 136]. In previous works from Nishi, it was stated that there is the possibility of the existence of an inhomogeneous network in the crosslinked rubber. [136] His results agree with the results of T_{2A}, T_{2B} and T_{2C} in this report. The mobile components such as chain ends (T_{2B}) and free chains (T_{2C}) are likely to be more influenced by applied stress than the less mobile components such as crosslinks and entanglements (T_{2A}). The assumption is that the strain reduces the free volume and as a consequence, the chain mobility is lowered. Fig.7.70 shows the model of a rubber network before and after deformation. The space into which chain ends can move is smaller in the deformed state and more pronounced than that in the undeformed state.
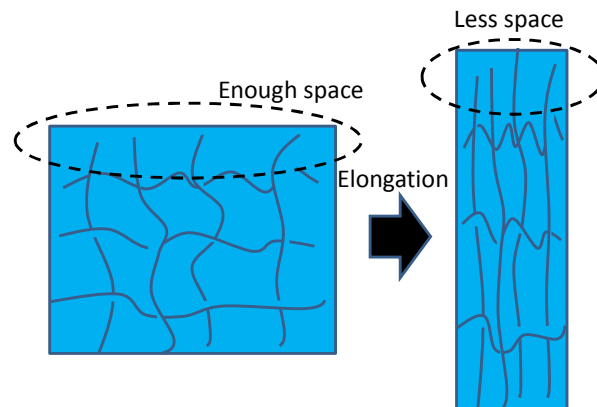
Fig.7.70 : Model of network deformation

Moreover, as seen Fig.7.69, the chain mobility of the CB filled material (EP3-CB-M) was more influenced by the elongation than that of unfilled materials. Mullins described the mechanism for these phenomena for stretched and the unfilled and filled materials [137]. The polymer phase is deformed by the elongation. However CB can be taken account as rigid particles which do not contribute to the deformation. Eventually, the polymer phase will get stretched more than the macroscopic (actual) elongation. This explanation is in good agreement with this chain mobility analysis.

In sum, the strain affects the chain mobility. This fact could be applied to the analysis of the relaxation process.

7.8.2 Correlation of physical relaxation and chain mobility

So far the discussion was for the effect of the deformation without aging. In this section, in order to understand the influence of physical relaxation on chain mobility, EP3 was aged under unstretched and stretched condition in N_2 in the closed tube at 150°C.

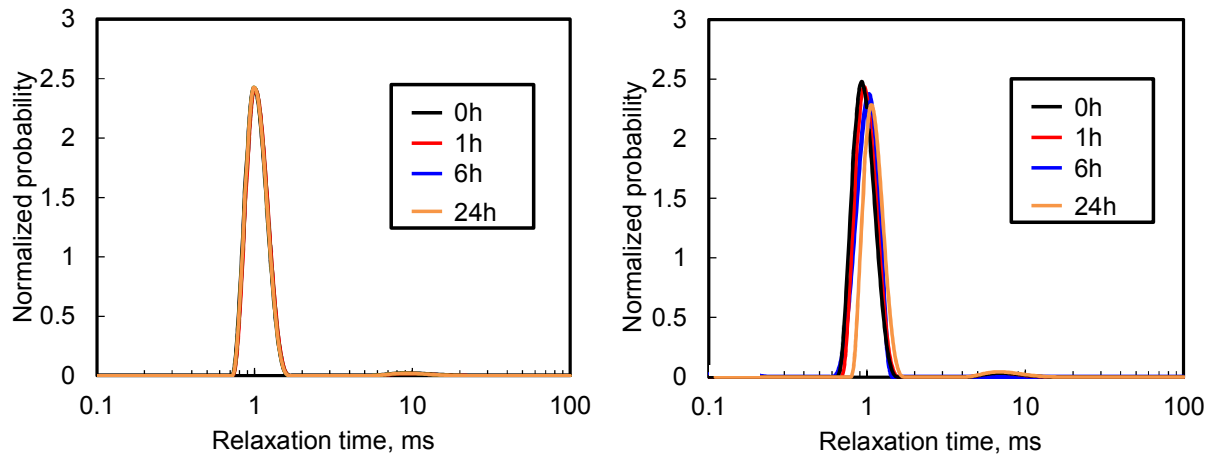NMR-ILT was performed and the results are shown in Fig.7.71.

Fig.7.71: NMR relaxation spectra of EP3 without stretching (left) and with stretching (right) in N₂

at 150°C

The peak max time of T_{2A} and the area corresponding peak are shown in Fig.7.72.

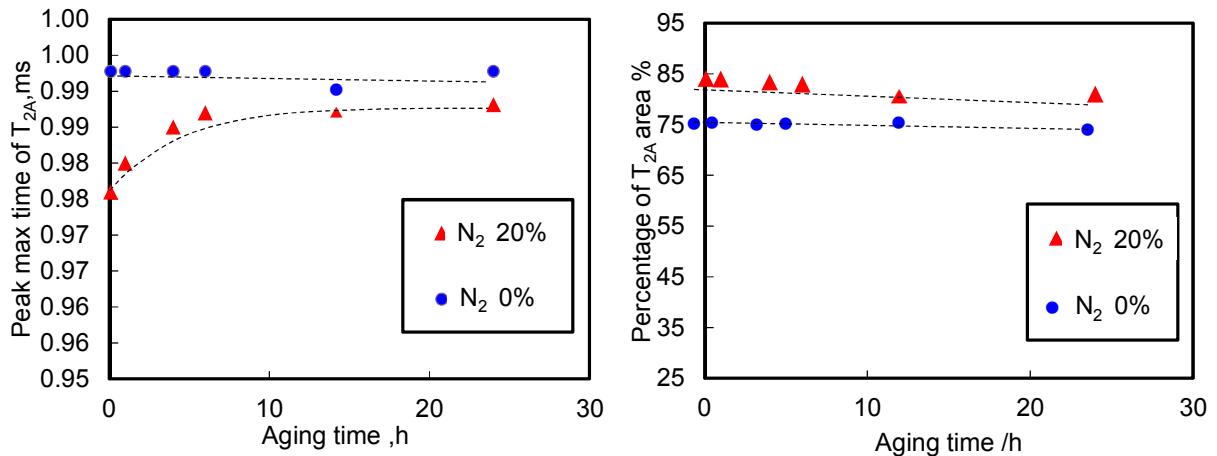Fig.7.72: Peak maximum time (left) and area (right) of T_{2A} during aging in N₂ without and with stretching at 150°C

Under stretched state (20%), the peak max time of T_{2A} gradually shifted higher as a function of aging time. The assumption of an increase of T_{2A} comes from disentanglements in crosslinking phase. This assumption is supported by the results of the test in N₂ without stretching. Where there was no significant change. Therefore it was possible to conclude that no chemical change took place in N₂ at 150°C because there was almost no oxygen in the NMR tube. In other words, as the aging under N₂ advanced, the peak max time at 20% elongation was

getting close to that at 0% elongation. This phenomenon can be explained from disentanglements leading to physical relaxation.

7.8.3 Correlation of chemical relaxation and chain mobility

In this section, the effect of stress on the thermal oxidation in air was investigated. The behavior of T_2 in air was completely different from that in N_2 as shown in Fig.7.73. Moreover, the time of peak max and peak area of T_{2A} during air aging is shown in Fig.7.74.
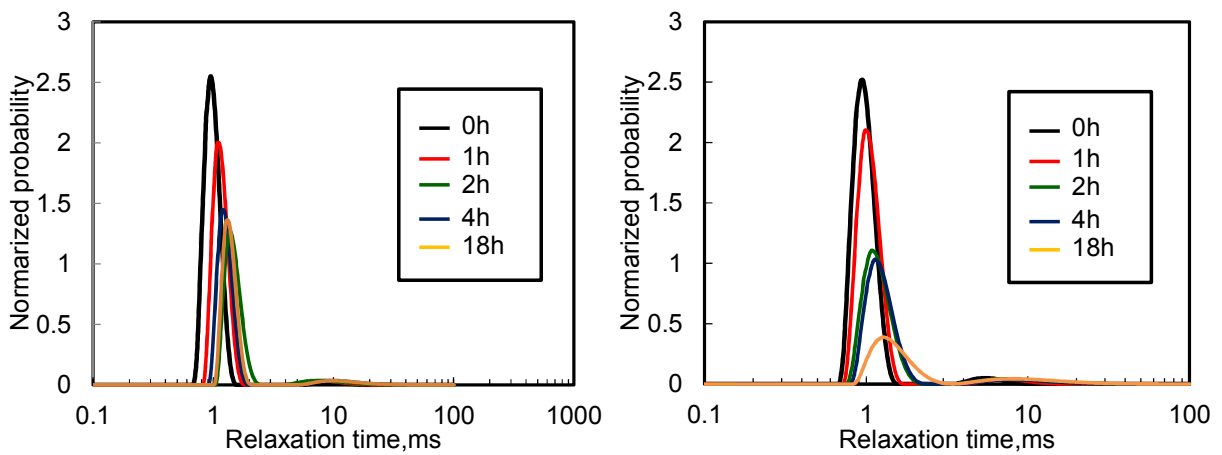

Fig.7.73: NMR relaxation spectra of EP3 without stretching (left) and with stretching (right) in air
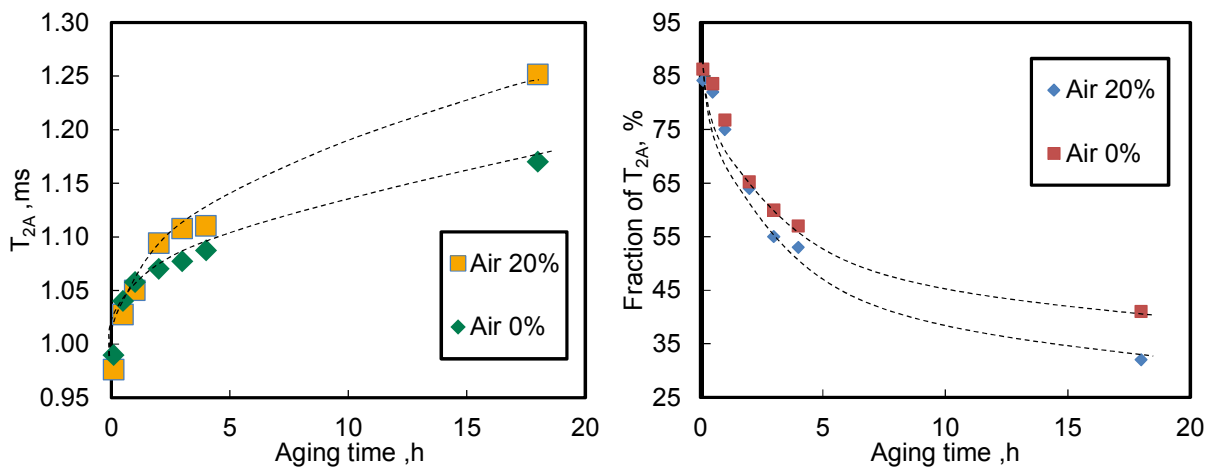
at 150°C

Fig.7.74: Peak time max (left) and area (right) of T_{2A} at 0% and 20% elongation in air at 150°C.

Although the samples were not submitted to the stress, the peak max time of T_{2A} values changed a lot because of chain scission due to the oxidation reaction of the polymer chain. In addition, the speed of increase of T_{2A} with stretching (at 20%) was higher than that without stretching. Supposing the several hypotheses for the explanation, in the deformation state not only chemical chain scission but also physical dentanglements should be taken in to consideration. As other possibility, the actual speed of thermal oxidation increases under stress compared to the undeformed. These effects cause a faster decrease of T_{2A}. Moreover, the activation energy can be calculated from peak area of T_{2A} as the same procedure in the section 7.4.5. The calculated value was 114 kcal/mol at 20% elongation. This value is lower than that without elongation (124 kcal/mol).

7.8.4 Summary

NMR under stretching condition shows the deformation shortened the relaxation time because of a restriction of chain mobility. This restriction of chain mobility released because of aging in N_2 .This comes from chain dentanglements. The deformation increased the speed of crosslink and entanglement phase.

7.9 Effect of deformation on thermal oxidation using chemiluminescence

In the previous section, the conclusion was that the speed, at which the rubber network breaks down is increased under deformation, was up by stress. For a further understanding of this effect, the investigation with chemiluminescence was done.

7.9.1 Physical property change in the deformed state

Typically, the physical relaxation process follows a logarithmic regression at low temperatures and within a short time [128]. The chemical process is seen as an accelerated decrease at high test temperatures and follows an exponential regression. The results of stress relaxation experiment at different temperatures are shown in Fig.7.75.
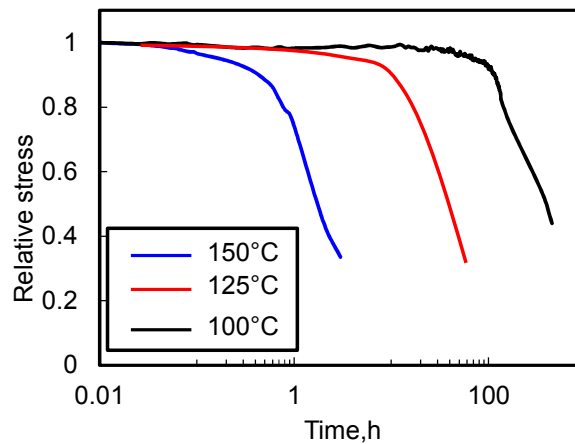

Fig.7.75: Stress relaxation curves at 100, 125 and 150°C in air

The threshold value, 50% of the initial force was used for the calculation of the activation energies. In addition, the relaxation tests were carried out under different values of elongations, as seen in Fig.7.76.
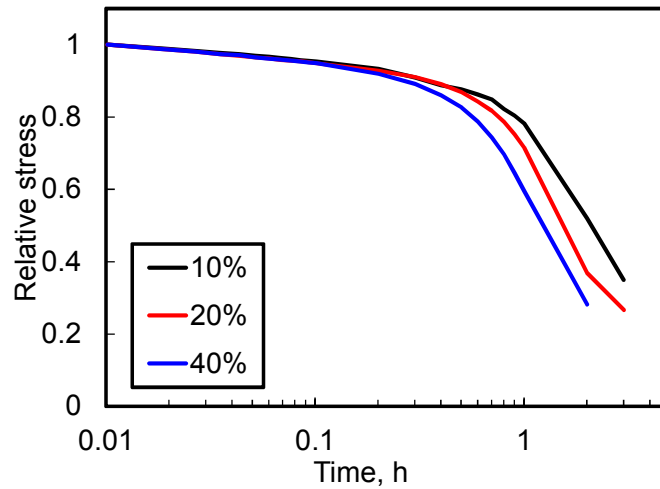
Fig.7.76: Stress relaxation curves at 10% ,20% and 40% elongation at 150°C

In order to calculate the activation energy, the log (time at 50% of F/F_0 from the beginning of test) and $1/T$ was plotted. The activation energy decreased depending on the elongation ratio as shown in Fig.7.77. where t is the time of 50% dropped of F/F_0 from the beginning of test, T is aging temperature.

To investigate the reason for this phenomenon, the chemical oxidation in the deformed state was analyzed.
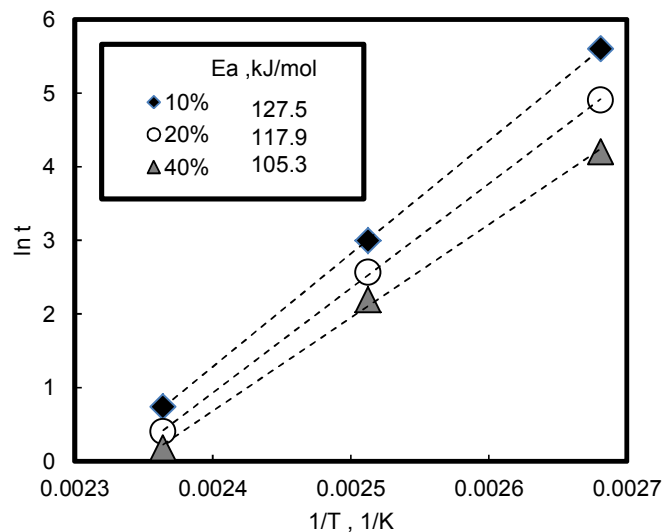
Fig.7.77: Arrhenius plots with different elongation ratio.

7.9.2 Thermal oxidative process in the deformed state

The mechanism of the oxidation process and luminescence emission of EPDM was proposed by Jirackova [112] .

This reaction links the chemiluminescence to the beta scission of alkyl radicals via the formation of a transient bi-radical. In other words, the light intensity is expected to be proportional to the rate of the polymer chain scission.

Fig.7.78 shows the chemiluminescence of the aging process with and without stretching at 125°C and 140°C. It is possible to convert the curves with (5.8) to describe the reaction rate values of k.
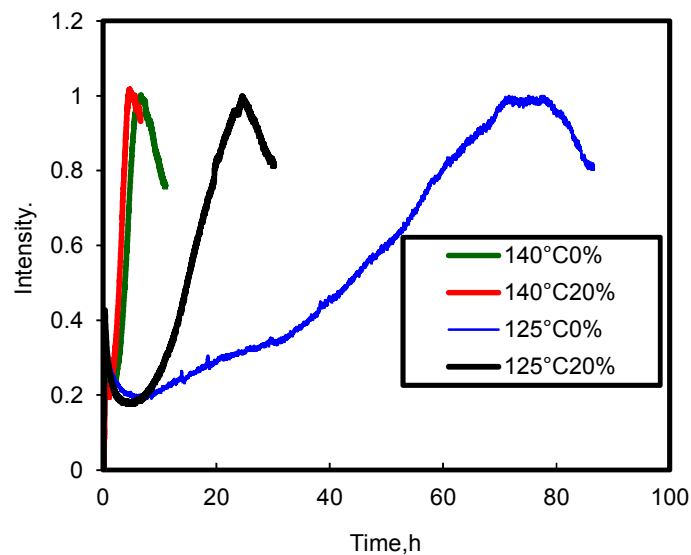
Fig.7.78: Chemiluminescence curves under stretching 0% and 20% at 125 and 140°C

Fig.7.79 shows the relationship of the reaction rate was calculated using the equation (5.8) between temperature and elongation.
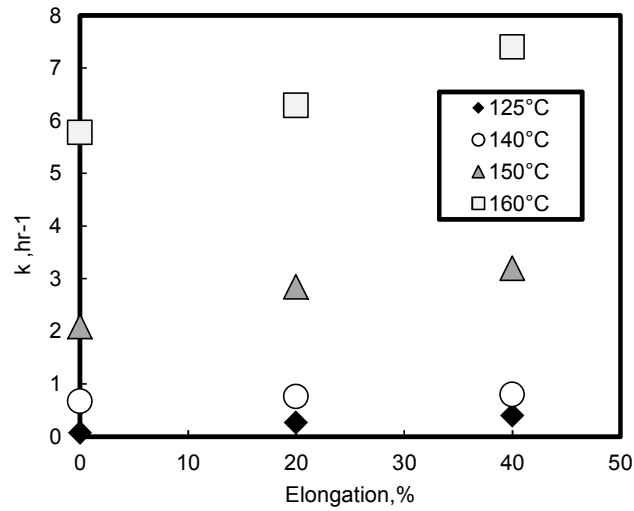
Fig.7.79: Relationship between reaction rate and stretching ratio

When the elongation increased, subsequently the reaction rate increased. In addition, the activation energy was calculated using the Arrhenius plot. The Arrhenius activation energy was plotted for unstretched and stretched specimens (Fig.7.80)
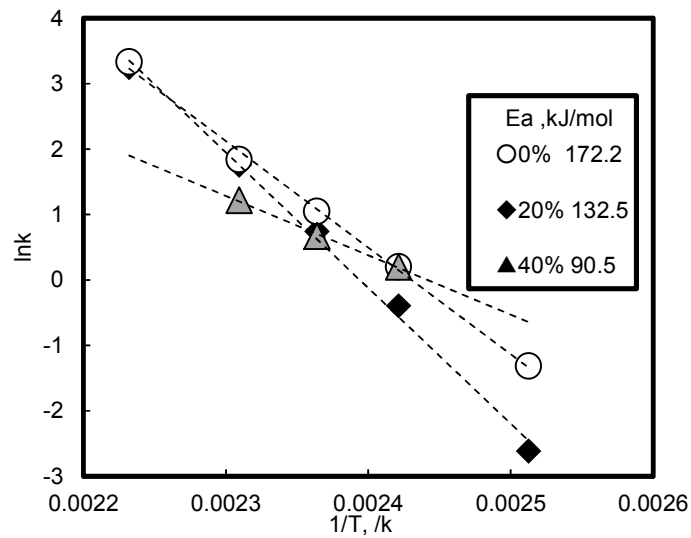
Fig.7.80: Arrhenius plot for calculating activation energy.

This result reveals a 40 kJ/mol decrease in the activation energy for the 20% stretched specimen. It shows that the decrease of the activation energy happens because of oxidation rate increased under the elongation state.

7.9.3 Analysis of oxidation reaction in combination with stress

To confirm the relationship of chemical oxidation reaction, the chemical oxidation reaction and product were analyzed using ATR_FT-IR (see Fig.7.81). The thermal oxidation was conducted using the samples (Thickness 2mm, length 30mm and width 30mm). The ATR-FT-IR spectra of crosslinked EPDM rubber shows the peak at 1714 cm^{-1} increasing in intensity as the time of aging increased.
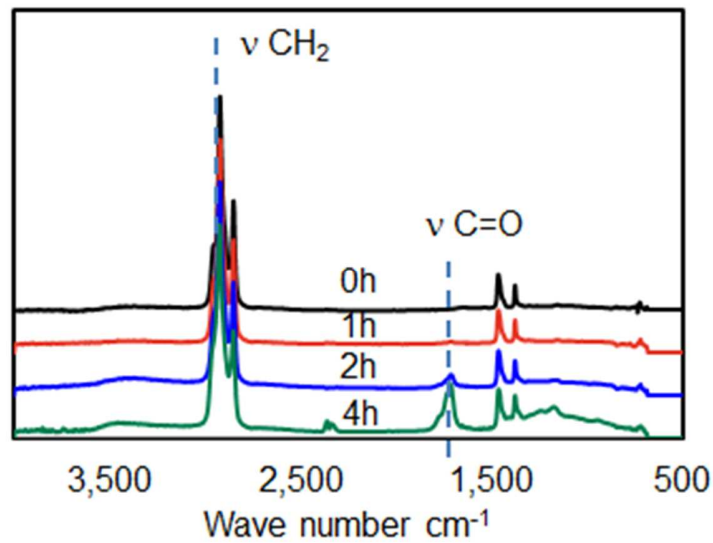
Fig.7.81: ATR-FT-IR spectra before and after aging at 150°C in air

This peak is assigned as symmetric stretching frequency of the C=O groups. The generation of C=O was due to oxidation at the main polymeric chain scission. The peak ratio of C=O at 1714 cm^{-1} and 2930 cm^{-1} as symmetric stretching frequency assigned CH$_2$ during an aging process showed in Fig.7.82.
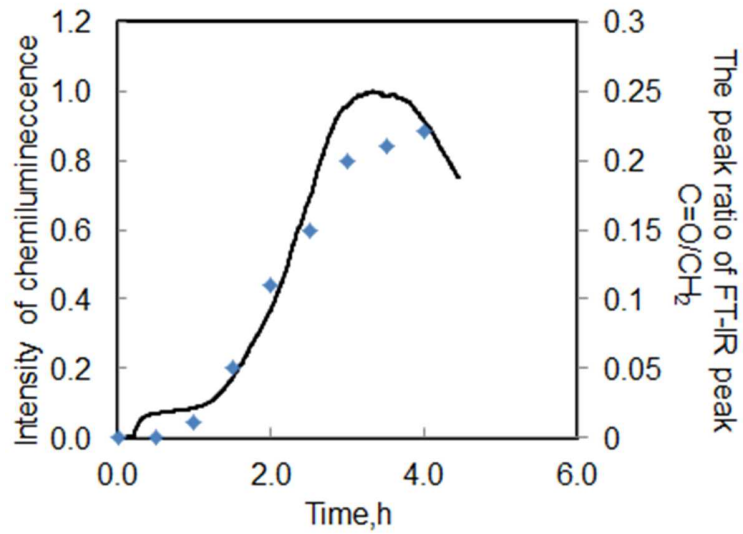
Fig.7.82: A comparison between chemiluminescence and signal ratio C=O/CH$_2$ by ATR-FT-IR

There is a positive relationship between the emission of chemiluminescence and the peak ratio of C=O and CH$_2$. This means that the chemiluminescence can be observed as the process of chain scission reaction by oxidation, especially in case of EPDM polymer.

The aging speed was shown in Fig.7.83 with comparison between the situation with and without stretching.
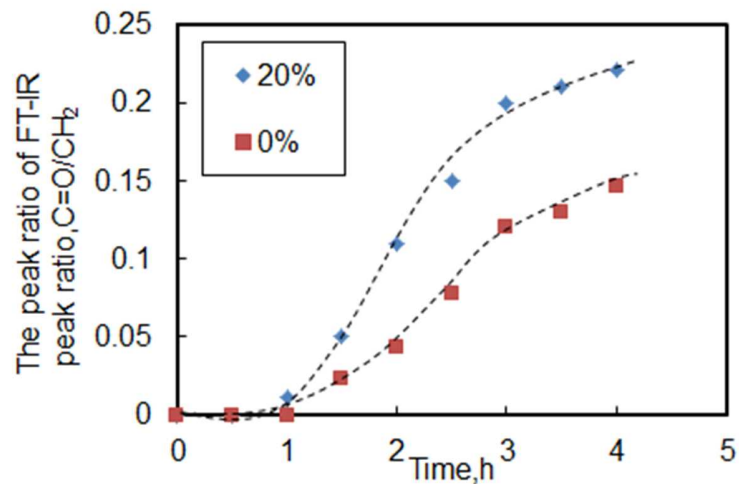
Fig.7.83: Relationship between reaction rate and stretching ratio

The aging speed of EPDM with stretching is higher than that without stretching. A hypothesis is, that additional reaction take place like the chain scission reaction by the stress, and so this leads to the radical concentration increasing.

7.9.4 Summary

In sum, the study shows that the stress significantly influenced the aging process of EPDM. Higher elongation leads to lower activation energy of the thermal oxidation reaction. The used method indicates that the beginning of the chemical degradation occurs with the stress relaxation. The changes of the polymer structure during the thermal oxidative aging processes can be traced by coupling chemiluminescence and physical relaxation test. ATR-FT-IR results proved that the chemiluminescence is a very useful tool to evaluate the chemical structural change during thermal oxidative aging. Furthermore the coupling of CL and relaxation test is a measurement technique which is useful to confirm the aging process of sealing materials in the deformed state significantly.

Chemical bond interchanges between crosslinks are occurring in the network when the rubber is maintained at strain during aging process. The interchanges might be regarded as a two stage process, the scission and rebuilding of crosslinks. Regarding the first stage, the scission happens by the chemical oxidation of polymer. This is the reason why the stress relaxation happens. So this technique was applied for understanding the structural change during the stress relaxation.

Stress induced chemiluminescence shows when the chemical change occurs, mainly the chain scission reaction. The early part of stress relaxation is dominated by physical relaxation one hour after the start of the test. Therefore the chemiluminescence amount is relatively small. On the other hand, one hour after the start of the test, the stress dropped significantly because of the emission of chemiluminescence linked to the amount of chain scission reaction. Besides , the curve from T_{2A} resulted by NMR can be overlapped in the same diagram in Fig.7.84. T_{2A} shows the amount of crosslinked network. The decrease of this shows the rapture of network.
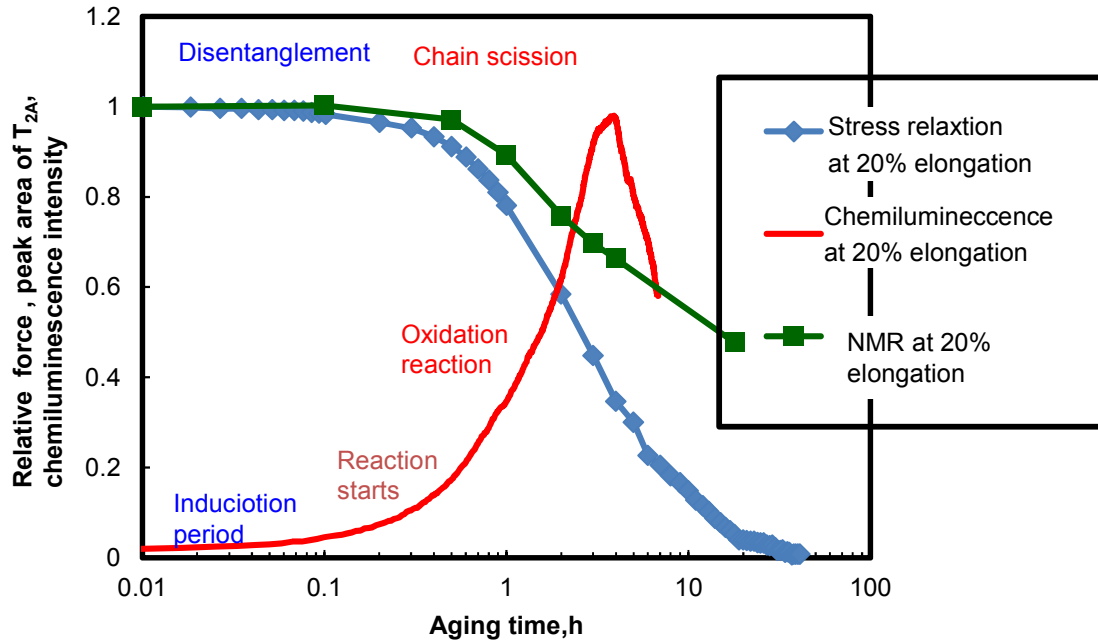
Fig.7.84: Combination analysis of stress relaxation, NMR and chemiluminescence

As well known, the activation energy of the thermal oxidation differs depending on the method [138]. The activation energy from three methods; stress relaxation, NMR-ILT and chemiluminescence are compared in Fig.7.85.
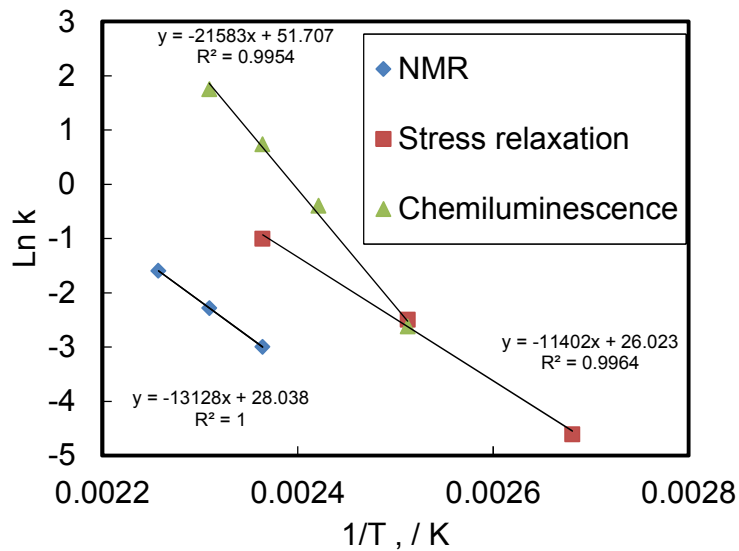
Fig.7.85: Arrhenius plot comparison of three methods

The results were obtained using the same materials EP3 and the same condition of aging (temperature range is from 100°C to 160°C). The activation energies from stress relaxation and NMR showed the similar results. However, the activation energy from chemiluminescence shows higher values. This difference might be led by the different observed phenomenon between NMR, stress relaxation and Chemiluminescence. Whereas the results of NMR and stress relaxation originated from the chain scission. However, the results of chemiluminescence originated from the chemical reaction taking place during thermal oxidation.

Table 7.3: Activation energies from three different methods

	Activation energy, kJ/mol	Measured parameters
Stress relaxation	117	Physical and chemical effect (Mainly, chain scission)
Chemiluminescence under deformation	135	Peroxide scission Generation of carbonyl function
NMR under deformation	114	Chain scission of network structure

Chapter 8

Conclusion

The achievements of this research can be divided into the following two areas of :

<u>Mechanism of the aging process of unfilled and filled EPDM</u>

- o Key influential factors of materials composition and the role of the different raw materials on aging process.
- o Influence of strain on the aging process

<u>Method development</u>

NMR relaxation spectra analysis (NMR using ILT data analysis)

- o Key factors of measurement execution and calculation parameters to ensure accuracy and reliability
- o Key factors of polymer structure of uncrosslinked and crosslinked rubber.

Analysis of material behavior under strain using NMR and chemiluminescence.

8.1 <u>NMR relaxation spectra analysis(NMR-ILT)</u>

<u>8.1.1 Key factors of the measurement and calculation parameters to ensure accuracy and reliability</u>

In order to confirm some experimental factors on the actual NMR relaxation, artificial noise added to ideal NMR relaxation and cut decay. It was found that the noise, a sufficiency of relaxation increased the peak width of spectra. These negatively affected the accuracy of the spectra.

<u>8.1.2 Key factors of polymer structure of uncrosslined and crosslinked rubber.</u>
<u>8.1.2.1 Effect of molecular weight and distribution of polymer</u>

With increasing the molecular weight of the polymer, the peak area of T_{2A} increased and T_{2B} decreased. Moreover, molecular weight distribution could correlate with the peak width of T_{2A} from NMR. These results indicated that T_{2A} originates from chain entanglement and T_{2B} originates from dangling ends. NMR-ILT can show the raw polymer structure such as amount of entanglements or length between entanglement(physical crosslinking point) or its distribution.

8.1.2.2 Effect of chemical cross link on chain mobility

Crosslinked rubber structure was correlated with NMR results. With increasing crosslink density, the peaks of NMR-ILT shifted to the left due to the restriction of polymer network chain mobility resulting from the chemical crosslinks. The T_{2A} peak max time can be correlated well with the crosslink density from swelling method. By introducing the chemical crosslinks, the area of T_{2A} increased and T_{2B} decreased. This result led that T_{2A} represents chemical crosslinks as well as chain entanglements. In addition, T_{2C} which has a longer relaxation time can be observed because of chain scissions as the side reaction of peroxide crosslink.

In sum, the occurring peaks can be attributed to the crosslinked part (T_{2A}), the dangling ends (T_{2B}) and the free chains (T_{2C}). T_{2C}, often gets neglected when using conventional exponential fitting techniques with NMR-ILT $T_{2C,}$ is detectable.

Thus NMR-ILT is powerful tool to clarify the crosslink structure as well as raw polymer structure so that this technique can be applied the analysis of structural change during aging.

8.2 Aging mechanism of crosslinked EPDM and the role of raw materials (ingredients)

NMR-ILT was applied to interpret the aging mechanism of crosslinked EPDM rubber. Besides, several key influential factors on the aging process were analyzed using this method as following.

8.2.1 Aging mechanism of crosslink structure

The crosslinked EPDM was aged in air at 150°C and analyzed using NMR-ILT. These results were in good correspondence to the physical tests performed such as hardness measurement and swelling test. NMR-ILT showed more precise information of crosslink structure such as T_{2A} ,T_{2B} ,T_{2C} additionally T_{2D}. T_{2D} is the rigid component resulting from the aging. This peak can be explained by the secondary network as a result of the chain recombination reaction following chain scission.

In summary, the results of NMR relaxation can detect the partial structural changes of rubber during the aging process in line with the model. Besides, T_{2A} is the important representative value of the crosslink structure which can be correlated with stress relaxation behavior. Several material factors as well as the effect of strain on the crosslink structure changes during the the aging process were evaluated using T_{2A}.

8.2.2 Effect of carbon black on aging

The investigation revealed the effects of carbon black.

1. Carbon black insignificantly affected the NMR relaxation spectra of uncrosslinked rubber. In other words, this method highly focuses on polymer chain mobility although the material contains inorganic fillers.

2. Higher surface of a carbon black led to reduced efficiency of peroxide crosslink reaction and thus resulted in reduced crosslink density of the materials. This resulted in a faster physical relaxation.

3. During the thermal oxidation process, carbon black behaved like an antioxidant. Higher surface of carbon black provided the less speed of the thermal oxidation of polymer.

8.2.3 Effect of ethylene content on aging

The difference in reactivity of ethylene and propylene was investigated. A smaller ethylene content (higher propylene content) led to a higher decomposition rate of the crosslink structure. This result was consistent with the tendencies seem in the stress relaxation experiments.

8.2.4 Effect of peroxide residue on aging

Insufficiently crosslinked materials led to a faster regression of the stress relaxation and antioxidant led to a slower one. In order to analyze the mechanism, the area of T_{2A} from NMR was measured during the thermal oxidation. This result indicated that the crosslink structure was damaged rather quickly by the residual peroxide agent.

On the contrary, antioxidant protected the crosslink structure against thermal oxidation causing chain scissions of polymer (stress relaxation).

8.2.5 Effect of co-agent

Incorporation of co-agent in the crosslink matrix led to a slower regression of the stress relaxation. In order to analyze the mechanism, the area of T_{2A} from NMR was measured during

the thermal oxidation. This result indicates that co-agent has a stabilizing effect on a thermal oxidation.

8.2.6 Effect of strain on the aging process

8.2.6.1 Analysis by means of NMR

NMR under stretching condition shows that the deformation of the rubber shortened the relaxation time because of the restriction of chain mobility. Under N_2 condition, this chain mobility restriction gradually released due to physical relaxation originated by chain dentanglements. Under air condition, the additional chain scissions took place and increased the relaxation time. Moreover, deformation increased the speed of degradation of crosslink and entanglements during the thermal oxidation.

8.2.6.2 Analysis by means of chemiluminescence

NMR results show the static stress significantly influenced the aging process of EPDM. For a further understanding, the chemiluminescence in deformation was applied.

Higher elongation led to a lower activation energy of the thermal oxidation reaction. The used method indicates that the beginning of the chemical degradation occurred with the stress relaxation. The changes of the polymer structure during the thermal oxidative aging processes can be traced by coupling chemiluminescence and physical relaxation test. ATR-FT-IR results proved that the chemiluminescence is a very useful tool to evaluate the chemical structural change during thermal oxidative aging.

Furthermore the coupling of different three methods, CL, NMR and relaxation test is a powerful technique which is useful to confirm the aging process of sealing materials in the deformed state significantly.

Chapter 9

Outlook

9.1. Further method development on crosslink structural analysis using NMR

The NMR signal of EPDM can be described as an exponential decay therefore ILT can be utilized. However, the observed NMR relaxation are not always to consist of perfect exponential curves. Especially, NR shows a Gauss part at the beginning of relaxation. In this case, ILT doesn't work well since the function of ILT consists of exponential functions. In order to solve this issue, the proposal idea is to utilize the Gauss function instead of an Exponential function as a kernel function.

$$M(t) = \int_0^\infty L(\tau)F(t,\tau)d\tau \qquad (9.1)$$

Here M(t) stands for the Gauss-experimental NMR data, L(τ) for the distribution function, which has to be determined, and F(t, τ) for the kernel function, in this case. Sectorized technique should be developed for the materials which contains Gauss functions in NMR relaxation.

$$F(t,\tau) = e^{-\left(\frac{t}{\tau}\right)^2} \qquad (9.2)$$

In another technique, recently, Multi Quantum NMR (MQ-NMR) or Double Quantum NMR (DQ-NMR) has been discussed to quantify the distribution of crosslink density [139, 140, 141, 142, 143, 144, 145]. The principal target is similar to NMR-ILT but these two methods use a different pulse sequence. Further investigation is necessary; this method can also help to reveal the crosslink density distribution in detail. The combination analysis of NMR-ILT and DQ-NMR could further insights of crosslink structure.

9.2 Further method development materials with aging process under the practical condition.

9.1.1 Static compressed condition

In this study, stretched materials are used but generally, actual seals in the field are used in a compressed state. For the investigation of this state, the diffusion of oxygen into the rubber matrix must be taken into account. Typically, diffusion of oxygen leads to an inhomogeneous aging state of rubber due to diffusion limited oxidation (DLO). This leads more complex aging

phenomena and is mainly important for the thicker parts. For this understanding further method development should be considered.

9.1.2 Contact media

In this study, thermal oxidation of materials are considered, In practical condition, liquid or gas can contact materials and degrade or swell rubber materials. This can be further interests on the study. However, this related to a lot of chemistry and physical chemistry so that the further method or test setup should be developed. For instance, they should be considered as below.

-Diffusion of base oil and additive.

-Chemical reaction of additives of lubricant on rubber

-Physical property change or rubber due to above diffusion and reactions.

9.2 Further investigation on the mechanism of stress relaxation varying material parameters

In this study, model compounds with only the most important raw materials were used. But industrial rubber materials have a larger variety of ingredients. These ingredients also possibly influence on the aging property of materials.

- Type of polymer i.e. NR, NBR, ACM, FKM etc.

- Type of crosslink i.e. sulfur cure, resin cure , amine cure, polyol cure etc.

- Mineral fillers i.e. Silica, Calcium Carbonate, Clay etc.

- Accelerators

- Plasticizers

- Co-agents

Literature

[1] Market research consulting, Gaskets and Seals Global Market Outlook 2017-2023 (2017)

[2] B. N. J. Persson and C. Yang, Journal of Physics: Condensed Matter **20**, 315011 (2018)

[3] K. T. Gillen, R. Bernstein and M. H. Wilson, Polymer Degradation and Stability, **87**, 2, 257 (2005)

[4] V. Plaček, et al., Polymer Testing, **28**, 2, 209 (2009)

[5] N. Grassie and G. Scott, Polymer Degradation and Stabilisation, *Cambridge Univ. Press* (1988)

[6] C. W. Lin, et al., Journal of Power Sources, **196**, 1955 (2011)

[7] M. Celina, et al., Polymer Degradation and Stability, **4**, 2, 493 (1998)

[8] T. Nakamura, et al., Polymer Degradation and Stability, **96**, 7, 1236 (2011)

[9] M. Gonokami, et al., Seikei-Kakou*, **24**, 335 (2012)

[10] Y. Aoyagi and H. Sano, International Elastomer Conference 184th Technical Meeting (2013)

[11] K. T. Gillen, M. Celina and R. Bernstein, Polymer Degradation and Stability, **82**, 25 (2003)

[12] K. Yokoyama, M. Okazaki and T. Komito, JSAE Review, **19**, 2, 123 (1998)

[13] C. P. Porter, et al., Journal of Applied Polymer Science, **135**, 45814 (2018)

[14] G. Smith, et al., Applied Surface Science, **90**, 357 (1995)

[15] K. Sadhan, Rubber Technologist's Handbook, **1**, 287 (2017)

[16] J. Aleman, et al., Pure and Applied Chemistry, **79**, 10, 1801 (2007)

[17] Bayer-Handbuch der Elastomer (2006)

[18] C. Guimon and B. Maxwell, Journal of Applied Polymer Science, **9**, 561 (1962)

[19] B. Maxwell and J. E. Heider, Trans. SPE, **2**, 174 (1962)

[20] H. T. Miller and G. E. Warnaka, Rubber Chemistry and Technology, **39**, 1421 (1966)

[21] L. R. G. Tresoar, The physics of rubber elasticity, *Oxford Classic Texts in the Physical Sciences* (1975)

[22] J. C. Salamone, Polymeric Materials Encyclopedia, **3**, *CRC Press* (1996)

[23] Mitsui chemicals, Catalog of Mitsui EPT

[24] B. Saville and A. A. Watson, Rubber and Chemistry and Technology, **40**, 1, 100 (1967)

[25] M. van Duin, KGK Kautschuk Gummi Kunststoffe, **4**, 150 (2002)

[26] S.Kodama, Organic chemistry, *Tokyo-kagaku-dojin Press* (1988)

[27] S. P. Manik and S. Banerjee, Rubber and Chemistry and Technology, **42**, 744 (1969)

[28] K. Hummel and J. Desilles, KGK Kautschuk Gummi Kunststoffe, **15**, 492 (1962)

[29] G. Heideman, et al., Journal of Applied Polymer Science, **95**, 1388 (2005)

[30] U. Giese, M. Santoso and R. H. Schuster, International Rubber Conference 2009

[31] U. Giese, M. Santoso and R. H. Schuster, 176th ACS-Meeting 2009

[32] A. T. Tobolsky, Properties and structure of polymers, *Wiley New York* (1962)

[33] A. N. Gent, Engineering with rubber: how to design rubber components, *Hanser Fachbuch* (2012)

[34] C. Prieß, et al., KGK - Kautschuk Gummi Kunststoffe, **4**, 16 (2014)

[35] R. D. Andrews and A. V. Tobolsky, Journal of Applied Physics, **17**, 352 (1946)

[36] J. G. Curro and E. A. Salazar, Rubber Chemistry and Technology, **50**, 5, 895-905 (1977)

[37] H. Eyring, Journal of Chemical Physics, **4**, 283 (1936)

[38] M. L. Williams, R. F. Landel and J. D. Ferry, Journal of the American Chemical Society, **77**, 3701 (1955)

[39] K. Watanabe, Rubber and Chemistry and Technology, **35**, 182 (1962)

[40] C. J. Derham, Journal of Materials Science, **1**, 1023 (1973)

[41] K. Murakami, Chemical rheology of polymer, *Asakura Publishing* (1968)

[42] ISO *11346:* 2014 Rubber, vulcanized or thermoplastic - Estimation of life-time and maximum temperature of use

[43] S. Kyung-do, et al., Journal of Applied Polymer Science, **34**, 223 (1987)

[44] J. G. Curro and E. Salazar, Journal of Applied Polymer Science, **19**, 2571 (1977)

[45] S. Ronan, *et al.*, KGK Kautschuk Gummi Kunststoffe, **4**, 182 (2009)

[46] M. Ito, Polymer, **23**, 4, 1515 (1982)

[47] T. Kusano and K. Murakami, Journal Polymer Science: Polymer Chemistry, **10**, 2823 (1972)

[48] K. Murakami, Kobunshi-kagaku, **21**, 602 (1968)

[49] I. V. Berezin and E. T. Denisov, The Oxidation of Cyclohexane, *Pergamon Press* (1996)

[50] I. Hermans et al., A European Journal of Chemical Physics and Physical chemistry*, **6**, 637 (2005)

[51] T. R. Talcott and S. L. Howard, Journal of Agricultural and Food Chemistry*, **47**, 5, 2109 (1999)

[52] P. Qiu-Hong, et al., Journal of Mass Spectrometry*, **44**, 633 (2008)

[53] M. Jack, Journal of Mass Spectrometry*, **38**, 4, 438 (2003)

[54] H. R. Prabhu, Indian Journal of Clinical Biochemistry*, **15**, 1 (2000)

[55] S. N. Zhurov and E. E. Tomashevsky, Physical Basis of Yield and Fracture*, Institute of Physics* (1966)

[56] A. A. Popov and N. N. Blinov, Polymer Degradation and Stability*, **7**, 1, 33 (1984)

[57] B. E. Krisyuk and E. V. Polianczyk, International Journal of Polymeric Materials and Polymeric Biomaterials*, **23**, 1 (1993)

[58] V. P. Efimov and Nikiforovsky, Journal of Mining Science*, **46**, 3, 260 (2010)

[59] J. R. White, Ageing studies and lifetime extension of materials, *Springer*, 475 (2012)

[60] J. Czerny, Journal of Applied Polymer Science*, **16**, 2623 (1972)

[61] B. Lánskáa, L. Matisová-Rychlá and J. Rychlý, Polymer Degradation and Stability, **61**, 1, 119 (1998)

[62] M. Porter, Developments in Polymer Stabilisation*, Applied Science Publishers* (1982)

[63] K. Jacobson, Polymer Degradation and Stability, **65**, 449 (1999)

[64] S. Hosoda, Y. Seki and H. Kihara, Polymer*, **34**, 22, 4602 (1993)

[65] A. Brydson, Rubbery Materials and their Compounds, *Elsevier* (1978)

[66] S. Kole, et al., Polymer Degradation and Stability*, **41**, 109 (1993)

[67] C. Gamlin, et al., Journal of Thermal Analysis and Calorimetry, **59**, 319 (2000)

[68] C. Gamlin, Thermochimica Acta*, **367**, 185 (2001)

[69] J. R. Shelton and L. William, Industrial & Engineering Chemistry Research, **46**, 816 (1954)

[70] E. Frank, Chemical Review, **46**, 155 (1950)

[71] A. G. Ferradino, Rubber and Chemistry and Technology*, **76**, 694 (2003)

[72] K. Fujiwara and H. Ueno, Nippon Gomu Kyokaishi*, **63**, 625 (1990)

[73] D. Brück and H. W. Engels, KGK Kautschuk Gummi Kunststoffe*, **44**, 1014 (1991)

[74] H. W. Engels, KGK Kautschuk Gummi Kunststoffe*, **12**, 47 (1994)

[75] G. Scott, Mechanism of Polymer Degradation and Stabilisation*, Springer* (1990)

[76] T. Kubota, Japanese Journal of Organic Chemistry*, **13** (1955)

[77] E. M. Bevilacqua, Journal of Applied Polymer Science*, **9**, 1, 267–277 (1965)

[78] H. W. H. Robinson and H. A. Vodden, Rubber Chemistry and Technology*, **29**, 1, 240-250 (1956)

[79] U. Giese, S. Thust and J. Stanko, International Conference on Polymeric Materials in Automotive and Slovak Rubber Conference 2017

[80] J. B. Donnet, Carbon Black, *Springer* (1991)

[81] M. J. Wang et al., Encyclopedia of Chemical Technology 5th edition*, Wiley,* 4, 761-803 (2004)

[82] Y. Fukahori, The mystery of rubber strength and weakness, *Posty Corporation* (2011)

[83] P. J. Hart, Carbon, **5**, 363-371

[84] K. Nakayama, et al., Journal of Applied Polymer Science, **108**, 4, 2578-2586 (2008)

[85] K. Nakayama, T. Watanabe, Ohtake and M. Furukawa, Journal Applied Polymer Science*, **89**, 2, 211-226 (2016)

[86] F. A. Hopf, R. F. Shea and M. Scully, Physical Review A*, **7**, 6, 2105–2110 (1977)

[87] M. J. Duer, Introduction to Solid-State NMR Spectroscopy, *Wiley-Blackwell* (2004)

[88] R. G. Brewer, et al., Laser Spectroscopy V*, 219-228, (1981)

[89] R. Folland and A. Charlesby, Polymer*, **20**, 207 (1979)

[90] K. Fukumori, T. Kurauchi and O. Kamigaito, Polymer, **31**, 2361 (1990)

[91] T. Nishi and H. Murray, Journal of Polymer Science: Polymer Physics Edition, **12**, 685-693 (1974)

[92] K. Bergmann and K. Gerberding, Colloid & Polymer Science*, **259**, 990-994 (1981)

[93] R. Folland and A. Charlesby, Polymer, **20**, 211 (1979)

[94] R. Folland and A. Charlesby, International Journal for Radiation Physics and Chemistry, **15**, 2–3 (1977)

[95] A. Charlesby and B. Bridges, European Polymer Journal*, **17**, 6, 645-656 (1981)

[96] M. S. Robert, et al., Polymer Degradation and Stability, **80**, 3, 443-450 (2003)

[97] J. Rehner and P. J. Flory, Journal of Physical Chemistry, **11**, 521 (1943)

[98] P. J. Flory, Principles of polymer chemistry, *Cornell University Press* (1953)

[99] ASTM D2765-16: Standard Test Methods for Determination of Gel Content and Swell Ratio of Crosslinked Ethylene Plastics, *ASTM International* (2016)

[100] L. Brannon-Peppas and R. S. Harland, Absorbent Polymer Technology, *Elsevier* (1990)

[101] V. M. Litvinov, W. Barendswaard and M. van Duin, Rubber and Chemistry and Technology, **71**, 105 (1998)

[102] V. M. Litvinov and M. Steeman, Macromolecules, **32**, 8476 (1999)

[103] S. Kaufman, W. Slichter and P. Davis, Journal of Polymer Science Part A, **2**, 9, 829 (1971)

[104] N. O. Goga, et al., Journal of Magnetic Resonance, **192**, 1–7 (2008)

[105] F. Delor, Polymer Degradation and Stability, **67**, 469-477 (2000)

[106] F. Delor, Polymer Degradation and Stability, **60**, 321-331 (1998)

[107] G. Teissedre, Polymer Degradation and Stability, **53**, 207-215 (1996)

[108] M. Santoso and U. Giese, Rubber Chemistry and Technology, **80**, 5, 762-776 (2007)

[109] L. Zlatkevich, Luminescence Techniques in Solid State Polymer Research, *New York: M. Dekker* (1989)

[110] G. A. Russell, Journal of the American Chemical Society, **79**, 3871 (1957)

[111] R. F. Vassil, Macromolecular Chemistry, **231**, 126 (1969)

[112] L. A. Jiráčková and J. Verdu, Journal of Polymer Science: Polymer Chemistry, **25**, 1295 (1987)

[113] M. L. Huggins, Annals of the New York Academy of Sciences, **44**, 4, 431-443 (1943)

[114] D. Moldovan, Macromolecular Chemistry and Physics, **211**, 14, 1579–1594 (2010)

[115] B. Blümich, et al., Journal of Magnetic Resonance, **161**, 2, 204–209 (2003)

[116] R. I. Chelcea, et al., Journal of Magnetic Resonance, **196**, 178 (2009)

[117] H. Uehara, et al., Journal of Macromolecules, **47**, 888 (2014)

[118] S. Chinn, et al., Polymer Degradation and Stability, **91**, 3, 555-564 (2006)

[119] W. Provencher, Computer Physics Communications, **27**, 213–229 (1982)

[120] W. Provencher, Computer Physics Communications, **27**, 229–242 (1982)

[121] R. Folland and A. Charlesby, Journal of Polymer Science: Polymer Letters Edition, **16**, 339-344 (1979)

[122] R. Folland and A. Charlesby, International Journal for Radiation Physics and Chemistry, **8**, 555-562 (1976)

[123] V. R. Land, et al., Polymer Engineering and Science, **18**, 15 (1987)

[124] I. Homeier, Y. Torrejon and U. Giese, KGK Kautschuk Gummi Kunststoffe, **1**, 44-51 (2017)

[125] H. Oikawa and K. Murakami, Polymer, **27**, 398 (1986)

[126] H. Oikawa and K. Murakami, Polymer, **25**, 1117 (1984)

[127] K. Fukumori, Material life Society, **2**, 59-67 (1990)

[128] A. N. Gent, Rubber Chemistry and Technology, **36**, 389 (1963)

[129] A. V. Tobolsky, I. B. Prettyman, J. H. Dillon, Journal of Applied Physics, **15**, 380 (1944)

[130] A. V. Tobolsky and M. C. Shen, Journal of Polymer Science, **2**, 6, 2513 (1964)

[131] W. Dietmar, A. Kömmling, M. Jaunich and D. Schulze, Kautschuk Herbst Kolloquium (2016)

[132] M. Ring, Progress in Polymer Science, **15**, 217-262 (1990)

[133] L. Shibryaeva, Thermal Oxidation of Polypropylene and Modified Polypropylene, *Russian Academy of Sciences* (2012)

[134] K. Steven, The Spring 167th Technical Meeting of the Rubber Division (2005)

[135] H. Oikawa and K. Murakami, Polymer, **23**, 1737 (1982)

[136] T. Chikaraishi, Journal of Macromolecular Science Part B*, ***19**, 3, 445 (1981)

[137] L. Mullins and N. Tobin, Journal of Applied Polymer Science, **28**, 9, 2993 (1965)

[138] M. Ito, Nippon Gomu Kyokaishi, **87**, 319-324 (2014)

[139] K. Saalwächeter et al., Applied Magnetic Resonance, **27**, 401 (2004)

[140] J. Addad. et al., Macromolecules, **30**, 4374 (1997)

[141] K. Saalwächter, et al., Journal of the American Chemical Society*, ***125**, 48, 14685 (2003)

[142] K. Saalwächter, et al., Journal of Chemical Physics*, ***119**, 6, 3468 (2003)

[143] K. Saalwächter, et al., Macromolecules, **38**, 9650 (2005)

[144] J. L. Valentin, Macromolecules, **34**, 125 (2008)

[145] J. L. Valentin, Macromolecules, **43**, 4210 (2010)

Appendix 1- List of abbreviation

BR   Butadiene rubber

NR   Natural rubber

SBR   Styrene-butadiene rubber

NBR   Nitrile-butadiene rubber

HNBR   Hydrogenated NBR rubber

CR   Chloroprene polymer

IIR   Butyl rubber

EPDM   Ethylene-propylene-terpolymer

ACM   Alkyl acrylate rubber

FKM   Fluoroelastomers

EU   Urethane rubber

VMQ   Silicone rubber

ENB   Ethylidene norbornene

DCPD   Dicyclopentadiene

VNB   Vinilidene norbonene

TAIC   Triallyl Isocyanurate

TAC   Triallyl cyanurate

TMTP   Trimethylopropane trimethacrylate)

NMR   Nuclear Magnetic Resonance

ILT   Inverse Laplace Transform

FTIR   Fourier Transform Infrared Spectroscopy

ATR   Attenuated Total Reflection

CL   Chemiluminescence

DSC   Differential Scanning Calorimetry

TGA   Thermal Gravimetric Analysis

Tg   Glass transition temperature

T_2 Relaxation time

Mn   Average number molecular weight

Mw   Average weight molecular weight

Appendix 2– List of Published Papers

1. Y. Aoyagi , U. Giese ,R. Kreiselmaier, Study on aging process of rubber material for sealing applications - A novel technique using chemiluminescence under stress -, International Rubber Conference 2016, Kitakyushu, Japan 2016

2. Y. Aoyagi, U. Giese, R.Kreiselmaier, A novel technique using chemiluminescence under stress, KHK 2016 (Kautschuk Herbst Kolloquium) Hannover, Germany, 2016

3. Y. Aoyagi, U. Giese, R. Kreiselmaier, Characterization of the aging process of EPDM using NMR and stress relaxation, J. Jungk, International Rubber Conference, Cleveland, USA, 2017

4. Y. Aoyagi, U. Giese, R. Kreiselmaier, J. Jungk, A novel approach to using inverse Laplace transformation of NMR regarding cued is aging, PMA 2017 (Polymer materials for automotive) Bratislava, Slovakia, 2017

5. Y. Aoyagi, U. Giese, J. Jungk, K. Beck, Characterization of the Aging Process of EPDM using NMR, DKT 2018, Germany,2018

6. Y. Aoyagi, U. Giese, J. Jungk, K. Beck, The analysis of aging processes of EPDM-elastomers using low field NMR and stress relaxation measurements, KHK 2018 (Kautschuk Herbst Kolloquium) Hannover, Germany, 2018

7. Y. Aoyagi, U. Giese, R. Kreiselmaier, Characterization of Stress Relaxation of cured EPDM using Chemiluminescence, Kautschuk Gummi Kunststoffe, August, 2017,19-23

8. Y. Aoyagi, U. Giese, J. Jungk, K. Beck, The analysis of aging process of EPDM elastomers using low field NMR with Inverse Laplace Transform and stress relaxation measurements, Kautschuk Gummi Kunststoffe, July, 2018,26-35.

Acknowledgement

Curriculum Vitae

Education and Work experience

April 2000- March 2004   Bachelor of Engineering, Waseda University Tokyo,
JAPAN

April 2004-March 2006   Master of Engineering, Waseda University Tokyo,
JAPAN

-Bachelor thesis title : An analysis of the decomposition reaction with vanadium
pentoxide as catalyst using Ab-initio molecular orbital simulation

-Master thesis title : An analysis of the decomposition reaction of dioxin using Ab-
initio molecular orbital simulation

April 2006- August 2015   NOK corporation, Japan

August 2015-September 2018   Freudenberg Innovation Technology

August 2015-September 2018   Deutsches Institut für Kautschuktechnologie e.V.